PERFORMANCE OF PORTLAND CEMENT CONCRETE CONTAINING CHEMICALLY BENEFICIATED HIGH LOSS ON IGNITION FLY ASHES WITH AIR ENTRAINMENT

by

Taye Oluwafemi Ojo

A thesis submitted to the faculty of
The University of North Carolina at Charlotte
in partial fulfillment of the requirements
for the degree of Master of Science in
Civil Engineering

Charlotte NC

2018

Approved by:

_____
Dr. Brett Q. Tempest

_____
Dr. Tara L. Cavalline

_____
Dr. Vincent Ogunro

ABSTRACT

TAYE OLUWAFEMI OJO Performance of Portland cement concrete containing chemically beneficiated high loss on ignition fly ashes with air entrainment (Under direction of Dr. BRETT Q. TEMPEST)

The use of fly ash as a partial replacement of Portland cement in concrete production has been widely accepted and has been proven to be a successful practice that enables production of economical durable concrete. However, following the Clean Air Act Amendment of 1990 power plants have started using the technology of adding activated carbon to the combustion chamber of coal plants to remove mercury and other contaminant from the exhaust. Consequently, the ashes produced in recent decades contain high quantity of unburned carbon which adsorb air entraining admixture in concrete. For resistance to stresses induced by freezing and thawing, concrete must be air entrained to prevent expansion of aggregate and cracks. The amount of air entraining admixture required to achieve a target air content in concrete can be difficult to predict and can vary significantly due to the presence of unburned carbon in fly ash.

The main objective of this study was to evaluate the performance of off-spec fly ashes that were chemically treated with a carbon blocker because they contain too much carbon to meet concrete use specifications. For this study, off-spec fly ash is the ash that do not meet North Carolina Department of Transport (NCDOT) specification for LOI limit in fly ash. Three off-spec fly ashes from three different power plants namely BU, MU and AU were used for this study, along with one on-spec fly ash BC which meets NCDOT specification for LOI, a marketable ash was also recovered which was used as a control. The off-spec fly ashes were chemically treated to reduce impact of unburned carbon on admixture adsorption and this treated ashes were used

to produce concrete specimens with varying air contents. Twenty different concrete mixtures, produced using the different treated and untreated ashes were batched and tested to provide insight on the durability performance and ability to predict the required air entraining admixture needed to achieve target air content in concrete containing treated ashes.

Durability of the concrete mixtures was measured through the use of compressive strength, surface resistivity, Super Air Meter test, air void analysis, and freeze thaw testing. Analysis of covariance (ANCOVA) was also performed for the response of durability factor, spacing factor and compressive strength to determine if the treatment process had any effect on the air void network, durability factor and strength of the concrete produced.

The variable dosage test showed that it was easy to predict the amount of AEA needed to achieve target air content in treated ashes and the control ash. For the untreated ashes, the relationship between AEA dosage and air content generated was scattered and inconsistent. This showed that it is difficult to predict the amount of AEA needed in untreated ashes due to the adsorptive nature of the unburned carbon. The air void analysis of the treated and untreated mixtures with air content greater than 5% meets the required specification for spacing factor to be frost resistant. Additionally, all mixtures with air content greater than 5% showed good freeze thaw performance. ANCOVA analysis demonstrated that the treatment of the fly ash did not significantly influence the durability factor, air void system and strength.

ACKNOWLEDGEMENTS

I greatly appreciate the opportunity, guidance and support provided by my advisor, Dr. Tempest and also for always pushing me to give my best. I would also like to thank other members of my committee, Dr Tara Cavalline for her genuine care, creativity and always been there when I felt lost. Dr Vincent Ogunro for his guidance, support, fatherly care and advice during the course of my studies. This material is based upon support from Duke Energy and this support is greatly appreciated.

My Mum and siblings for making me the man I am today by supporting me in every way. Without my Mom, I will not be where I am today and would have never been on the path to achieve my goals.

I would also like to thank Wesley Maxwell, Gregory Loftin, Blake Biggers, Ross Newsome, Mark Fitzner and Gunnar Wright for their help in batching and testing of concrete for this research project.

I would not be the man I am today without all of these wonderful people. I am proud of who and where I am today. For this, I am forever grateful and I thankful.

TABLE OF CONTENTS

LIST OF TABLES

LIST OF FIGURES

CHAPTER 1: INTRODUCTION

The objective of this study was to evaluate the performance of fly ashes that were chemically treated because they contained too much carbon to meet concrete use specifications. Although fly ash is a material that is often utilized in concrete for a variety of purposes, it must meet American Association of State Highway and Transportation Official (AASHTO) and various state agencies specifications for it use. Carbon in fly ashes, measured as loss on ignition, interferes with air entraining admixtures and makes it difficult to reliably achieve the required amount of entrained air during mixing to ensure frost durability. Therefore, the experiments that are described in this report were intended to measure the reliability of achieving specified air content with treated ashes as well as to determine whether the resulting air void network was sufficient to protect the concrete from freezing damage.

Due to the Clean Air Act Amendment of 1990[1], which had the objective of reducing air pollution, power plants that produce fly ash as a by-product of coal have employed a strategy of adding activated carbon to the gas stream of coal combustion chamber as a method of removing mercury and other contaminants from the exhaust. This method of adding activated carbon has resulted in the production of higher carbon content fly ash. The carbon particles in the fly ash tend to adsorb air entraining admixtures (AEA) making it difficult to predict the amount of AEA required to achieve a targeted air content in concrete mixtures for frost resistance.

To prevent problems associated with predicting the amount of AEA required for target air content, several standard specifications have set limits for percentage of carbon measured as loss on ignition that should be present in fly ash for use in portland cement concrete. The American Society of Testing and Materials have

established a limit of 10% for Class N, 6% LOI for Class F and Class C fly ashes (ASTM C618) [2], The North Carolina Department of Transportation (NCDOT) [3] sets the limit to 4% LOI for Class C and Class F ashes while American Association of State Highway and Transportation Official (AASHTO M295) [4] sets the limit to 5% for Class C and Class F ashes.

1.1 Scope of Research

A series of tests such as foam index, iodine adsorption and loss on ignition were performed to characterize the unburned carbon in fly ashes obtained from several power plants supplying ash to the Southeastern United States market. Several other tests were also performed to evaluate the characteristics of concrete produced with chemically treated and untreated ashes such as slump, air content, mechanical properties and durability performance. The off-spec ashes were chemically treated by adding a carbon blocker and it should be noted that the treatment is proprietary treatment approach which is not developed or applied by this study. The research was done by comparing performance of concrete mixtures made with treated ashes to concrete mixtures made with untreated ashes. The control mixture was made with a marketable ash which does not require any chemical beneficiation to meet current specifications for use in concrete production. The concrete mixtures prepared for this study were pavement mixtures typically used by NCDOT with local cements and aggregates used in the field. Mechanical tests and durability tests were performed on each mixture at various ages of curing. The quality of air void network of each mixture was also evaluated by performing air void analysis to determining the air void parameters such as hardened air content, spacing factor and specific surface.

1.2 Organization of Thesis

Chapter 1 provides an overview of the purpose and objectives of this research work. Chapter 2 provides a literature review that gives details about air void network in concrete, forms of unburned carbon in fly ashes, carbon mitigating technologies as well as summary of laboratory research findings of other researchers. Chapter 3 provides a description of materials used, concrete mixture batched, preparation of tests specimens and the test procedures used. Chapter 4 gives the results from all the laboratory tests performed. Chapter 5 provides discussion and analysis of laboratory tests as well as statistical analysis to further substantiate some of the earlier conclusions. Chapter 6 provides the conclusions of this study as well as recommendation for future research.

CHAPTER 2: LITERATURE REVIEW

2.1 Air Entrained Concrete

Concrete contains capillary pores which in service are often partially or entirely filled with water. As temperature decreases to the freezing point, water turns to ice and stresses are developed. If these stresses are greater than the strength of the concrete, the concrete will rupture and cracks will develop, allowing additional water to penetrate the concrete. With subsequent cycles of freezing, the concrete further deteriorates until it can no longer serve its intended purpose.

Various theories and hypotheses have been put forward to explain the freezing damage mechanism in concrete by researchers like Powers [5] and Pentalla [6]. Powers [5] in his extensive study proposed the hydraulic pressure and critical saturation theory to explain the frost damage mechanisms. The hydraulic pressure theory proposed by Powers states that damage in concrete due to frost action is caused by build-up of hydraulic pressure as a result of resistance to flow of unfrozen water in the capillary pores. Hydraulic pressure is produced due to the resistance of the matrix to movement of water flow. When a pore is saturated, the expansion during freezing results in excess water flowing away from the freezing part. This is based on law of thermo-dynamics which describes diffusion as movement from a high energy to a low energy zone. Because cement paste does not expand, as water freezes, unfrozen water is pushed out of the capillary pores. This flow then generates hydraulic pressure in the capillary pores which builds up over time. Figure 2.1 shows various stages of the damage mechanism during freezing. Before freezing in stage 1, the water in both upper and lower pores are at low pressure. The cold front, which is the boundary of an advancing mass of cold and warm air enters the upper pore, increases the hydraulic

pressure in the upper pore and subsequently exposing surrounding concrete to high pressure water. The hydraulic pressure increases over time which leads to deterioration of the cement paste between the capillary pores.

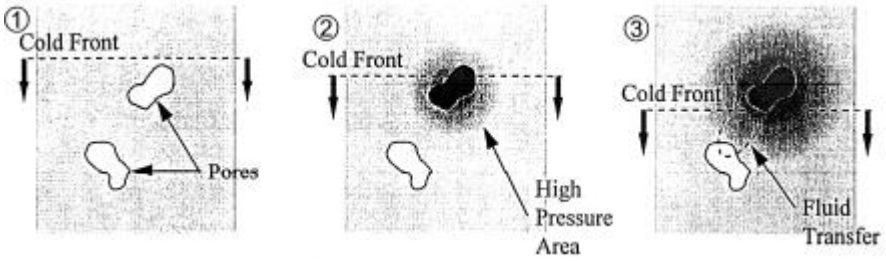

Figure 2.1: Stages of freezing damage mechanism using the hydraulic pressure theory [7]

Pigeon et al [8] reported that the magnitude of hydraulic pressure correlates with the rate of freezing and characteristics of the pore system. The characteristics of the flow distance affects the frost performance of the concrete, and an increase in the distance between freezing zone and the nearest unfilled void will result in high flow resistance and hence high hydraulic pressure.

Contrarily, osmotic pressure develops as a result of water moving towards the freezing part in the pore system. In an investigation to study the effect of moisture condition on damage development during cyclic freezing and thawing, using vacuum saturation and partial saturation with exposure to wet environment. It was reported that vacuum saturated concrete show less resistance to freezing and thawing cycles, completely failed at 13 cycles [9].

The critical saturation theory proposed by Powers [10] states that water increases by about 9 percent when it freezes which generates a hydrostatic pressure and since the capillary pores are completely saturated, the pressure increases because the pores cannot accommodate additional volume of ice created. As the hydrostatic pressure increases and exceeds the tensile strength of the cement paste, the cement

paste cracks and ruptures. The build-up of the effect of consecutive freeze thaw cycles gradually leads to excessive expansion and scaling of the concrete.

Powers and Helmuth [11] also put forth the osmotic pressure and capillary ice growth theory to explain experimental results which were not in agreement with the hydraulic pressure theory. The osmotic pressure and ice growth theory is based on the hypothesis that ice attracts unfrozen water, and that water in the capillary pores contains soluble substances which implies that water in capillary pores is not entirely pure. The temperature at which water freezes depends on the size of the pores. Water cannot freeze in smaller pore because surface tension is sufficiently great, hence unfrozen water moves from fine pores to coarse pores as shown in Figure 2.2. Osmotic movement of unfrozen water leads to pressure build-up which increases the internal stresses in the paste. The potential damage of paste due to freezing can be prevented by creating air voids to compete with the capillary pores, since air void contains a little water, ice can form on the walls of air voids as shown in Figure 2.2 thereby attracting the unfrozen water from the smaller pores.

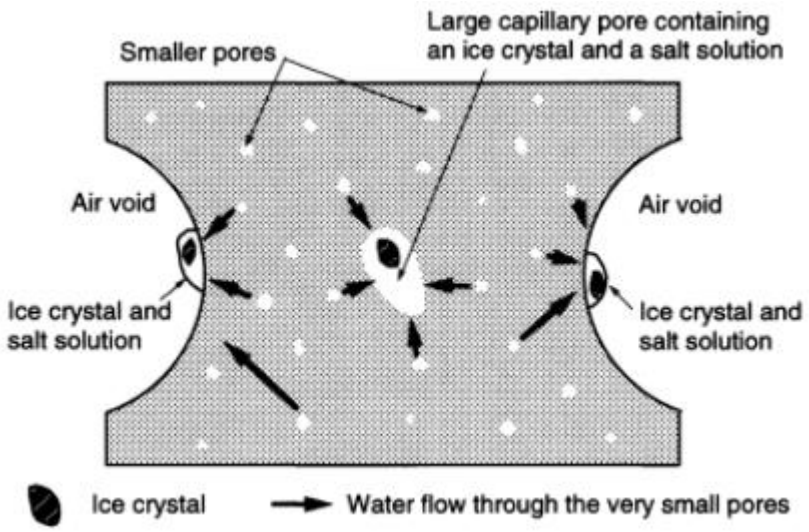

Figure 2.2: Illustration of osmotic and capillary ice growth theory [12]

Consequently, to produce concrete that is able to withstand wear, stress and eventually damage in freezing and thawing zones, a properly distributed air void network must be developed. Air entrainment is the intentional creation of controlled amount of tiny disconnected air bubbles in concrete through the addition of air entraining agents. The agents are typically surfactants and are commonly to as air entraining admixtures (AEA). Air entraining admixture stabilizes air bubbles which are produced from the mechanical agitation action of the mixing machine. The volume and spacing of air bubbles in concrete are key characteristics that provide the ability of concrete to withstand freezing and thawing actions. [13] The finer the gradation of air bubbles, the higher the ability of the hardened concrete to withstand freeze-thaw action. If the volume of air voids is too low or the air voids are not closely spaced in the hardened concrete, the concrete is susceptible to damage due to freezing and thawing actions. When concrete is air entrained, pores are stabilized; during freezing the pressure pushes water from the capillary voids to the entrained voids which prevent the concrete from cracking, as the air bubbles are capable of being compressed. The bubbles also improve the workability of concrete, reduce segregation and bleeding of concrete.

2.1.1 Air Void Network

Air is present in concrete as gas bubbles which are trapped as a result of mixing, transporting and placing. These bubbles range in sizes and shapes, from fine voids to coarse voids. They can change size, shape, be removed and expand during vibration. When concrete hardens, these bubbles are fixed in one position and create a hollow space called air void. Typically, air voids vary in size from 0.0004 in (0.01 mm) to 0.004 in (0.1 mm) and usually have a diameter of about 0.002 in (0.0508 mm) [14]. Figure 2.3 shows the size range of air voids typically found in hardened concrete.

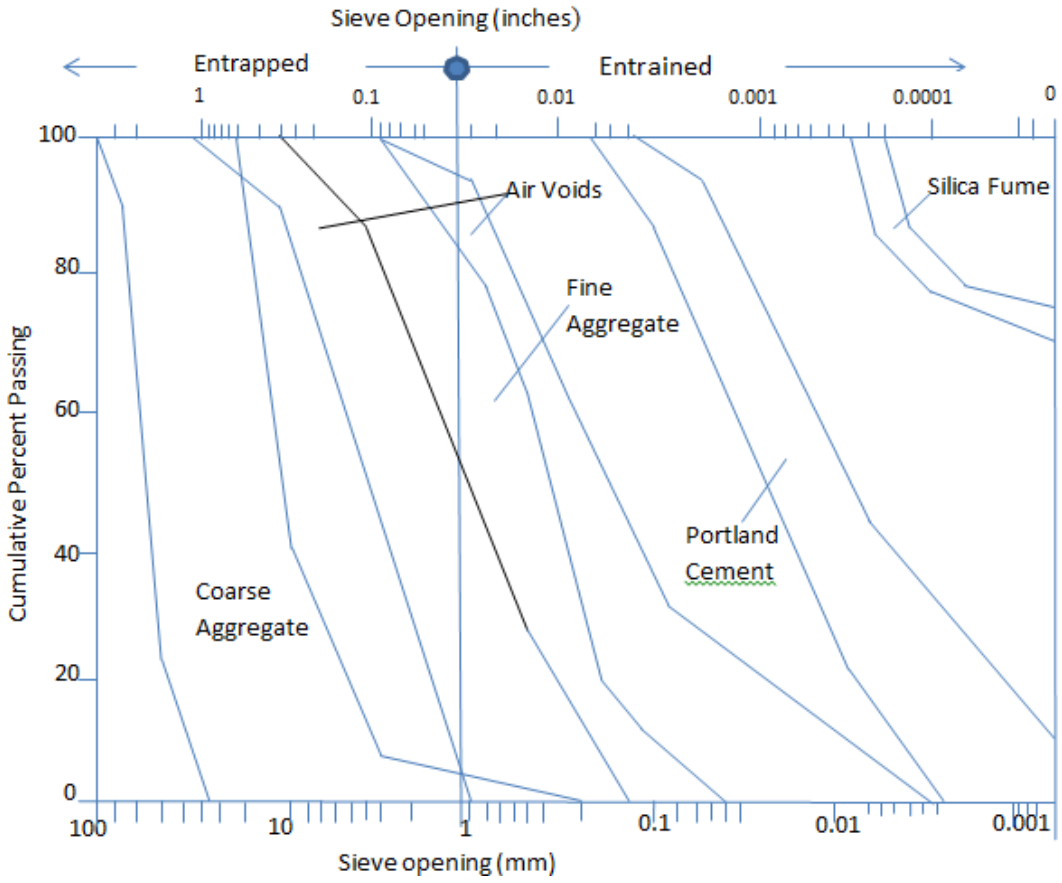

Figure 2.3: Size range of Voids in Hard Concrete [14]

As shown in Figure 2.3 above, voids in concrete can be categorized as entrained voids and entrapped voids.

2.1.1.1 Entrained Voids

Entrained voids are small sphere-like voids shaped into folds during mixing of concrete. These bubbles are stabilized and retained through the addition of AEA in concrete. Addition of AEA shifts the air void gradation to the finer side and retains the air trapped during mixing and vibration. Entrained bubbles are smaller than 0.04 in (1.016 mm) and which are uniformly distributed throughout the concrete [14]. A typical air entrained concrete has a total volume percentage of entrained air between 2 – 6 % as compared to 1.5 % of entrapped air in a non-entrained concrete [15].

Entrained air is also known to increase slump, volume and plasticity of fresh concrete [16] [17].

2.1.1.2 Entrapped Voids

Unlike entrained voids, entrapped voids are created during improper mixing, placing and consolidation of concrete. These voids are coarse voids which are irregularly shaped voids, typically larger than 0.04 in (1.02 mm) in size [14]. These voids do not provide considerable resistance to freeze-thaw actions because they are disconnected and too large in size.

2.1.2 Air Content and Air Void Spacing

The air void system in concrete can be characterized by different parameters such as the number of bubbles, volume of bubbles, spacing between each bubble and bubble size distribution in the cement paste. Of all these parameters the spacing and size distribution of the bubbles are generally the most important parameters to predict the durability of the concrete to freeze and thawing actions [13]. The determination of the parameters of the air void in hardened concrete is currently performed based on guidelines from The American Society of Testing Material Standard (ASTM C457) [18].

ASTM C457 [18] 'Standard Test Method for Microscopical Determination of Parameters of Air Void System in Hardened Concrete' defines the spacing factor as the maximum distance between any points to the nearest air void. It is recommended by Powers [5] that the spacing should not be greater than 0.008 in (0.20 mm) for moderate exposure of the concrete. Larger values may be used for mild exposure and smaller values for severe exposure of the concrete especially if the concrete is in contact with deicing chemicals. The size of these bubbles is also important and ASTM

C457 defines the specific surface as the average surface area of the voids per unit volume in hardened concrete. For adequate resistance to freezing and thawing, it is recommended that the specific surface should be greater than 600 in^2/in^3 (23.62 mm^2/mm^3) [5].

Air content and air void system quality in concrete depends on mixture proportions, chemical admixture used, temperature and the aggregates size [4]. The required air content and size/spacing characteristics in a particular concrete is dependent on the environmental exposure of the concrete. American Concrete Institute (ACI) gives different recommended air content for frost resistant concrete based on maximum aggregate size, a severe and moderate exposure which is shown in Table 2.1.

Table 2.1: Recommended Air Content for Frost Resistant Concrete [16]

Maximum Aggregate Size (in)	**Average Air Content (%)**	
	Severe Exposure	***Moderate Exposure***
3/8	7-1/2	6
1/2	7	5-1/2
3/4	6	5
1	6	5
3/2	5-1/2	4-1/2
3	4-1/2	3-1/2
6	4	3

In a research conducted by Felice et al [19] to investigate fresh and hardened air void parameters and cyclic freezing durability of concrete, it was reported that using modern AEA with a minimum air content of 3.5 % can provide protection from freeze stresses in concrete. An acceptable air content is achieved when the size of the bubbles is smaller than 0.05 in (1.27 mm) and the distance between air bubbles is no

more than 0.008 in (0.20 mm) [19]. Typically, air content of between 5 % and 8 % are specified in regions of freezing weather to provide resistance to freeze and thaw actions in concrete to offset the effect of bubble system that is larger and of lower quality at a given volume of air.

For concrete to withstand freeze and thaw action, there must be sufficient distribution of well-spaced air voids. Other than the Super Air Meter (SAM) [24] which gives an indication of the quality of the air bubbles, there is no specific quality control test to adequately measure the size of bubbles and distribution of air voids, hence the volume of air is generally used to specify the durability of concrete in freezing zones. From the freeze-thaw damage theory, concrete only requires a little volume of air void for expansion hence it is not the volume of this air voids that is critical but good network of closely distributed air voids. However, in research by Ley et al. [20] it was shown that as the volume of air in concrete increases, the spacing of air voids decreases and small bubbles tend to be evenly distributed, which leads to resistance to stresses from freezing and thawing.

According to Klieger [21] et al., similar to the spacing factor the volume of air also plays an important part in the performance and durability of concrete to freeze and thaw actions. Klieger et al. [21] suggested that the minimum required air volume in the paste for frost resistance is 18% using vinson resin as an AEA available as at the time. They methodically changed the volume of air in the concrete specimen and evaluated the freeze-thaw performance of the specimens. Specimens having less than 18% paste air volume were susceptible to freeze and thaw actions. Klieger's work was completed without performing hardened air void analysis to evaluate the total air volume in the concrete and the test methods used today are very different from

modern methods. For instance there are differences in the curing, freezing and evaluation of failure compared to what is used today.

The total volume of air in a concrete mixture represents the air content in the concrete mixture which is generally measured by pressure and volumetric test methods. These tests are performed in accordance to "Standard Test Method for Air Content of Freshly Mixed Concrete by the Pressure Method" ASTM C231 [22] and "Standard Test Method for Air Content of Freshly Mixed Concrete by the Volumetric Method"
ASTM 173[23] respectively. These tests only measure the total air void volume in a concrete mixture, but do not give a good indication of the quality of the air void network in the concrete mixture. In a recent research study carried at Oklahoma State University by Ley and Tabb [24], a modification of the pressure method was introduced to measure the spacing factor of air void system using data from the pressure method results. This research has led to the development of a new test device that measures the quality of the air void system in a fresh concrete mixture. This new device is called the Super Air Meter (SAM).

2.1.3 Super Air Meter (SAM)

The Super Air Meter is specialized equipment that measures both the air void volume and the air void spacing in a fresh concrete. The device consists of a digital pressure gage and pressure pump as shown in Figure 2.4 below. Air void spacing has been shown in various research to be a better indicator a concrete resistance to freeze-thaw durability that air volume and until recently, there was no way to determine this in the field before concrete is placed and hardened. The SAM specimen preparation method is similar to the method used to perform air content testing using the Type B meter from "Standard Test Method for Air Content of Freshly Mixed Concrete by the

Pressure Method" ASTM C231 [22] . However, the SAM test method uses incrementally higher pressure events instead of one single pressure procedure as is used in "Standard Test Method for Air Content of Freshly Mixed Concrete by the Pressure Method" ASTM C231 [22] . The deformation of the concrete is studied at 14.5 psi, 30 psi and 45 psi and the pressure is released and the procedure is repeated to measure the deformation. The difference between the first pressure step and the second pressure step is used to calculate the SAM number. A study by Ley et al. [25] has shown that the SAM number is directly correlated to the air void spacing in concrete. It was reported that a SAM number of 0.20 correlates with the spacing factor of 0.008in limit which is the standard limit to provide resistance to rapid freeze and thaw actions [5]. This threshold of 0.20 SAM number can vary up to 0.32 [25].

Ley and Tabb [24] measured the freeze thaw durability of fresh concrete using the overpressure method; they investigated the validation of the SAM by using 50 different concrete mixtures that had different workability, air void distribution and different admixtures. It was reported that 94 % of the data examined with SAM correlated with the ASTM C 457 hardened air void analysis. The SAM has been shown to be a useful tool to analyze and investigate the freeze thaw durability of concrete before it is placed.

Figure 2.4: Super Air Meter (SAM)

2.2 Carbon in Fly Ash

About 25% of the world's energy production is fueled by coal [26]. According to the United State Energy Information Administration [27], in 2015 the United States produced about 4.1 trillion kilowatts hours of electricity with 30 % of total electricity from coal, producing 44.3 million tons of fly ash in the process as by product. Only 54 % of the fly ash produced is used beneficially and the rest is dumped in landfills as solid waste [28]. In a 2015 America Coal Ash forecast report prepared by American Road & Transportation Builders Association, the total electricity generation from coal is projected to increase substantially as shown in Figure 2.5 below. With the projected increase in electricity generation from coal-fired plants, it follows that the quantity of fly ash produced will also increase. It was forecasted from 2013 through 2033 that fly ash production will grow 3.8 % over the forecast period [29].

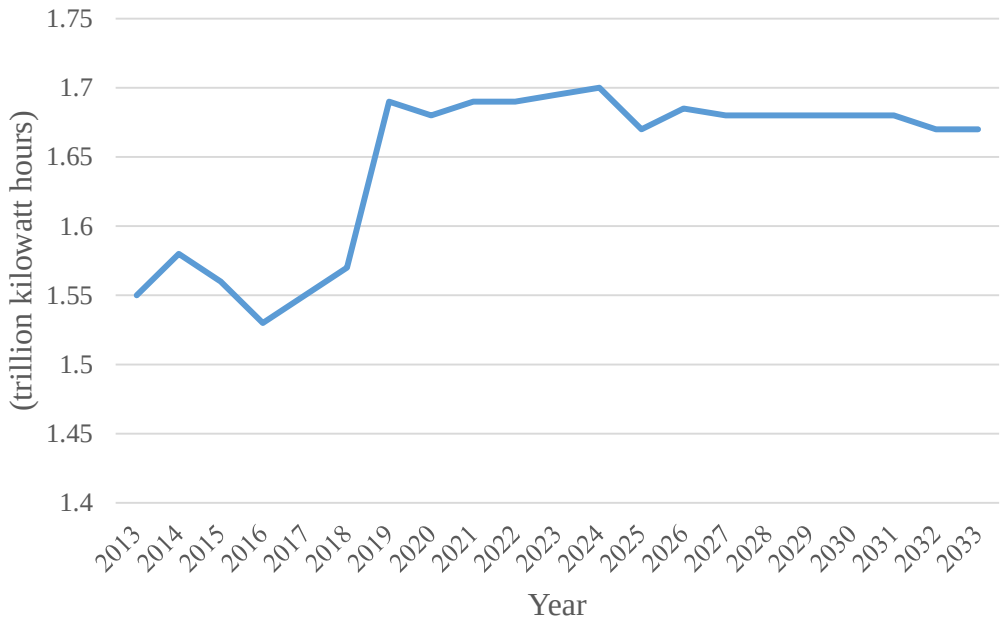

Figure 2.5: Coal Generated Electricity, 2013-2033[29]

Currently, the major use of fly ash is in concrete production. However, it was not until the 1940s that fly ash use was widely accepted. Fly ash use in concrete is a successful and well-accepted practice to produce durable concrete. When used as a supplementary cementitious material in concrete, fly ash improves the concrete properties and performance. Fly ash has been shown to reduce the water demand in concrete compared to concrete without fly ash [30], this beneficial use of fly ash also helps to solve the environmental problems associated with ash disposal. It has also been established that the use of fly ash in concrete generally increases resistance to chloride penetration [30], reduces heat of hydration [31], increases later age concrete strength and reduces permeability [31]. However, over the years not all fly ash produced can be used in concrete due to the high amount of unburned carbon present in the fly ash which adsorbs AEA.

In a petrographic examination by Hower et al [32] studying different high carbon fly ashes, it was shown that the unburned carbon in fly ash is not visually uniform. Inertinite particles, isotropic coke and anisotropic coke were identified as the three very small distinct types of unburned carbon in fly ash. Inertinite particles are the oxidized form of carbon which are entrained during combustion prior to melting while the other forms of carbon particles are the non-oxidized form and have gone through molten stage. The three carbon types also have different physical and chemical properties. These differences in properties might also be reflected in the absorption properties as regards to AEA [33]. Another study has also classified unburned carbon in fly ash produced from low-NOx pulverized coal combustion as soot and coal char [34]. Anisotropic is when the properties of a material vary with different crystallographic orientation while a material is said to be isotropic when the

properties are the same in all directions. Figure 2.6 below shows a photomicrograph of the carbon particles present in fly ash.

a) Isotropy [33]

b) Anisotropy [33]

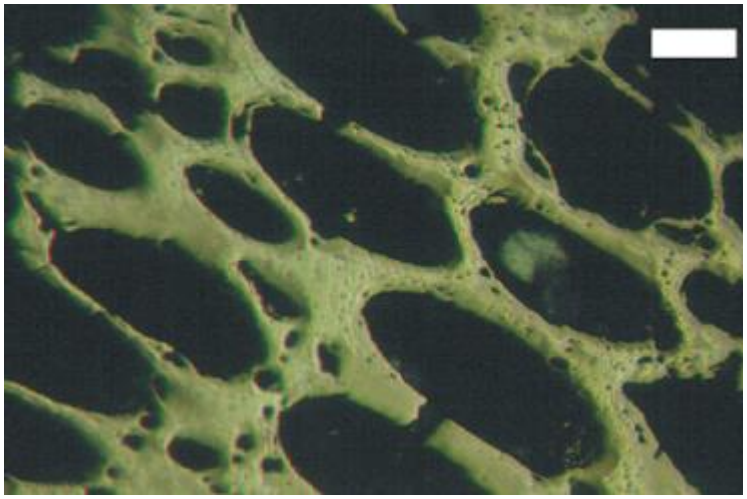

Inertinite [35]

Figure 2.6: Representation of forms of carbon particles

Inertinite particles are generally formed at high temperatures during coalification due to forest and peat fire at temperature range of 1112 °F – 1292 °F (600 °C-700 ˚C). It escapes during combustion and is carried by the flue gas to the electrostatic precipitator where it is added to the unburned carbon present in fly ash, collected at the electrostatic precipitator. Isotropy carbon particles are poorly ordered

and when viewed in polarized light they have similar optical properties in various positions when rotated while, anisotropic carbon are well ordered and have optical properties that vary when rotated. The degree of anisotropism and relative size and shape of the anisotropic particles in the unburned carbon depends on the petrographic rank and type of the coal [32] [33].

Not much is known about the individual absorptive properties of the different forms of carbon particles present in the unburned carbon in fly ash because the process to extract each particle is a cumbersome task. For instance, it is not known if a fly ash composing of mainly isotropic particles will absorb the same amount of AEA as a fly ash containing predominantly anisotropic or inertinite particles [33].

However, in a study by Maroto et al [33] to characterize the differing forms of unburned carbon in fly ash, the research team successfully developed a method to isolate the different types of carbon particles present in fly ash. They separated two fly ash specimens using triboelectrostatic enrichment followed by density gradient centrifugation with high density lithium polytungstate media. Density gradient centrifugation is the process of separating different particles based on densities which uses a gradient material that is capable of providing higher densities and low viscosity. Maroto et al [33] used lithium polytungstate aqueous solution as the separation media because it is non-toxic, has high stability and it provides high density solutions.

It was reported that for the two fly ash specimens, the density of the three unburned carbon types is similar despite the differences in the starting coal or fly ash source from which they were derived. In regard to adsorptive properties for both fly ash specimens, the surface area of the unburned carbon particles is generally low ranging from 10 – 60 m^2/g (7000000 – 42000000 in^2/lb) and most of the pores range

from 2 – 50 nm ($7.874x10^{-8}$ - $1.9685x10^{-6}$ in) in width. The surface area increases linearly as a function of particle density and inertinites has the lowest surface area with isotropy and anisotropy exhibiting intermediate and highest surface area respectively. Additionally, isotropy particles contained a higher level of oxygen than anisotropy and inertinites

2.2.1 Effect of High Carbon Fly Ash on Air Entrainment

The effect of the fly ash on the amount of AEA required to properly entrain air bubbles is a major challenge facing the use of fly ash in concrete. When fly ash is used in air entrained concrete, the unburned carbon will absorb the air entraining admixture, resulting in production of concrete with an inadequate air void network [13]. This adsorbing nature of fly ash is not due to the fly ash itself but due to composition of the contaminants present in the fly ash. This unburned carbon content is usually measure by performing a loss on ignition test (LOI).

In a study conducted by Gebler and Krieger [35] to determine the effect of fly ash on air void stability, they discovered that the higher the carbon content of a fly ash, the higher the amount of air entraining admixture that is required to achieved a specified air content than concrete without fly ash. These tests were performed by investigating 10 fly ashes having different geographical origin and chemical properties. The research also showed that the higher the air entraining admixture the greater is the air loss on extended mixing of concrete.

In one investigation on control of air content in concrete [36], it was reported that the air content in concretes decrease as loss on ignition in fly ash increases. This is due to the absorption of the air entraining admixture by the carbon particles present in the fly ash, this resulted in the AEA not being able to perform it intended use. To

mitigate the effect of this carbon, more AEA must be added until it can no longer be absorbed.

Freeman et al [37] reported that most carbon present in fly ash is of the form of distinct, fused particles with a very macro-porous structure. They conducted an investigation on the interaction of carbon in fly ash with AEA using four fly ashes specimen having LOI value ranged from 1.5 to 16 wt%. This study showed that very little AEA was needed to stabilize air bubbles in concrete without high carbon fly ash, but when carbon containing fly ash was added the requirement for AEA increased substantially to thrice the amount needed for low carbon fly ash.

2.2.2 Standard Specifications for Fly Ash Use in Concrete

The widely used specifications for fly ash in North America is The American Society of Testing and Materials 'Standard Specification for Coal Fly Ash' (ASTM C618) [2] and American Association of State Highway and Transportation Official 'Coal Fly Ash and Raw or Calcined Natural Pozzolan for Use in Concrete' (AASHTO M295) [3]. ASTM C618 [2] classifies fly ash into three classes based on it source of origin and chemical composition. The three types of fly ash are Class N, Class F and Class C. Class N are raw or calcined natural pozzolans. Class F fly ash is typically produced from burning anthracite or bituminous coal and sometimes from lignite. Class F fly ash has pozzolanic properties. Class C fly ash is normally produced from burning lignite or subbituminous coal. Class C fly ashes sometimes have some hydraulic cementitious properties which made them widely used in concrete work. Class C ash materials typically have calcium contents that are higher than Class F fly ashes.

Due to the negative effect of fly ash carbon on air entrainment, the standard making organizations have established limit for percentage of carbon measured as LOI in Carbon. Table 6 below presents the LOI limit established by different standard organizations and state highway authorities (North Carolina, South Carolina and Tennessee State Departments of Transportation). American Concrete Institute (ACI) [16] Committee 201 on durability of concrete also recommends some guidelines for production of concrete under freezing conditions. This includes adequate curing before first freezing cycles and appropriate air entrainment.

Table 2.2: LOI limits established by different specifications

Agency	**ASTM C618**	**AASHTO**	**NCDOT**	**SCDOT**	**TDOT**
LOI Limit	6%	5%	4%	5%	5%

2.3 Air Entraining Admixture

Air entraining admixtures are materials other than portland cement, water and aggregate that is added to concrete, during or immediately before mixing to entrain air. Air entraining admixtures are generally known to improve workability, produce improved resistance to frost action and high durability. The American Society of Testing and Material standard (ASTM C260) [38] "Specification for Air-Entraining Admixtures for Concrete" outlines specific requirements that all admixtures used in concrete must meet. This specification sets performance requirements and limits on the effect of the admixture on compressive strength, flexural strength, setting time, maximum shrinkage and bleeding.

2.3.1 Types of Air Entraining Admixture

There are many chemicals used for entraining air in concrete. These products could be a mixture of more than one chemical. Most contemporary air entraining admixtures are liquids produced from wood resins or from synthetic detergents. The

chemical surfactants used as AEA are substances which consist of long chain molecules with a polar group at one end. These surfactants can be classified as anionic, cationic and non-ionic based on the nature of the charge of the polar portion of the molecules. If it is positively charged it is referred to as cationic. If negatively charged it is anionic, and if it electrically neutral it is non-ionic. Anionic surfactants are generally used in concrete works because they provide more stability to entrained air void than other class of surfactants [39]. The most widely used air entraining admixtures in the United States are formulated from vinsol resins and Polycarboxylates [40]. Commercially available admixture can be grouped into the following seven categories [41]:

1) Salt of wood resins

These are the most widely used AEA, and are surfactants generally derived from the process of recovering solvents and resins from pine wood stumps. They are insoluble and classified as anionic. The neutralization of these types of admixtures is done with sodium hydroxide and this solution is what different AEA formulations are based. They are preferred to other types of admixtures because they provide more stability to entrained air bubbles.

2) Salts of petroleum acid

These are derived as by product of petroleum refining. It is generally the sludge left over after treatment of petroleum product with sulfuric acid which produces white olive oil. The sludge is then neutralized with sodium hydroxide, however if it is neutralized with triethanolamine, agents of organic salts of sulfonated hydrocarbon are produced. Salts of petroleum acid can be anionic, cationic or non-ionic. This type of admixture is not effective because the air void system produced is not stable in concrete [42].

3) Salts of proteinaceous materials

This class of AEA are derived from product of animal processing. They are a mixture of salts of complex carboxylic and amino acid. These surfactants are usually anionic and cationic in nature. They are not commonly and generally used in concrete works because the stability and quality of air bubbles that they provide is doubtful and questionable.

4) Salts of sulfonated lignin

These are derived generally as by product of production of paper. The surfactant are anionic and are comparatively poor air entrainers when compared to other types of AEA available. They are mostly used as water reducers and retarders in concrete.

5) Synthetic detergents

Synthetic detergents consist usually of alkali metal salt of strong acid with an inorganic salt usually sodium sulfate. They are also referred to as alkyl aryl sulfonates which are complex left over from petroleum refining that are condensed using benzene. The product is usually neutralized to get the soluble salt. The surfactant is generally nonionic and anionic in nature, hence they are not widely used because of the unstable air void generation associated with nonionic admixtures.

6) Organic salts of sulfonated hydrocarbons

These class of surfactants are anionic and generally derived from by-products of refining petroleum, just like the salts of petroleum acids. The major difference is the material used to neutralize the substance. The neutralization is usually done using triethanolamine to produce agents of sulfonated hydrocarbons.

7) Fatty and resinous acids

Fatty and resinous acids are produced from the saponification of animal tallow which results in an insoluble calcium salt. The aqueous phase is saturated using calcium hydroxide which also results in the production of oils like vegetable oil and coconut oil. These surfactants can also be produced from tall oil which is a by-product of the paper industry. They are usually anionic surfactants. As stated earlier, a good admixture is able to generate a stable air void system however, admixtures derived from fatty acid are generally used in air entrainment because the calcium salts of this surfactants is insoluble [17].

Of all these admixtures, the most common air entraining agents in the United States available commercially are vinsol resin which is formulated from salts of wood resin. They are generally favored because they provide greater stability to the entrained air in concrete than other class of surfactants [32], and increase resistance to scaling from de-icing salts[33]. Some common commercially available AEA are formulated from Vinsol resin and ASTM C 226 [43] "Standard Specification for Air-Entraining Additions for Use in the Manufacture of Air- Entraining Hydraulic Cement" declared Vinsol resin acceptable for use in concrete to test resistance to rapid freeze and thaw actions.

It has been shown that vinsol resin admixtures generally produce concrete with better strength than synthetic air entraining admixture. In one of such studies by Ansari et al [44] to investigate the reduction in concrete strength using synthetic admixtures, they experimented with concrete mixtures containing synthetic and vinsol resin admixture and the strength gained was determined for 7, 14, 28 and 28 days. It was reported that the 14 days compressive strength of the specimen that contains synthetic admixture was about 30 % lower to the compressive strength of the

specimen that contains vinsol resin because vinsol resins produced smaller bubbles than the synthetic admixture. Additionally, petrographic analysis of the specimens also showed that vinsol resins produced smaller air bubbles in the concrete needed for frost resistance compared to synthetic admixture; this explains the low compressive strength associated with synthetic admixture due to the larger air bubbles.

Tanesi and Meininger [45] also showed in their study to evaluate the freeze thaw resistance of concrete with marginal air content that concrete mixture with 3.5% air content is adequate for freeze thaw performance, when vinsol resin based air entraining admixture was used compared to when synthetic admixture was used. The reason for this could not be explained Tanesi and Meininger [45] but it can be inferred from Ansari et al [44] who reported that Vinson resin based admixture produce smaller bubble size which is required for frost resistance when compared to synthetic admixture.

2.4 Measurement of Carbon Quantity

High unburned carbon in fly ashes generally make their use not beneficial to concrete. The AEA required to stabilize air bubbles in concrete are greatly influenced as high carbon content ashes require greater AEA to produce concrete that has adequate air content. Consequently, different test methods have been developed to characterize the un-burn carbon in fly ash. They are:

1) Loss on Ignition
2) Foam Index
3) Iodine Adsorption
4) Fluorescent method

2.4.1 Loss on Ignition

The loss of ignition method consists of intense heating a specimen of the fly ash and measuring the change in mass of the ash between oven drying and 750 ± 50 °C. This test is usually performed in accordance to 'Standard Test Methods for Sampling and Testing Fly Ash for Use in Portland Cement Concrete' ASTM C 311[46], which was modified from the LOI procedure for hydraulic cement described in ASTM C114[47]. ASTM C311[46] specified that 1g of the remaining ash specimen from the determination of the moisture content should be intensely heated to a constant mass over an uncovered porcelain at 1292 ± 122°F (750 ± 50°C). The standard specifies that the test should be performed with an initial heating period and at least 5 min for all subsequent periods. The LOI value of the specimen is the percentage change in mass of the specimen after heating.

Several researchers have observed that the LOI result could be unreliable because it overestimates the amount of organic carbon since the ignition mass loss is not due to burning of organic carbon alone. It measures other potential reactions such as oxidation of sulfur and iron minerals. Experimental results of 70 fly ash specimens showed that LOI test overestimates unburned carbon by at least 20% in 30 fly ash specimens [48] In a study conducted by Mohebbi et al [49], it was reported that using a thermo-gravimetric analysis in non-oxidizing atmosphere, followed by air revealed that burning carbon in high temperature does not only produce combustible carbon oxidation, but that other decomposition reactions also take place.

The individual mass change due to different reactions cannot be individually identified by the LOI test. However researchers have proposed a modification to the test so that a more reliable result can be achieved. One of such proposition was made by Harris et al [50]. They suggested that the ASTM C 311[46] test be modified so that

the mass loss is recorded after 60 minutes exposure to temperature range of 572 °F – 932 °F (300 °C – 500 °C). Its assumed that the organic carbon content of the ash can be estimated by measuring the mass loss which occurs between heating the specimen to 572°F (300°C) for 60 min and heating the specimen to 932 °F (500 °C) in 60 min. Due to the unreliability of LOI test, Thermo-gravimetric analysis techniques have been suggested to replace the LOI test in estimating the unburned carbon content in fly ash [48] [49].

2.4.2 Foam Index Test

The foam index test involves titrating a slurry of fly ash and water with a known concentration of AEA solution. The fly ash slurry is agitated with the AEA solution for a short time and left to rest. The foam index test is a useful method to estimate the absorption of AEA by carbon particles in fly ash. The foam index is the total volume of AEA added to the test specimen until stable foam is formed. It has a high level of subjectivity because it has not been standardized by organizations like ASTM. Therefore, no fully standardized procedure to perform the test exists. However, several foam index test procedures have been proposed and used by researchers [51] [52]. The procedures used by various researchers include a range of variables like mass of fly ash, cement in slurry, dimension of container and agitation time. The variation in the test result is mostly due to the agitation speed and the subjectivity of when stable slurry foam is formed.

It has been suggested that agitating the container with a mechanical shaker reduces the variance in result and ensures a consistent result. In a study conducted by Harris et al [51] to examine the subjectivity of the foam index test, they noted that performing the foam index test without a standardized shaking technique gives variable results. Harris et al [51] performed four tests with seven test specimen each.

Two tests were performed with mechanical shaker and the other two were performed manually. It was reported that the mechanical shaker produced a more consistent result and allowed the operator to perform concurrent test. It was also observed that it allows the operator to monitor the test and have adequate time to add AEA to the test specimen.

Several studies have been conducted to compare the fly ash carbon characterization tests. In a study conducted by Ahmed [52] to quantify the adsorption capacity of fly ash using 14 fly ash specimens, the results showed that LOI alone cannot be used to characterize adsorption capacity of fly ash. It was reported that the foam index test correlates well with the LOI test at higher LOI values and at lower LOI, inconsistent with the LOI results. Experimental results by Sutter et al [53] have shown that the relationship between LOI test and foam index test is reasonable but the inconsistency is high due to the subjective nature of the foam index test. This is also due to the fact that LOI measures the loss in mass and not the adsorption of AEA by carbon. When the total time of foam index test is consistent, it provides a better representation of the adsorption capacity than the LOI test [53].

2.4.3 Iodine Adsorption Test

The iodine adsorption test involves the determination of the adsorption capacity of fly ash using standard aqueous solution of iodine. This test is usually performed in accordance to “Standard Test Method for Carbon Black Iodine Adsorption Number” ASTM D1510 [54]. ASTM defines the iodine number as the mass of iodine adsorbed by 1 gram of carbon in an aqueous solution of 0.05N. The test involves a weighed specimen of carbon black mixed with standard iodine solution of 0.05N and the mixture shaken and filtered. The excess iodine is then titrated with standard sodium thiosulfate solution.

Sutter et al [53] have evaluated the testing procedures to determine the modification necessary for the foam index test. They evaluated the procedure based on characterization of coal fly ash, effect of carbon on air entrainment, characterization of strength activity and testing environment. They evaluated the testing protocols with fly ash specimens from 30 sources, 47 AEA types and 3 sources of portland cement. It was reported that there is need for improvements in test and specifications for fly ash used in concrete to better identify the property affecting the concrete performance. Due to the sulfur and lime content which interfere with the result obtained and low adsorption capacity of fly ash, researchers have developed a modified test procedure for determination of adsorption capacity of carbon in fly ash.

One such modification by Sutter et al [53] which is slightly different from the ASTM procedure, but based on the same principle of adsorbing iodine from solution and determining the amount absorbed. This method proposes that fly ash should be pre-treated with hydrochloric acid (HCl) to remove sulfates and lime prior to performing the iodine number determination. The procedure involves mixing 4 weighed specimens of fly ash with iodine solution and filtering ash iodine solution to separate the ash from the iodine solution. The resulting iodine is titrated with sodium thiosufate and hence the amount of iodine adsorbed by 1g of fly ash is determined for each fly ash specimen and an isotherm plot of the absorption generated. The fly ash iodine does not use AEA in its procedure, therefore it does not measure the absorption capacity of AEA by fly ash but it an accurate test to specify fly ash based on the adsorption capacity.

The work of Sutter et al [53] has led to the development of ASTM WK47573 [55] "New Test Method-Standard Method of Test for Determination of Iodine Number of Coal Fly Ash". This latest standard procedure is similar to ASTM D1510 [54] but

the iodine solution concentration to be used is 0.025N and the fly ash is to be pre-treated with HCl to remove sulfates and lime that might be present in the ash specimen. This particular research study showed that the iodine adsorption test gives an accurate measurement of adsorption capacity of fly ash when compared to the foam index and LOI test. Both tests are only suitable as an indicator rather than as a measurement of adsorption capacity of fly ash, in that they provide a good indication of the adsorption capacity but cannot be used for quantification of the adsorption capacity of fly ash.

In an extensive study by Ahmed [52] comparing results of currently used adsorption capacity tests and new developed method called direct adsorption isotherms, it was reported that LOI only correlated to adsorption capacity of fly ash at high LOI values and does not provide a good correlation at low LOI values. In this study, isotherm tests were developed to characterize the adsorption processes on several cements and fly ash specimens. The adsorption isotherms consist of individual Erlenmeyer flasks which contain various masses of fly ash and various concentrations of AEA, kept at equilibrium at constant temperature. It should be noted that the iodine adsorption test utilizes iodine for measurement while the direct isotherm tests utilizes AEA for measurement which enables users to determine the quantity of AEA adsorbed by fly ash in a concrete mixture. It was reported that the foam index results showed a clear trend with fly ash iodine number and correlated to the capacity measured using the direct adsorption isotherms. Similarly to Sutter et al [53], Ahmed [52] concluded that the foam index and LOI test provide a good indicator of adsorption capacity of fly ash while the iodine adsorption test is a suitable tool to quantify adsorption capacity of fly ash and its suitability for use in concrete work.

2.5 Carbon Mitigating Techniques for Fly ash

The presence of excessive unburned carbon in ashes is a serious issue in predicting the quantity of AEA to produce adequate air content required for freeze-thaw durable concrete. Consequently, there is need to able to remove carbon from ashes or render incapable in adsorbing AEA in concrete. Different techniques have been developed to reduce the high carbon in fly ash before use in concrete. The nature of these treatment processes range from chemical treatment to mechanical treatment. These treatment methods include thermal treatment (carbon burnout), chemical treatment ("carbon blocker"), supercritical carbon water oxidation, ozone treatment and electrostatic carbon removal.

2.5.1 Carbon Burn-out

Of all the treatment processes for fly ash, carbon burn-out (CBO) is one of the most common forms of carbon removal. This treatment method has been implemented and in use commercially for years without having effect on the pozzolanic properties of the fly ash produced. Studies by Fox [56] to determine the effect of thermal beneficiation of high carbon fly ash, using four fly ash specimens from different sources have shown that there is no significant reduction in the pozzolanic activity of fly in concrete. These specimens were heated from 932 °F – 1200 °F (500 °C to 1200 °C) and it was reported that the effect of higher temperature carbon burn out on the pozzolanic properties should depend on the lime content and the maximum temperature. This suggests that a reduction in pozzolanic activity of high lime fly ash is possible.

A typical commercial CBO system consists of a fluid combustor, heat exchanger, turbine generator and cyclone, silos and a control room as shown in Figure

2.7 below. The carbon burn out process combust the carbon in fly ash and produces a low carbon fly ash. During this continuous process, heat is recovered and sent back the power plant. The rate at which the ash is transferred to the fluid bed is auto-regulated at every point in time and it is determined by the temperature profile of the fluid bed. The process to separate carbon from fly ash begins at the fluid combustor which is a bubbling fluid bed, operates at temperature of approximately 1000 °F (538 °C).

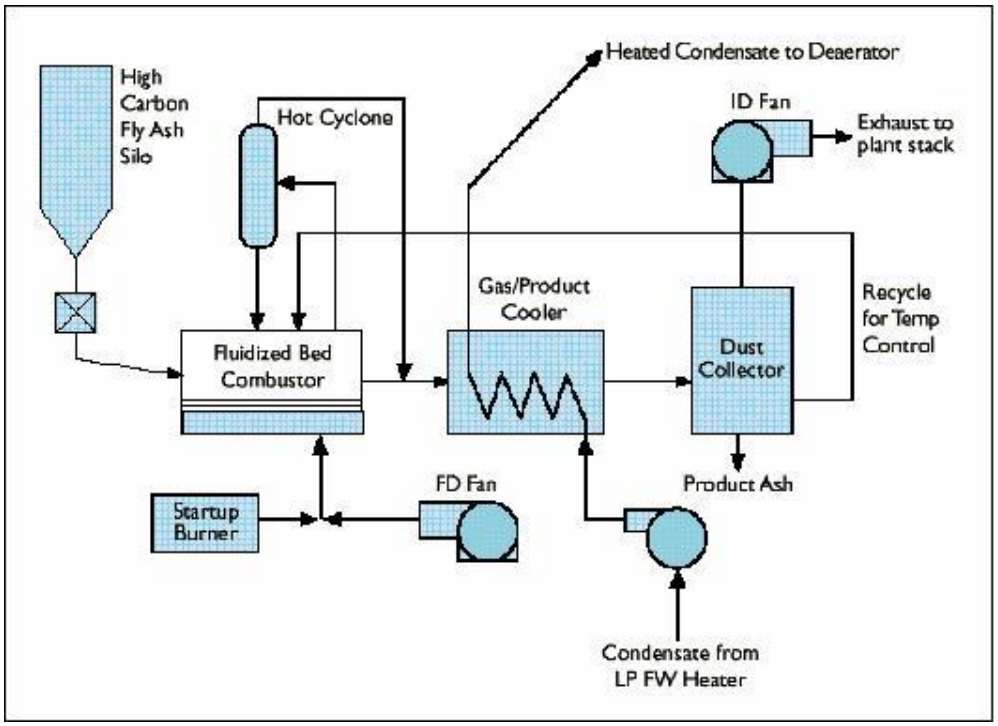

Figure 2.7: Typical CBO Process [57]

The high carbon fly ash is fed through the combustor and low carbon fly ash exits the combustor. This fluid bed combustor continues in steady state without outside assistance and the start-up process is fuelled by bunker A oil, as soon as the carbon begins to ignite the start-up burner system shuts off allowing the system to be fuelled by the residual carbon. The CBO system includes an induced draft (ID) fan and forced draft (FD) fan. The ID fan extracts air from the combustor while the FD

fan forces air to the combustor, controlled in such a way that the system operates under a negative pressure. The product ash and flue gas is transported through the system by motive power created by these fans. Typically the fly ash exits the FBC at approximately 1350 °F and the ash and the flue gas are separated by the cyclone and bag house installed in the plant. The major advantage of a CBO system is that there is no problem of waste disposal since there is no solid and liquid waste. Carbon-dioxide which is a major environmental problem is also not created during this process; this makes treating fly ash for use in concrete a benefit since for every ton of fly ash use as a replacement of cement in concrete 0.8 tons of CO^2 is not created. [58]

The labor cost of a CBO system is considerably low because majority of the operation is controlled from a control station which allows two people per shift to control plant operation. However, the high cost of construction, implementation and energy cost of maintaining a commercial CBO system is high. This is the major drawback of a CBO system which makes this treatment process less appealing to use.

The Wateree station of South Carolina Electric and Gas is the first full scale commercial application of CBO which started operation in 1999 [59]. It is a two-unit 772 MW plant located southeast of Columbia South Carolina with a capacity to process about 180000 tons (163293253 kg) per year of fly ash. Wateree station has consistently showed the efficiency to produce fly ash of 2.5 % LOI from a range of feedstock [59]. Several commercial CBO systems like Winyah station of Santee Cooper which began operation in 2002 with a capacity to produce 170000 tons (154221 metric tons) of fly ash per year, Brayton Point and Chesapeake both of Dominion, South Carolina have been implemented.

2.5.2 Chemical Treatment (i.e. Carbon Blocker)

The absorptive properties of the un-burned carbon in fly ash can be made inactive by treating the fly ash with chemical reagents. Unlike the CBO system, the chemical treatment method does not necessarily remove the unburned carbon but it renders it not further adsorptive of AEA. Carbon blocker is the most common chemical treatment use for fly ash in the United States. This chemical makes most fly ash suitable to achieved desired amount of air entrainment in production of concrete. This treatment method to treat higher carbon content fly ash was developed by the partnership between Fly Ash Direct (a Cincinnati based waste management company) and BASF chemical company. The treatment binds the carbon molecules in fly ash thereby subsiding the absorptive nature of the carbon and rendering the fly ash on-spec for concrete use.

The treatment process begins with a small specimen of fly ash tested for LOI or adsorptive characteristics in other to determining the dosage of the carbon blocker to be used. The fly ash is transported through pneumatic pipelines to a venturi. The chemical is then added to the fly ash based on the pre-determined dosage required. Due to the low pressure in the venture, the chemical is atomized and mixes with the fly ash in a uniform manner. The treated fly ash is then transported to the other installed pipelines and recovered in a bag.

Because of the ease of use and simplicity of this treatment process, it is easy to implement commercially and in large scale. The large scale process is in form of a permanent unit installed at the power plant. Unlike the CBO treatment process, the carbon blocker unit requires less than 3 months to design and build. It can be easily installed and operated at power plants with only minor modification to the current fly ash unloading systems and little disruption to current operations. Another advantage

the carbon blocker has over other carbon mitigation technique is that, it's cost effective to implement. Various power plants in the United States like Avon Lake Generating Station (Avon Lake, Ohio), Joppa Generating Station (Joppa, Ill.), Fayette Power Project (La Grange, TX) and Oklaunion Generating Station (Vernon, TX) have taken advantage of this technology to treat fly ash for commercial use.

Studies have been conducted to determine the effectiveness of carbon blocker in controlling the adverse effect of carbon. One of such studies was conducted by Miller et al. [60], the study was designed to determine if concrete made with fly ash treated with carbon blocker will have stable air entrainment while meeting standard specifications. The concrete specimens were tested for air content, compressive strength, rapid freeze tests and petrographic analysis. It was reported that the treated ash exhibited higher level of air entrainment than untreated specimens. It was concluded that the treatment effectively controlled the adsorption of AEA by carbon, does not have any adverse effect on the strength of the concrete and does not affect the air bubble size and spacing.

Notable chemical treatment of fly ash that has been used in the past involves treating of fly ash with calcium polysulfide. Calcium polysulfide is an alkaline aqueous solution produced by boiling lime (CaO) in water in the presence of sulfur. The aqueous solution is produced to force the ionic charge of metal elements to a positive state with sulfur atom in a negative state. The material produced is not limited by the loss on Ignition requirement in various specification standards. [61]

2.5.3 Electrostatic Carbon Removal

This treatment process is based on the use of electric field to separate carbon from fly ash. The electrostatic carbon removal machine consists mainly of two electrodes, ash stream, carbon stream belts and rollers which are the only moving

parts of the machine as shown in Figure 2.8 below. The electrodes could be parallel or louvered, which are similar in construction but with major difference in the separation zone. For the louvered separator, the plates are louvered compared to parallel in the parallel plate separator.

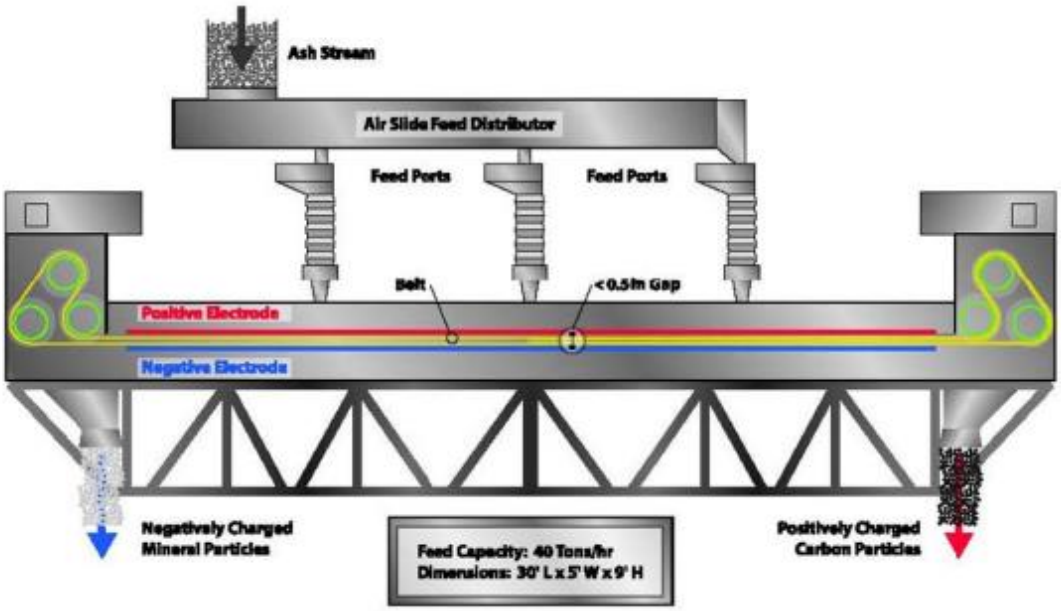

Figure 2.8a: Schematic of Separation Technologies Separator [62]

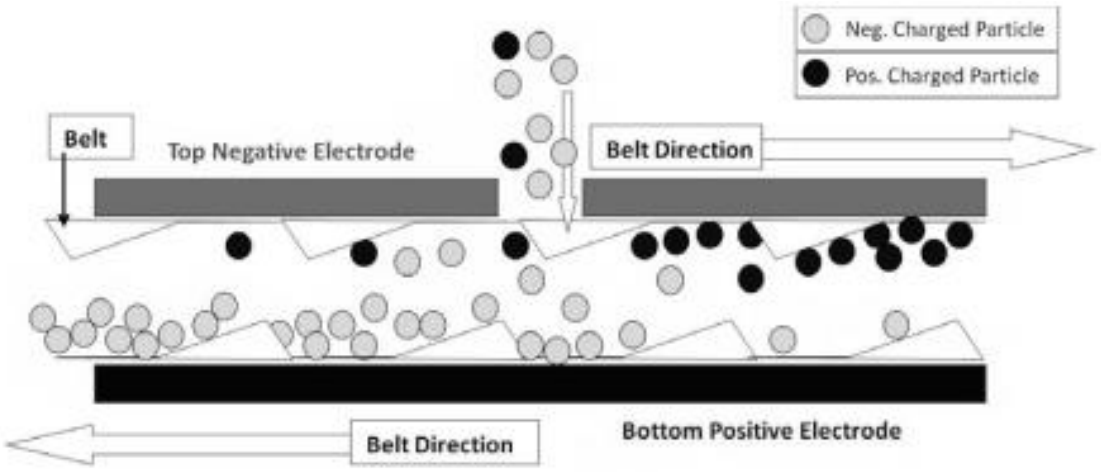

Figure 2.8b: Details of Separation Zone [62]

Unburned carbon and ash have different chemical and physical properties. This difference allows their particles to be electrically charged to opposite polarity.

The process to separate the carbon from the ash begins by feeding the ash into the thin gap between the electrodes, the particles are charged up by the electric field which is created applying direct current to the parallel plate electrodes. As the carbon is positively charged up, it is attracted towards the negative electrodes while the negatively charged minerals are attracted towards the positive electrode. The belts move each particle adjacent to each electrode towards opposite end of the separator. The plates then direct the separated particles into either ash stream or carbon stream. The low carbon content fly ash is then collected and used for concrete works while the recovered carbon can be used as fuel. The process is entirely dry and requires no additional material other than the fly ash and no waste is produced. The general features of an electrostatic carbon separator include the belt speed, thin space between electrodes and high voltage.

Various electrostatic separator systems have been developed and the efficiency of such system evaluated. Research by Stencel et al. [63] developed a working bench scale that uses pneumatic transport-based system. The operation of the system consists of feeding twenty-five fly ash specimens of high LOI fly ash to the tribo charging unit using a vibratory feeder, the particle then flows out from the separation chamber in streams. It was reported that fourteen of the ash specimens had 50 % recovery rate with less than 3 % LOI. A model produced by Stencel et al [63] was estimated to require a processing energy of less than four-KW-hour/ton for a 20 ton/hr (18.14 metric ton/hr) system. The total cost which includes electricity and direct labor was estimated to be $3/ton ($3.3/metric ton) for a 20 ton/hr (18.14 metric ton/hr) system.

The commercial application of electrostatic carbon separation has been developed in the United State by Separation Technologies Inc (ST). ST began

operation of the first commercial electrostatic based fly ash processing plant in 1999 at Brayton Point Station, Massachusetts [56]. Due to the successful development of the electrostatic carbon separation at Brayton station, several commercial electrostatic system has been installed by ST. Currently, some of the operating systems are Progress Energy Roxboro station in North Carolina, Constellation Brandon shores station in Maryland, WPS Power development Sunbury station in Pennsylvania, Jacksonville Electric Authority in Florida and South Mississippi Electric Morrow station in Mississippi [64].

2.5.4 Supercritical Water Oxidation

Supercritical water is a fluid which has temperature and pressure above the vapor-liquid critical point. At this critical point, the properties such as liquid and gas like behavior vary with change in temperature and pressure, and the liquid and gas phases cannot be distinguished. Water under supercritical conditions is non-polar, the normal water with dielectric constant of 78.5 changes to non-polar liquid with a much lower dielectric constant below 5 [65]. Supercritical water possess a low density which depends on some conditions, this low density and other properties allows it to mix with organic molecules and gases.

Supercritical water oxidation separation of carbon from fly ash is based on the principle that under supercritical conditions, organic compounds that contain carbon are oxidized and carbon dioxide is produced in the process. Supercritical water separation is a technique that uses the high temperature and pressure that exceeds the critical point of water properties to destroy the organic compounds and toxic pollutants [65]. The properties of water above the critical point such as ionic product, viscosity, conductance, diffusivity and solvent ability are different from water at

ambient temperature and these unique properties makes the oxidation of carbon possible.

A typical supercritical water oxidation bench scale consists of 3 inlets where water, fly ash and oxygen are pumped and compressed to a pressure of between 0.0038 – 0.0044 psi (26 – 30 MPa) into the system separately [66]. The reactants are mixed and preheated before transporting them to the reactors where oxidation takes place. After oxidation has taken place, the solid specimen is cooled and water-gas separation takes place.

The efficiency of this method in the removal of organic compounds has been demonstrated in various studies. In the study by Thompson et al. [65] to determine the efficiency of supercritical oxidation to remove unburned carbon in fly ash, using 7 fly ash specimens with a bench scale system, it was reported that ashes with LOI greater than 20 % had the best removal efficiency. Out of the seven specimens investigated, the process reduced the LOI to less than 5 % in six of the specimens. It was suggested that the removal efficiency depends on how reactive the ash type is and the nature of the residual carbon which is related to the petrography of the coal.

Supercritical water oxidation has been shown to be effective in removing a considerable amount of unburned carbon in fly ash. However the major drawback in the use of this method is the production of carbon dioxide during this process. With increase in environmental protection laws and concerns for greenhouse effect, release of carbon dioxide into the atmosphere is not beneficial.

2.5.5 Ozone Treatment

Ozone treatment is a method by which ozone is directly applied to fly ash at room temperature which reduces the absorptive properties of the carbon. This process

reduces the foam index of the treated ash. Hurt et al [67] have developed an inexpensive and practical ozone treatment process which is reported to deactivate and reduce the surfactant absorptivity of carbon without negatively changing the properties of the fly ash specimen.

The apparatus includes an ozonator and a chamber where the fly ash is poured. The ozonator generates an ozone containing gas which is passed through a conduit into the chamber. Forcing the ozone through the bed of fly ash in the chamber has greater effect than simply blowing the ozone over the fly ash. This operation can be performed at ambient temperature however it's not unusual to also perform it at 150 °C which is the average handling and storage temperature of fly ash [67]. The effect of the ozone on the surfactant absorptivity depends greatly on the concentration of the ozone.

Ozone treatment is advantageous in that, it is simple to apply, it produces no high carbon waste product [62] and it is less expensive when compared to other physical methods available to mitigate the effect of carbon on fly ash. The major cost to operate an ozone treatment is associated with the electricity requirement. Gao et al [68] estimated the cost of electricity based on vendor data to be 7 kW-hr/lb (55.6 KJ/g), with electricity cost of 1 - 2 cents, the cost of electricity to operate ozone treatment is about 0.3 - 1.2 $/ton ash (0.33 – 1.3 $/metric ton ash). However, its major drawbacks are toxicity of ozone which is very harmful to humans, hence care needs to be taken during the process and since ozone treatment does not necessary decrease the unburned carbon in fly ash other treatment processes are preferred.

Chapter 3: Experimental Materials and Methodology

3.1 Materials

3.1.1 Cementitious Materials

The cementitious material used for concrete production was Type I portland cement and fly ash. A total of three fly ash sources were used for this research to evaluate the effect of the carbon content in the adsorption capacity and benefit of chemically treating high LOI fly ashes. The three fly ash sources used for this study were three coal power plant stations in North Carolina. Ashes from each of these facilities were unmarketable due to having carbon contents in excess of specified limits. A portion of the fly ash recovered from each source was chemically treated to evaluate the effect of the treatment process on the high LOI fly ash. Additionally, one fly ash specimen meeting the specified LOI limits and other standards (currently marketed to concrete manufacturers) was also obtained and used as a control.

In total, seven fly ashes specimens were used in this study. These ashes represent the on-spec, off-spec treated and off-spec untreated ash sets. The mixture designates that contained treated fly ash were denoted with ‘T’ preceded by the first letter of the fly ash plant name while the mixture that contained untreated fly ash were denoted with ‘U’ preceded by first letter of the fly ash plant name . The control ash which contained low LOI and deemed suitable for use in concrete without chemically treating it is denoted by ‘BC’. Table 3.1 relates the fly ash source with the codes used throughout this report.

Table 3.1: Fly ash specimen codes

Fly Ash Specimen	**Codes**
Plant B (Control ash)	BC
Plant B (Untreated)	BU
Plant B (Treated)	BT
Plant A (Treated)	AT
Plant A (Untreated)	AU
Plant M (Treated)	MT
Plant M (Untreated)	MU

3.1.2 Admixtures

The air entraining admixture used for this research was Master Air AE200 from BASF which meets the requirements of 'Standard Specification for Air Entraining Additions for Use in the Manufacture of Air Entraining Hydraulic Cement' ASTM C226 [43]. The data sheet for this product is included in Appendix A, Figure A1

3.1.3 Aggregates

The aggregates used for the concrete mixtures were sand as fine aggregates and gravel as coarse aggregates. Crushed granitic gneiss stone gravel No 67 was used as coarse aggregate with maximum particle size of 1 inch. Both the fine and coarse aggregates meet the specification of ASTM C33 [69] "Standard Specification for Concrete Aggregates" and are commonly used in NCDOT paving operations. The coarse aggregate used in this study came from a quarry in the Piedmont region of North Carolina near the city of Cary. The fine aggregate used for this research is natural silica sand which also came from the Piedmont region of North Carolina, specifically from a pit in Lemon Springs, North Carolina. The result of the sieve analysis for coarse aggregate is given in Appendix A, Table A1

The density of the coarse aggregate (dry rodded unit weight) was 96.5 lb/ft^3 (1 545.78 kg/m^3), the relative density (specific gravity) was 2.62 with an absorption capacity of 0.8 %. For the fine aggregates, the fineness modulus of the sieve analysis was 2.72; the result of the sieve analysis for fine aggregate is provided in Appendix A, Table A2. The density (dry rodded unit weight) of the fine aggregate was 97.2 lb/ft^3 (1556.99 kg/m^3, the relative density (specific gravity) was 2.44 with an absorption capacity of 0.18 %.

3.1.4 Mix Design

The concrete mix design used in this research project is concrete pavement mixtures which are typically used for concrete pavement in North Carolina. The typical mixture has a water cementitious material (w/cm) ratio of 0.48. The mix design used for concrete production is presented in Table 3.2 below. The experimental program consisted of producing three mixtures per fly ash specimen where the quantity of AEA was varied to achieve a low air content of between 0 to 4%, target air content of between 5 to 7% and a high air content of greater than 7%. The slump was expected to vary for each mixture since air content is known to strongly affect workability. Each mixture was produced in 2.7 ft^3 (0.077 m^3) batches. The labelling of each mixture followed a sequential order according to when they were made.

Table 3.2: Mix proportions

Material	Quantity (lbs)	Quantity (kg)	Quantity (lb/cy)
Coarse aggregate	179.8	81.6	1798
Fine aggregate	109.4	49.6	1094
Cement	46.0	20.9	460
Fly ash	13.7	6.2	1370
Water	29.1	13.2	291

The test methods used to characterize the ash and concrete materials are shown in Tables 3.2-3.4.

Table 3.2: Fly ash characterization tests

Characteristic	**Test Method**	**Numbers of replicates per Ash**
Foam index	Procedure proposed by Harris [51] and Ahmed [52]	3
Iodine adsorption	ASTM WK47573 [55]	3
Loss on ignition	ASTM C 311[46]	3

Table 3.3: Fresh concrete tests

Characteristic	**Test Method**	**Replicates per Mixture**
Slump	ASTM C143 [71]	1
Air content, SAM Number	Ley et al. [24]	2

Table 3.4: Hardened concrete tests

Characteristic	**Test Method**	**Replicates per Mixture**	**Specimen Type**	**Testing Interval**
Compressive strength	ASTM C39 [73]	3	4 in x 8 in (100 mm x 200 mm) cylinder	7, 28, 56 and 90 days
Surface resistivity	AASTHO TP95 [72]	3	4 in x 8 in (100 mm x 200 mm) cylinder	7, 28, 56 and 90 days
Modulus of elasticity	ASTM C469 [75]	3	6 in x 12 in (150 mm x 300 mm) cylinder	28 days
Freeze thaw	ASTM C666 [76]	3	4 in by 4 in x 12 in long (100 mm x 100 mm x 300 mm long) prism	14 days
Air void analysis	ASTM C457 [18]	3	concrete specimens cast in take-out food boxes	14 days

Concrete samples were prepared with constituent materials and mixing proportions that are typical of pavement mixtures used by the North Carolina Department of Transportation (NCDOT). The materials are described below, with additional details

3.2 Fly Ash Characterizations Tests

A series of tests was conducted on all the seven fly ash specimens (including the treated and untreated versions of the ashes) to estimate the required amount of AEA required to achieve a target air content and to also determine if chemically treating high LOI fly ash affects the ability to reliably achieve entrained air targets. The impact of the carbon content on air entrainment was measured with multiple standardized procedures. These tests include foam Index test, iodine adsorption test performed using procedures in 'New Test Method for Determination of Iodine Number of Coal Fly Ash." ASTM WK47573 [55] and loss on ignition test performed using procedures in "Standard Test Methods for Sampling and Testing Fly Ash or Natural Pozzolans for Use in Portland-Cement Concrete." ASTM C 311[46].

3.2.1 Foam Index Test

The foam index test is used to provide a prediction of the degree of adsorption of AEA by unburned carbon in fly ash. This test provides an estimate of AEA required to overcome the adsorptive action of fly ash by dropwise addition of AEA until a slurry solution is formed. The foam index test was performed using procedure proposed by Harris [51] and Ahmed [52]. Specimens were prepared from 0.07 oz. (2 g) of fly ash and 0.28 oz. (8 g) of cement to make a total of 0.35 oz. (10 g) cementitious material. A 3.38 fl. oz. (100ml) Master Air AE200 AEA was placed in an 8.45 fl. oz. (250 ml) Erlenmeyer flask and 30 fl. oz. (900 ml) of distilled water was added to make 33.8fl. oz. (1000 ml) AEA solution. The cementitious material was then placed in a cylindrical glass container and 1.69 fl. oz. (50 ml) of distilled water was then added. Next the container was sealed and agitated by hand in a vertical motion in approximate rate of 40 – 50 cycles in 15 seconds. After agitating, a 0.0012 in^3 (0.02

ml) single drop of AEA solution containing the 3.38 fl. oz. (100 ml) of AEA and 30 fl. oz. (900 ml) of distilled water was added using a digital pipette, and the container was sealed and then agitated at the same rate as before.

After 15 seconds of agitation, the container was opened and allowed to rest undisturbed for a period of 45 seconds, to allow the foam to reach a stable state. Next, the liquid-air interface was examined to see if there was formation of foam covering 100 % of the liquid-air interface. Figure 3.1a shows an incomplete foam coverage of the liquid-air interface, additional drops of AEA was added and the container agitated until there is a stable formation of foam at the liquid-air interface; at this point the end point was reached as shown in Figure 3.1b below. When the foam covered 100 % of the liquid interface, the test was terminated, and the end point reading was taken. A blank determination was also performed according to the above procedure using 0.022 lb (10 g) of cement with no fly ash to determine the relative foam index of the fly ash.

Figure 3.1a: Incomplete foam coverage

Figure 3.1b: Foam index test end point (100% Foam Coverage)

3.2.2 Iodine Adsorption Test

The iodine adsorption test is used to obtain the quantitative value of the adsorption of fly ash. Results of this test provide an expression of the adsorption capacity of carbon in fly ash based on the mass of iodine adsorbed per gram of carbon. The iodine adsorption test was performed for all the specimens in accordance with 'New Test Method - Standard Method of Test for Determination of Iodine Number of Coal Fly Ash.' ASTM WK47573 [55]. Pre-mixed 0.025N sodium thiosulfate and 0.025N iodine solution were acquired from Lab Chem and Ricca Chemical Company respectively and used for this test. A blank iodine determination was first performed by titrating 25ml of standard iodine solution with standard sodium thiosulfate solution to determine the volume of sodium thiosulfate required to neutralize 25 ml of iodine solution. After the blank determination, the fly ash specimen was pre-treated with 5 % wt HCL to remove sulphur which might interfere with the test results. A 0.66 lb (300 g) of the fly ash specimen and 2.65 lb (1200 g) of HCL was weighed out and placed inside a wide mouth metallic container. The mixture was then placed on a hot plate

and heated to boiling for 5 minutes. After boiling, the hot mixture was left to cool to ambient temperature. Next the cooled mixture was filtered with 0.30 ft (90 mm) Whatman grade 2V 8 μm filter paper and the filtrate was dried at 230 °F (110 °C) in an oven for 24 hrs to a constant weight. Once the specimen was dried, it was pulverized with a mortar and pestle then sieved with sieve No 200 until 0.088 lb (40 g) of the specimen was collected.

The 0.088 lb (40 g) pre-treated ash specimen was placed in an 8.45 fl.oz. (250 ml) Erlenmeyer Flask containing 3.38 fl. oz. (100 ml) of 0.025N iodine solution and was sealed with paraffin to minimize iodine volatilization. A magnetic stirrer bar was added to the flask and the solution was stirred on a stirring plate for 5 minutes. After stirring, the mixture was filtered using a grade 2V 8 μm filter paper until 0.85 fl. oz. (25 ml) of the solution was collected. Using a pipette, the 0.85 fl. oz. (25 ml) solution was placed in an 8.45 fl.oz. (250 ml) Erlenmeyer flask and a digital burette with 0.02 ml increment was filled with 0.025N standard sodium thiosulfate solution which was used to titrate the 0.85 fl. oz. (25 ml) solution. The titration process continued until the color of the mixture turned pale yellow as shown in Figure 3.2a, after which four drops of 1 % starch solution were added to serve as an indicator during the titration process as shown in Figure 3.2b. The titration continued until a colorless solution was obtained as showed in Figure 3.2c.

Figure 3.2a: Pale yellow solution after addition of 0.025N sodium thiosulfate solution

Figure 3.2b: Black solution after addition of 1% starch solution as indicator

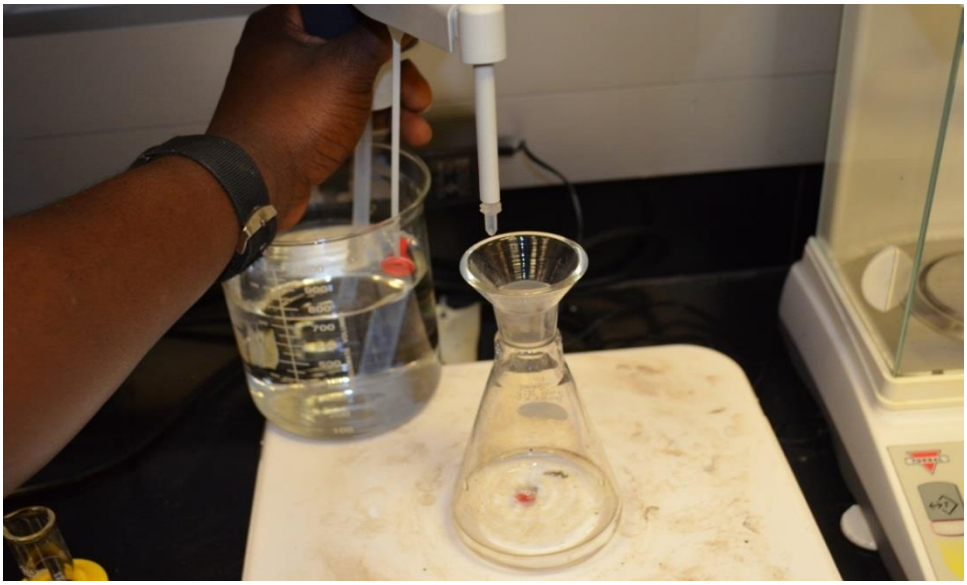

Figure 3.2c: Colorless Solution (End of Test)

The final volume of 0.025N sodium solution used was recorded and the iodine adsorption number was calculated using Equation 1.

$$I=\frac{B-S}{B} \times \left(\frac{V}{M}\right) \times N \times 126.9 \qquad (Eq.\ 1)$$

Where:

I = Fly ash iodine number (g I / kg coal fly ash)

100 = volume of standard iodine solution equilibrated (mL)

126.9 = Equivalent mass of iodine (meq / mL)

B = Volume of standard sodium thiosulfate solution

S = Volume of standard sodium thiosulfate required for titration

N = normality of the iodine solution meq/cm^3

M = Weight of fly ash specimen

3.2.3 Loss on Ignition test

The loss on ignition (LOI) test was performed in accordance to ‘Standard Test Methods for Sampling and Testing Fly Ash or Natural Pozzolans for Use in Portland

Cement Concrete' ASTM C 311[46] and the recommendations made by Harris [52]. A 0.071 oz (2 g) specimen of fly ash was weighed in porcelain crucibles and placed in an oven at 230 °F (110 °C) for 4hrs. After drying, the specimen was placed in the desiccator to cool for 30 minutes. 0.035 oz (1 g) of the oven-dried specimen was weighed in a porcelain crucible and placed in a muffle furnace heated to 1382 °F (750 °C) as showed in Figure 3.3a. The specimen was ignited at 1382 °F (750 °C) for 30 mins, cooled in a desiccator as showed in Figure 3.3b for 30 mins and then weighed. The loss on ignition was calculated using equation 2.

$$\text{LOI} = \frac{\text{Initial weight-Final Weight}}{\text{Initial weight}} \times 100 \qquad \text{(Eq. 2)}$$

Figure 3.3a: Specimens of fly ash heating in muffle furnace

Figure 3.3b: Specimens of fly ash cooling in desiccator

3.3 Concrete Production

A total set of twenty-one concrete mixtures were made to analyze the effects of high LOI fly ashes adsorption capacity on the air content and to demonstrate the ability to entrain air in high LOI fly ashes that are chemically treated. The production of the concrete mixtures was performed in accordance to 'Standard Practice for Making and Curing Concrete Test Specimens in the Laboratory' ASTM C192 [70]. Several days before mixing, the required quantity of coarse aggregates were taken from the stockpile and put in a rectangular wooden tray, placed under a fan to allow all the materials come to room temperature while the fine aggregates were oven dried for 24 hours to remove moisture. The inside surface of a 4 ft^3 (0.113 m^3) capacity mixer was dampened with small quantity of water before mixing to lubricate the mixer. The coarse aggregates were added to the mixing drum followed by addition of the fine aggregates. The quantity of water needed for the mixture was divided into two equal parts with one part containing the desired dosage of AEA. The portion

containing AEA was then added to mixture in the moving drum to be agitated by the aggregate.

The next step was the addition of the cementitious materials (both cement and fly ash) and the remaining mix water. The drum was covered to allow the cementitious materials to fully mix with the aggregates in order to avoid spillage and once all the materials had been added to the drum the timer was started. The mixture was mixed for a period of 3 minutes, allowed to rest for 3 minutes and finally mixed for 2 more minutes. After mixing a series of tests were performed on the fresh concrete immediately after production. These tests include slump test, determination of air content, temperature and unit weight.

3.3.1 Fresh Concrete Tests

This section contains results from fresh concrete properties such as slump test and air content. The slump and air content were measured as part of correlation to the durability tests of the mixtures.

3.3.1.1 Slump Test

The slump test was performed for each of the concrete batches in accordance with the procedure outlined in 'Standard Test Method for Slump of Hydraulic Cement Concrete' ASTM C143 [71]. First, the slump mold and the tamping rod were damped with water and the mold placed on a flat rigid metal surface, held firmly without movement as showed in Figure 3.4a. Fresh concrete from the mixer drum was placed in the slump mold using a scoop. The concrete was placed in 3 layers with each layer rodded 25 times uniformly across the cross-section. The last layer was heaped with excess concrete just above the mold, rodded and the top was struck off with the tempering rod by rolling the rod on the surface of the concrete. Once the surface was struck off, the base of the mold was cleared to prevent interference with the slumping

concrete. The mold was then removed by raising it in a vertical motion with no lateral or twisting motion and then placed just beside the slump as showed in Figure 3.4b, with the tempering rod placed on the mold. The vertical difference between the top of the mold and the displaced original center of the top surface of the specimen was recorded as the slump.

Figure 3.4a: Slump mold held firmly to prevent vibration

Figure 3.4b: Measurement of slump

3.3.1.2 Air Content Test (Super Air Meter)

The air content of the concrete was determined using the Super Air Meter (SAM). The SAM procedure is a modified ASTM C231 [22] 'Standard Test Method for Air Content of Freshly Mix Concrete by Pressure Method' type B meter. After completing the conventional testing the meter is moved into second mode of operation that measures the deformation of the concrete under higher pressures. The internal surface of the SAM was first dampened with water before beginning the test. Fresh concrete was scooped into the SAM apparatus in three layers with each layer consolidated twenty-five times with a rod. The final layer was levelled with the inside of the bowl and the rim of the bowl was cleaned properly as shown in Figure 3.5a to allow the top cover to seal the bowl properly. The top of the device was then attached to the bowl by clamping opposite arms at the same time. One of the petcocks was opened and filled with water as shown in Figure 3.5b until water started flowing out through the second petcock, at this point the petcocks were closed one after the other; this was done to remove trapped air at the bottom of the device.

Figure 3.5a: Fresh concrete in SAM bowl with rim cleaned properly

Figure 3.5b: SAM test in progress

Once the petcocks had been closed, the gauge on the device was turned on and setup to run the SAM test. First, the fresh concrete was pressurized by applying 14.5 psi (0.10 N/mm^2) as prompted by the device, next the lever was held down for 10 seconds and the bowl was hit once by a mallet. The total air content is provided after this first pressure step and this process was repeated for 30 psi (0.20 N/mm^2) and 45 psi (0.31 N/mm^2) respectively. At this point the gauge displayed the air content of the fresh concrete. The pressure from the top and bottom of the chambers was released by opening the petcocks and the valves. Once this was done, the test was performed again using the same concrete specimen without removing the top cover, the petcocks were filled with water and the test was repeated for pressures of 14.5 psi (0.10 N/mm^2), 30 psi (0.20 N/mm^2) and 45 psi (0.31 N/mm^2). After this has been done, the device displays the SAM number and the air content of the concrete.

3.4 Preparation and Curing of Test Specimens

Concrete specimens were cast in accordance to the procedure outlined in ‘Standard Practice for Making and Curing Concrete Test Specimens in the

Laboratory.' ASTM C192 [70]. For the surface resistivity and compressive strength test, 4 in (100 mm) diameter by 8 in (200 mm) deep cylinders was made. For each batch, nine cylinders were made in order to provide three cylinders for testing at each of 7, 28, 56 and 90 days. The concrete specimens were removed from their molds after 24 hours, labelled and wet cured in a moist curing room as showed in Figure 3.6 for compressive strength test at their respective age. The curing room has water sprinklers attached to the walls which sprinkle water on the specimens throughout the designated curing period. The atmospheric conditions in the room is maintain such that the specimens in storage are moist at all times. Adequate water spray and distribution was maintained at all times.

Figure 3.6: Concrete specimens in curing room

Three 6 in x12 in (150 mm x 300 mm) cylinders were also made and cured for 28 days in the curing room for the determination of modulus of elasticity and compressive strength test. To determine the durability of the concrete specimens, three 4 in x 4 in x12 in (100 mm x 100 mm x 300 mm) long beams were made and cured for 14 days for freeze thaw testing as well as three rectangular prisms for air

void analysis. The rectangular prisms are 3 in x 3 in (76 mm x 76 mm) at the base, 4 in x 4½ in (100 mm x 100 mm) at the top and with a height of 4½ in (100 mm).

3.5 Hardened Concrete Tests Procedures

This section includes details regarding testing of hardened concrete included surface resistivity test, modulus of elasticity determination, compressive strength test, rapid freeze thaw test and air void analysis.

3.5.1 Surface Resistivity Test

The surface resistivity test was performed in accordance to 'Standard Method of Test for Surface Resistivity Indication of Concrete's Ability to Resist Chloride Ion Penetration.' AASHTO TP95 [72]. The surface resistivity specimens were the same 4 in x 8 in (100 mm x 200 mm) cylinders used for the compressive strength. The test was performed prior to compressive strength testing to ensure the surface had not been damaged. The test was performed on all the cylinder specimens used for compressive strength testing. Three cylinders were tested after 7, 28, 56 and 90 days of curing. The test was performed with a four-point Wenner probe; this instrument consists of four equally spaced co-linear electrodes. First the concrete specimen was placed on two supports as shown in Figure 3.7a and the surface of the specimen was dampened with wet towel before each reading, to ensure consistent an accurate measurement. After dampening, the specimen was examined for air voids along the line of placement of the probes and the probes were set to avoid these types of surface imperfections. The probe was then placed in contact with the concrete cylinder specimen as shown in Figure 3.7b. The device applied an alternating current to the outermost electrodes and automatically provides a reading of the resistivity measured

between the probes. The readings were taken at 0, 90, 180 and 270 degree face of the concrete cylinder specimen.

Figure 3.7a: Concrete cylinder specimen on supports

Figure 3.7b: Surface resistivity test in progress

3.5.2 Compressive Strength Test

The compressive strength test was performed in accordance to the procedure outlined in ‘Standard Test Method for Compressive Strength of Cylindrical Concrete

Specimens' ASTM C39 [73]. The 4 in x 8 in (100 mm x 200 mm) cylinders were tested for strength immediately after the surface resistivity test. Three cylinders were tested at each of the following ages: 7, 28, 56 and 90 days after casting. Two unbonded caps were used in accordance to 'Standard Practice for Use of Unbonded Caps in Determination of Compressive Strength of Hardened Concrete Cylinders.' ASTM 1231[74]. After placing the cylinder in the testing machine, the load rate was maintained between 150 – 200 psi per second (1034 – 1379N/mm per sec) until failure of the test specimen and the ultimate strength of the cylinder was recorded.

3.5.3 Modulus of Elasticity

The modulus of elasticity (MOE) and poison's ratio tests were performed on the concrete specimen at 28 days of curing. The MOE and Poisson's ratio were performed on the same specimen in accordance to 'Standard Test Method for Static Modulus of Elasticity and Poisson's Ratio of Concrete Compression.' ASTM C469 [75]. For each of the batches, three 6 in x 12 in (150 mm x 300 mm) cylinders were made, cured for 28 days and tested.

Prior to determination of MOE, the 4 in (100 mm) by 8 in (200 mm) cylinders were tested to compressive failure and the load at failure was recorded. The 6 in by 12 in (150 mm x 300 mm) cylinder was fitted with a combined compressometer and extensometer such that the compressometer was centered along the cylinder making the deformation experienced by the cylinder equal to ½ the gage reading. A load equal to approximately 40 % of the load at which it was anticipated to fail was estimated from the load at failure of the 4 in x 8 in (100 mm x 200 mm) cylinder and was applied to the cylinder to seat the gage, then the load was released and adjustments were made if necessary to ensure the compressometer was properly seated. Starting near zero, the load was re-applied at continuous rate of movement with intervals of

5000 lb (2267962 kg) and the deformation was taken at each load interval. The cylinder was loaded until when the longitudinal strain was approximately 0.00050 and the corresponding load at a gage reading of 0.0008 in (0.020 mm) was recorded. The load was increased to approximately 40 % of the estimated load at failure of the cylinder and the corresponding load and gage reading were recorded. The test was also performed for the other two specimens in each batch and modulus of elasticity of each mix was calculated by averaging the three values obtained per the calculations.

3.5.4 Rapid Freeze Thaw Test

The rapid freeze-thaw test was performed in accordance to 'Standard Test Method for Resistance of Concrete to Rapid Freezing and Thawing.' ASTM C666 [76] to determine the durability of the concrete specimens. For each batch of concrete mixtures, three 4inch by 4 in x 12 in long (100 mm x 100 mm x 300 mm) concrete prisms were made. The specimens were cast in a steel mold tightened with bolts on all four corners, compacted on a vibrating table and demolded 24 hours later. Specimens were then placed in a moist curing room for 14 days as stipulated by ASTM C666 [76]. When the age of the specimens was 14 days, the specimens were removed from the curing room, wrapped in plastic wrap with wet burlap and placed in the freezer to stop the curing process. This was done in order to produce a group of eighteen specimens at a time, which is the total number of specimens the freeze thaw chamber can test at one time. As groups of eighteen specimens were prepared, and the chambers were available, specimens were removed from the freezer and placed in a tank filled with water for 48 hours to gradually thaw them.

After thawing, the fundamental transverse frequency and weight loss of each specimen were measured using a Rigol DS1052E digital oscilloscope, Omega Engineering ACC-PS2 accelerometer and a scale. The digital oscilloscope was set to

Fast Fourier Transform (FFT) mode and the specimens were tested as shown in Figure 3.8a. The determination of fundamental transverse frequency was performed in accordance to 'Test Method for Fundamental Transverse, Longitudinal, and Torsional Resonant Frequencies of Concrete Specimens.' ASTM 215 [77]. After testing, the specimens were each placed in a metal container with a small metal rod separating the specimen and the bottom of the steel container. The steel container with the specimen in it was then filled with water and placed in the freeze thaw apparatus as showed in Figure 3.8b. The freeze-thaw cycles consisted of alternately lowering the temperature of the specimens from 40 °F to 0 °F (4.4 °C to -17.8 °C) and raising it from 0°F to 40°F (4.4°C to -17.8°C) within 2.5 - 3 hours to make one cycle. After 30 cycles, the apparatus was tuned off and the specimen allowed to thaw for approximately three days before testing for weight loss and fundamental transverse frequency.

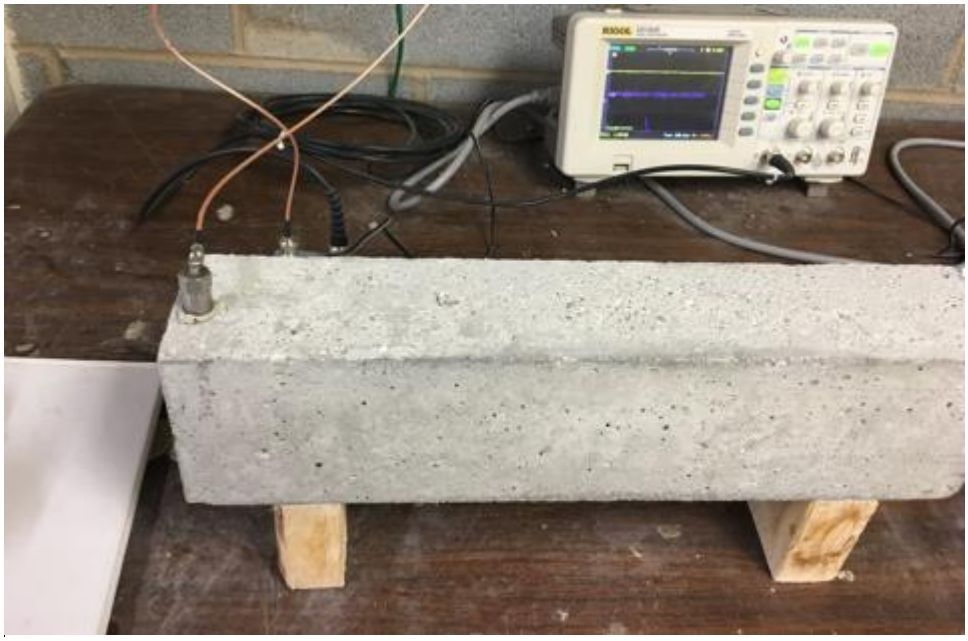

Figure 3.8a: Testing for fundamental transverse frequency setup

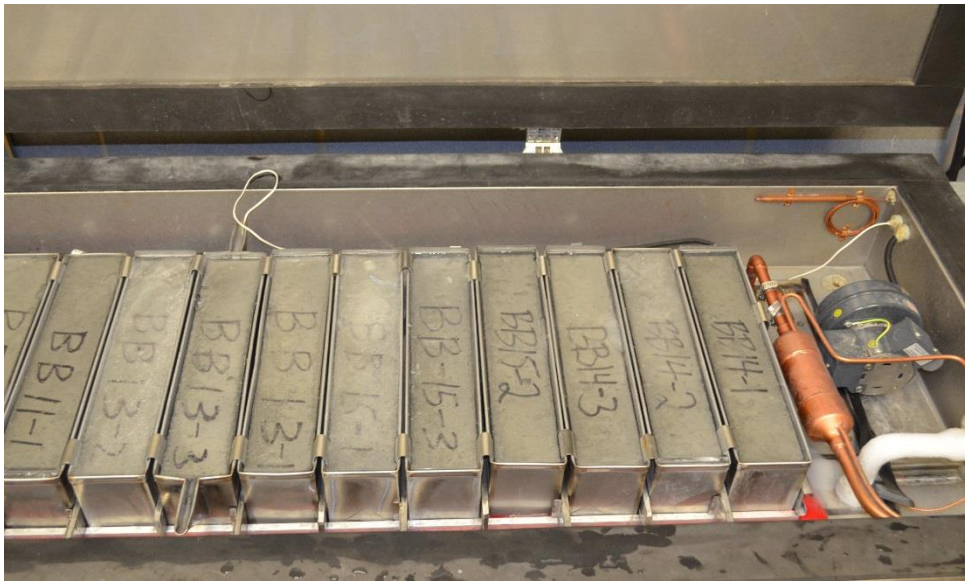

Figure 3.8b: Concrete specimen in freeze thaw apparatus

The specimens were removed for testing when they were in a thawed condition at 30 cycles, cleaned to remove any concrete scales and tested for fundamental frequency as well as weight loss. Before returning the specimens into the freeze-thaw apparatus in a predetermined order, the containers were cleaned out and fresh water was added. The air-entrained concrete specimens were subjected to 300 cycles of freezing and thawing.

3.5.5 Air Void Analysis

The air void parameters that characterize the air void system were evaluated in accordance to test method stipulated by ASTM C457 [18]. In this research both the manual modified point count method and an automated method were used. To use the automated method, calibration of the system must be performed with a minimum of 30 specimens whose air void parameters have been determined using the manual method, after this other specimens can be analyzed using the automated system. Six specimens set from this study were analyzed using the modified point count method. The results of the six specimens from manual counting were combined with results of

twenty-four specimens which had been manually evaluated for air system parameters per ASTM C457 as part of an independent study earlier conducted. This set of thirty manually evaluated specimens served as the calibration set for the automated process. The specimens used for calibration were selected to provide a diverse range of air content and air void characteristics. After calibration, the automated method was used to analyze the remaining unknown specimens. The specimen preparation for the manual count and the automated method are similar but with additional surface preparation for specimens utilized for the automated method. This additional preparation will be discussed in detail in subsequent sections.

3.5.5.1 Specimen Preparation

For each mixture, three concrete specimens cast in take-out food boxes as shown in Figure 3.9a were cured for 14 days. After curing, the specimen was sawn perpendicular to the layers in which the concrete was placed, and a flat specimen was obtained. The surface preparation of the specimen begun by attaching the specimen to an automatic polisher shown in Figure 3.9b and silicon carbide abrasive (grit) of nominal size 150 μm (0.0059 in; no 100) was applied to the bowl of the polisher.

Figure 3.9a: Concrete Chinese boxes

Figure 3.9b: Concrete specimen attached to auto-polisher

The polisher was started and allowed to grind the surface of the specimen for approximately 15mins. After each grinding, the polisher and the specimen were cleaned gently and thoroughly to remove grinding compound, the process was continued with nominal grit sizes of number 240, 320, 600, and 1000 until the surface is suitable for microscopic observation as shown in Figure 3.9c. The surface was ready for microscopical examination when it reflected a distant light source when viewed at a low angle. After a satisfactory specimen was obtained, the specimen was placed in an ultrasonic cleaner as shown in Figure 3.9d to effectively remove grit powder on the surface and in air voids.

Figure 3.9c: Polished Concrete specimen

Figure 3.9d: Polished Concrete specimen in ultrasonic cleaner

3.5.5.2 Modified Point Count Method (Manual Counting)

Six of the specimens were analyzed using the modified point count method described in ASTM C457 [18]. The modified point count apparatus used comprised of a microscope and support, microscope lamp, counter and a platform connected to Eest-West and North-South lead screws which was designed in a way that a concrete specimen placed on the platform can be moved at equal intervals by turning the

screws; the apparatus setup is shown in Figure 3.10a. The well-polished surface of the concrete specimen was placed on the platform of the point count device, adjustment and focusing was done to minimize the need for refocusing. The index line of the microscope was then placed on the upper corner of the specimen. The surface of the specimen was observed at a magnification of 50x by moving the concrete specimen from the east to the west through operation of the E-W screw.

Figure 3.10a: Manual point count apparatus setup

At the end of each transverse line, the E-W screw is reversed, and the number of each air voids intersected is recorded on a separate counter whether a stop is made or not. Once a transverse line was completed, the N-S screw was used to change the index point to a different transverse line and the process was started again until the whole specimen surface was covered with minimum transverse length of 95 in (2413 mm) as specified by ASTM C457[18]. Figure 3.10b shows transverse lines on a section of the concrete specimens.

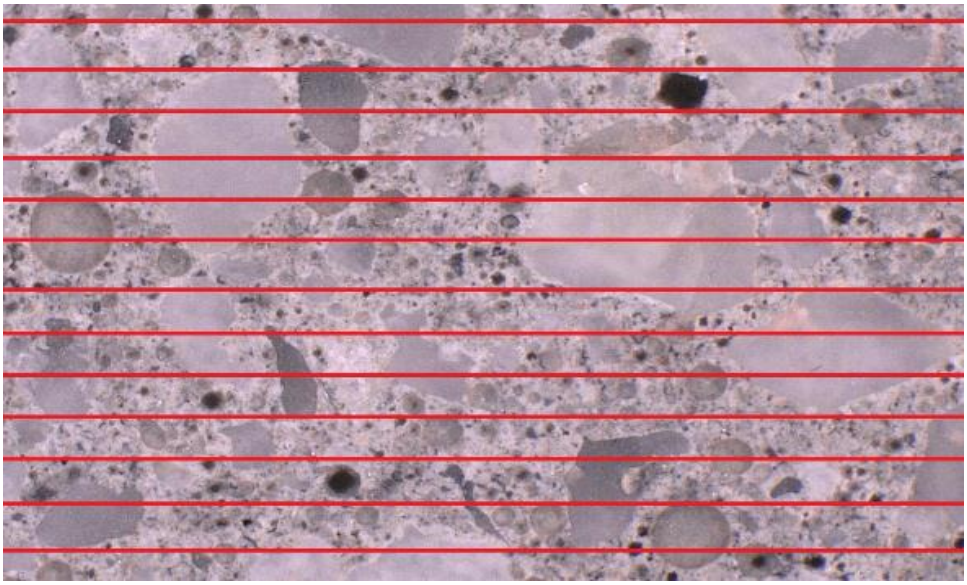

Figure 3.10b: Transverse line on a concrete specimen

From the above process, the data obtained are

N = total number of air voids intersected

S_t = total number of stops

S_a = number of stops in air voids

Sp = number of stops in paste

I = E-W translation distance between stops

The air void parameters were calculated using the following equations;

Air content (A) = $\frac{Sa}{St}$ x 100

Total transverse length (T_t) = $St\ x\ I$

Void frequency = $\frac{\mathrm{N}}{Tt}$

Spacing Factor (Ĺ): $4.342\acute{\mathrm{L}} = \frac{Tp}{4\mathrm{N}}$

3.5.5.3 Automated Air System

The automated method used to analyze the specimens for air void parameters was the software routine, “Bubble Counter” which is based upon ASTM C457 [18]

method A. The macros collected the image of the polished surface using a flatbed scanner, and the polished specimen was rendered black and white by application of black ink and then a fine white powder. The automated method was developed at Michigan Technological University by Petersen et al. [77]. Bubble Counter requires an initial analysis to be performed on a minimum of 30 specimens to calibrate the system, after this initial analysis the optimization routine is run, producing optimum threshold values that are based upon convergence with the results obtained from manual air void parameters determinations of the 30 specimens. Once the calibration/optimization is done, any specimen with unknown air void parameters can be determined. Figure 3.11 shows a flow chart of the process followed to analyze the specimens using Bubble Counter.

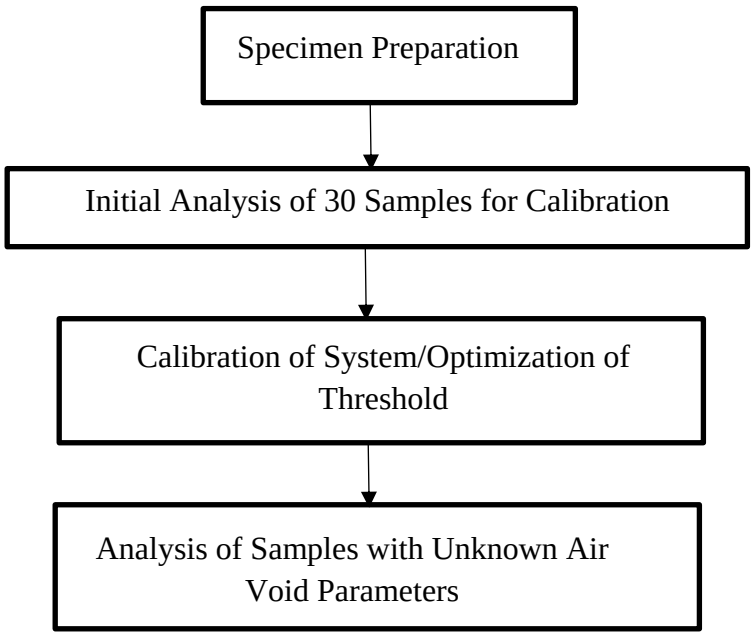

Figure 3.11: Flow chart for automated air system

3.5.5.3.1 Specimen Preparation

The specimen preparation started by following the process described in section 3.6.5.1 above. After a satisfactory flat polished concrete specimen has been achieved,

the surface of the specimen is then treated with black ink and white powder to aid in distinguishing air voids and other components such as aggregates.

Using a Pigma BB black marker from Sakora Color Products Corporation, the polished surface was darkened horizontally by covering the surface with overlapping parallel lines. After this, the specimen was rotated 90 degrees and darkened again by applying overlapping parallel lines for maximum coverage. Once an evenly darkened polished surface was achieved, white powder with size of 2 microns was distributed over the entire surface. For this project, 2 micron wollastonite powder manufactured by Nyco was used. This powder is similar to the powder utilized by Peterson et al [78]. The powder was then pressed into the air voids using a sharp flat metal blade and excess powder was removed from the surface of the concrete specimen by gently scarping with the edge of the blade. When air voids are not fully packed with powder, the powder was re-applied to specific areas as needed. After air voids are fully packed with powder, the surface of the specimen was gently darkened again to increase the contrast between white and black, and to remove excess powder from the surface. A well-prepared specimen showing contrast between aggregates and air voids is as shown in Figure 3.12a.

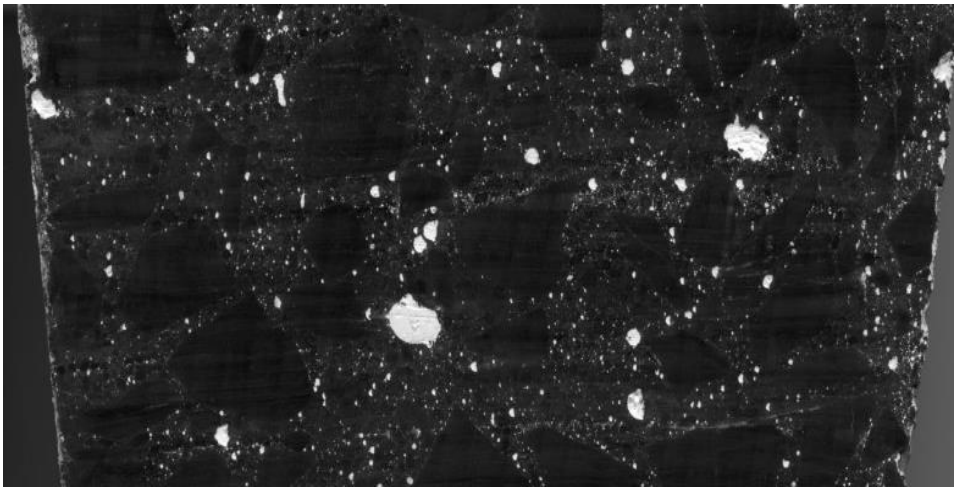

Figure 3.12a: Prepared specimen showing contrast between aggregates and air voids

3.5.5.3.2 Initial Analysis

Bubble Counter is a scanner based system that counts air voids intercepted by a series of single-pixel-wide lines extracted from a high resolution scanned image of well-polished concrete specimen. It measures the length of chord traversed which allows the calculation of air content and void frequency.

Each specimen was scanned in 8-bit grayscale mode that is 125 dpi and saved in TIFF format. The scanned specimen is opened in Bubble Counter and a representative area of the concrete specimen was selected for analysis and the bubble counter prompted for input of properties and analysis parameters as shown in Figure 3.12b. For the analysis, the number of traverse performed per specimen was 400, aggregate top size was 0.75 in (19 mm), and aggregate volume fraction was 0.75. Based on the properties provided, the macros extracted a number of traverse lines from the image after stretching the image pixels intensity.

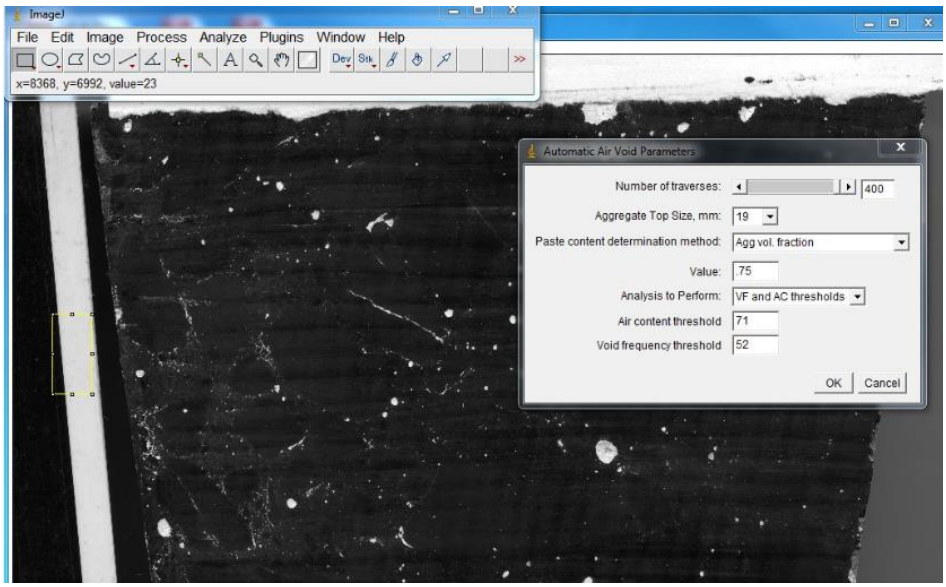

Figure 3.12b: Properties input prompt

White pixels were counted as voids and black pixels were counted as paste or aggregates in the specimen. After conclusion of the initial analysis, a dialog box containing the results summary is displayed as showed in Figure 3.12c.

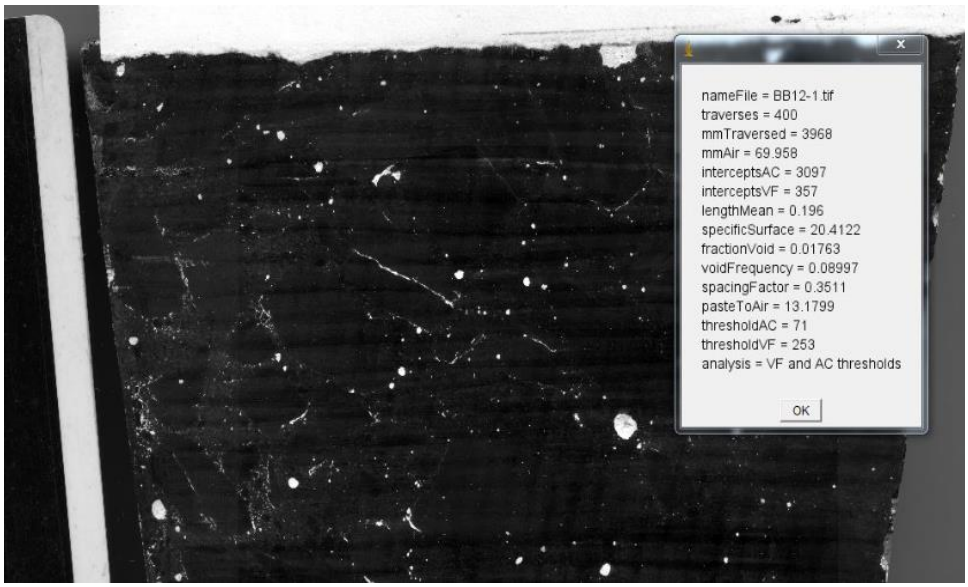

Figure 3.12c: Results summary interface

3.5.5.3.3 Calibration of System/Optimization of Threshold

Due to the fact that the colors of scanned image are not entirely black or white, Bubble Counter gives the user the opportunity to apply thresholds which discern the levels at which brighter pixels are air void and darker pixels are aggregate or paste. This process is called optimization/calibration of threshold. In other to assure the accuracy of the reported output results, Bubble Counter requires optimization of thresholds using the initial analysis results and results of manual air void analysis. Optimization was done by obtaining the results of the manual air void analysis performed on the thirty specimens and the results from initial analysis using Bubble Counter. A total of thirty specimens with wide range of air content and void

frequency was used to optimize Bubble Counter. The optimization routine was then performed, which produced optimum threshold values for both air contents and void frequencies that are based upon convergence with the results from manual air void determinations.

3.5.5.3.4 Analysis of Specimens

Once Bubble Counter was optimized, the calibrated specimens were re-analyzed and subsequently, specimens with unknown air void parameter was analyzed. The arithmetic mean of the optimized threshold values was used as threshold to analyze all the remaining specimens with unknown air void parameters.

3.5.5.3.5 Reliability of Automated Method

Table 3.3 presents the air void parameters of the specimens used for calibration using the automated system and standard manual method. The allowable difference between measurement of air content as stated in ASTM C457 [18] is 0.82 % for within laboratory and 1.16 % for between laboratory. As shown in Table 3.2, the average difference in air content measured by the two methods is 0.62 % which is less than both the allowable difference in within laboratory and between laboratory stated by ASTM C457[18]. This shows that results from the automated method is comparable to results from manual method.

As for the spacing factor, the average difference between the two methods was calculated to be 30.3 % which is more than the 22.6 % for within laboratory but less than 56.9 % for difference within laboratories specified by ASTM C457[18]. In summary, the results from the automated method are comparable with results from standard manual method.

Table 3.5: Air void parameters for calibration specimens

Specimen	Manual Air Content (%)	Automated Air Content (%)	Manual Spacing Factor	Automated Spacing Factor	Absolute Difference Air content (%)	Absolute Difference Spacing Factor
2A	5.9	6.0	0.0669	0.0911	0.1	0.0241
36048	3	2.5	0.191	0.369	0.5	0.178
38024	3.1	3.6	0.152	0.230	0.5	0.079
3B	3.3	4.3	0.210	0.150	1	0.0594
4A	4.9	5.1	0.159	0.106	0.2	0.0523
4B	5	5.1	0.162	0.117	0.1	0.0442
5A	5.5	5.0	0.0822	0.117	0.5	0.0353
5B	5.5	4.7	0.0863	0.132	0.8	0.0463
6A	6.3	6.1	0.0790	0.0932	0.2	0.0141
6B	5.9	6.8	0.0845	0.0695	0.9	0.0149
7A	5	4.5	0.113	0.144	0.5	0.0321
7B	5.1	4.9	0.106	0.141	0.2	0.0354
9A	5.9	5.3	0.104	0.108	0.6	0.00526
9B	5.7	5.9	0.122	0.0961	0.2	0.0260
9L126E	4.4	5.5	0.215	0.147	1.1	0.0670
9R240E	5.3	6.3	0.177	0.160	1	0.0161
BB12	2	1.8	0.720	0.443	0.2	0.276
BB13	9.4	9	0.0300	0.0724	0.4	0.0424
BB18	12	9.2	0.0212	0.0200	2.8	0.00114
BB24	2.2	2.1	0.720	0.563	0.1	0.156
BB25	1.6	1.0	0.719	0.592	0.6	0.126
R146B	5.2	5.2	0.147	0.105	0	0.0413
R163CC	4.3	4.5	0.169	0.125	0.2	0.0438
TF150N	4.4	3.6	0.146	0.142	0.8	0.00333
TF22N	5.5	3.1	0.154	0.193	2.4	0.0390
TL163D	4.6	3.5	0.147	0.175	1.1	0.0284
TLI63E	4.3	4.8	0.165	0.266	0.5	0.100
Average					**0.62**	**0.0589**

In addition to the allowable limits stated in ASTM C457 [18] comparison, a graphical correlation is presented in Figure 3.13a and Figure 3.13b. The correlation between the air content results obtained from manual method and automated method

is presented in Figure 3.13a while Figure 3.13b presents correletion for spacing factor. For the air content, there is a correlation of approximately 82% between the manual method and automated method while for the spacing factor, there is approximately 80% correlation between both methods.

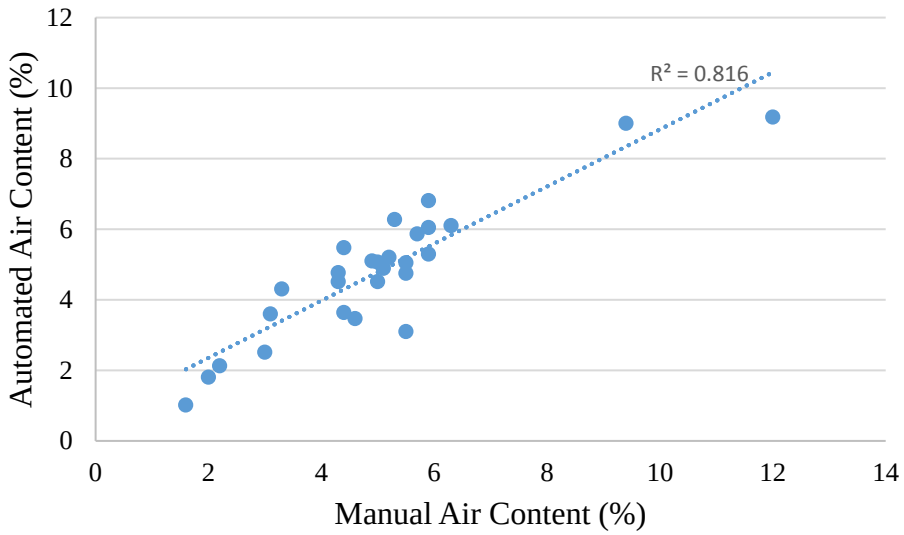

Figure 3:13a: Air Content, Manual vs Automated Method

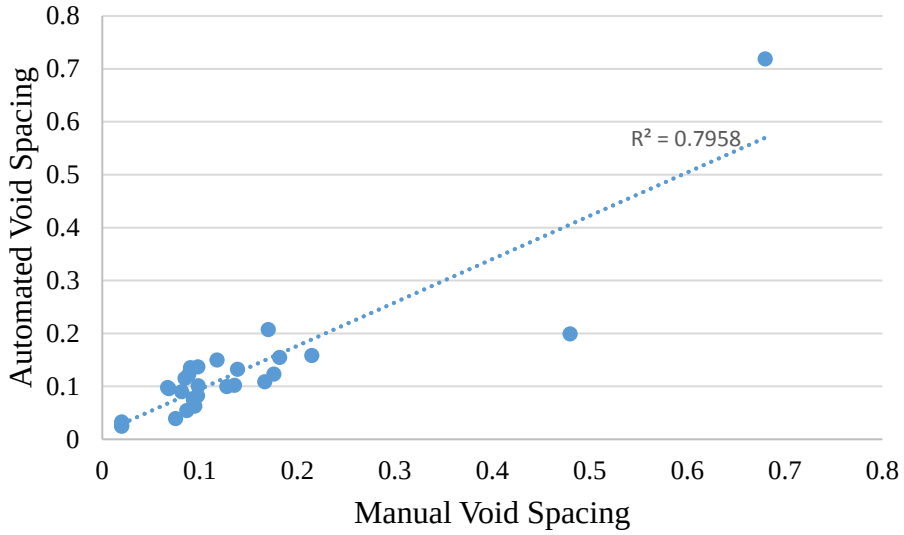

Figure 3:13b: Spacing Factor, Manual vs Automated Method

CHAPTER 4: TEST RESULTS

4.1 Fly Ash Characterization Tests

The results of the characterization tests performed on all the fly ash specimens are presented below. This section summarizes the foam index, iodine adsorption and loss on ignition tests results.

4.1.1 Foam Index Test Results

The results obtained from the foam index performed on the fly ash specimens are presented in Table 4.1. This table summarizes the quantity of diluted AEA and number of drops. The quantity of AEA used was determined by multiplying the number of drops and the volume of a single drop of AEA. As mentioned in procedure section, the single drop of AEA used is 0.02 ml. The foam index is the volume of diluted AEA solution added in the test while specific foam index is the undiluted AEA per 100 kg of cementitious material. As shown in Table 4.1, the BC and BT have the lowest interaction with AEA followed by AT and MT. The treated ashes generally required fewer drops of AEA to form a foam. The chemical treatment of off-spec ashes was expected to cause a reduction in the rate of adsorption of AEA. However, MT required more drops of AEA than BU, suggesting that the form of carbon in off-spec Plant M Ash is aggressive in adsorption of AEA than the form of carbon in off-spec Plant B Ash. This could also mean that the capacity to absorb AEA varies for differing forms of unburned carbon. Also, since the treatment process does not remove unburned carbon in off-spec ashes, rather it makes the carbon particles ineffective by neutralizing the adsorptive capacity, the premise could be true.

Table 4.1: Foam Index result

Fly Ash Specimen	Foam Index (No of drops)	Foam Index (ml of diluted AEA)	Specific Foam Index (ml of AE/g fly ash)
BC	12	0.24	0.024
BT	14	0.28	0.028
BU	20	0.40	0.040
AT	17	0.34	0.034
AU	26	0.52	0.052
MT	21	0.42	0.042
MU	39	0.78	0.078

4.1.2 Iodine Adsorption Test Results

The results obtained from the iodine adsorption test performed on the fly ash specimens are presented in Table 4.2. This table presents the iodine number of each fly ash specimen. From the results obtained, it can be concluded that BC has the lowest adsorption capacity compared to BT and BU. BU and BT showed similar adsorptive capacity, however the treatment process was able to reduce the iodine number by 0.18 mg. A similar trend was observed for ashes from Plant A and Plant M, the treated ash from Plant A showed less adsorptive ability when compared to the untreated ash from plant A and there was a reduction of 0.74 mg in the iodine number. The iodine number of MU is almost twice that of MT, this difference could be because Plant M ash has a lot of unburned carbon than both Plant A and B ashes.

Table 4.2: Iodine Adsorption result

Fly Ash Specimen	Iodine Number (mg of I/kg of fly ash)
BC	1.11
BT	3.07
BU	3.25
AT	3.11
AU	3.85
MT	3.48
MU	6.85

4.1.3 Loss on Ignition Test Results

The results from the loss on ignition test performed are presented in Table 4.3. This table summarizes the percentage of unburned carbon present in each fly ash specimen.

Table 4.3: Loss on Ignition results

Fly Ash Specimen	LOI (%)
BC	1.60
BT	5.59
BU	5.59
AT	8.67
AU	8.67
MT	7.70
MU	7.70

4.2 Variable Air Dosage and Fresh Concrete Results

The results from the fresh concrete and variable air dosage tests performed are presented below. The objective of the variable air dosage test is to show whether it is possible to successfully entrained air, by increasing the dosage of AEA until the carbon cannot adsorb it anymore. Table 4.4 presents the variable air dosage and fresh concrete test which includes SAM, slump and unit weight. Figure 4.4 through Figure 4.6 shows the variation of the AEA dosage and the ability to entrain air. In Table 4.4, the AEA dosage is the amount of AEA added to the mixtures to achieve the target air

content, SAM 1 and SAM 2 are the results of air content and SAM number measured by two different SAM operators simultaneously. Four of the results were removed from the analysis because the SAM number was greater than 0.7. Per information from the developer of the device, these values are not possible and are likely due to leakage in the meter (Ley, personal communication, January 15, 2018). The mixtures that contain treated ash are denoted with "T" preceded by the first letter of the ash plant name while the mixtures that contain untreated ash are denoted with "U" preceded by the first letter of the fly ash plant name. The number at the end of the specimen ID represents the low, target and high air content ranges.

Table 4.4: Fresh Concrete Results

Specimen ID	**AEA Dosage (oz/cwt)**	**SAM 1 (%)**	**SAM1 no**	**SAM 2 (%)**	**SAM2 no**	**Slump (in)**	**Temp (F)**
MT1	0	2.1	0.73	1.9	0.11	4	70
MT2	5.03	5.4	0.38	5.1	0.41	4	68
MT3	33.5	9.6	0.15	9.2	0.20	3.5	69
MU1	1.51	1.5	0.30	1.7	0.25	2.5	74
MU2	43.55	6.0	0.16	5.8	0.13	3	74
MU3	36.85	8	0.39	7.6	-	4	75
BC1	0	1.6	0.45	1.7	0.20	2.5	83
BC2	3.92	5.8	0.23	5.8	0.14	4	80
BC3	8.38	13.8	0.29	13.7	0.26	4.5	71
AT1	0	3.0	0.31	2.7	0.33	2.7	72
AT2	5.03	5.1	0.11	5.3	0.19	2.5	73
AT3	12.56	9.5	0.24	9.8	0.27	4	72
AU1	5.37	2.3	0.63	2.2	0.45	7	78
AU2	16.75	6.7	0.24	6.7	0.36	8.5	76
AU3	29.31	12.4	0.19	12.7	-	5	78
BT1	0	3	-	3	0.77	5	76
BT2	5.03	5.7	-	5.9	0.41	4	75
BT3	16.75	11.6	0.22	11.9	0.28	3.5	72
BU1	0	3.0	0.49	2.7	0.45	2.8	72
BU2	6.7	5.5	0.12	5.3	0.20	2.5	73
BU3	16.75	8.5	0.22	8.7	0.24	4	72

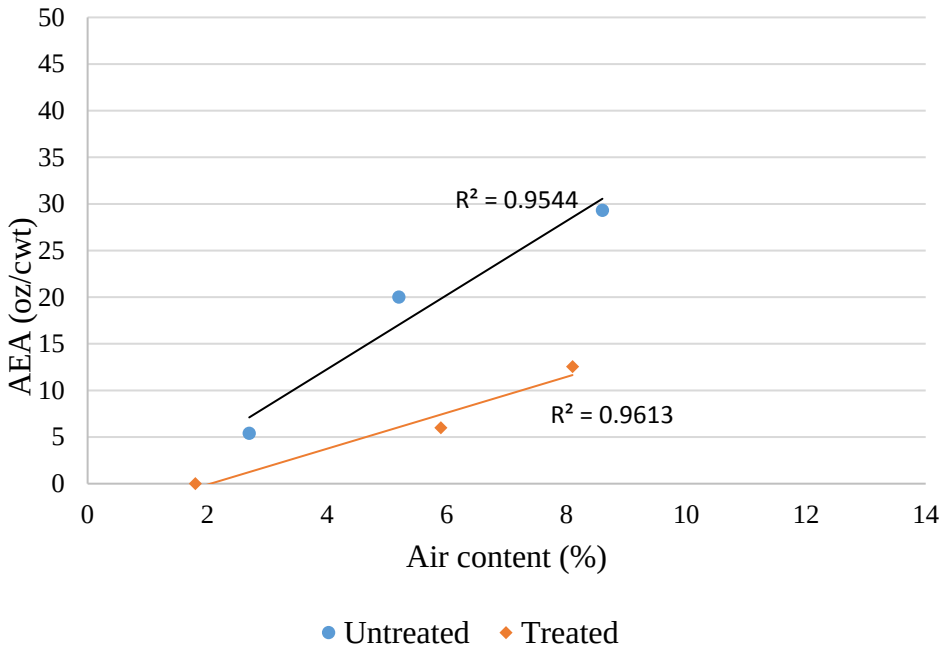

Figure 4.4: Air Content vs Air Dosage for Plant A treated and Untreated Ash

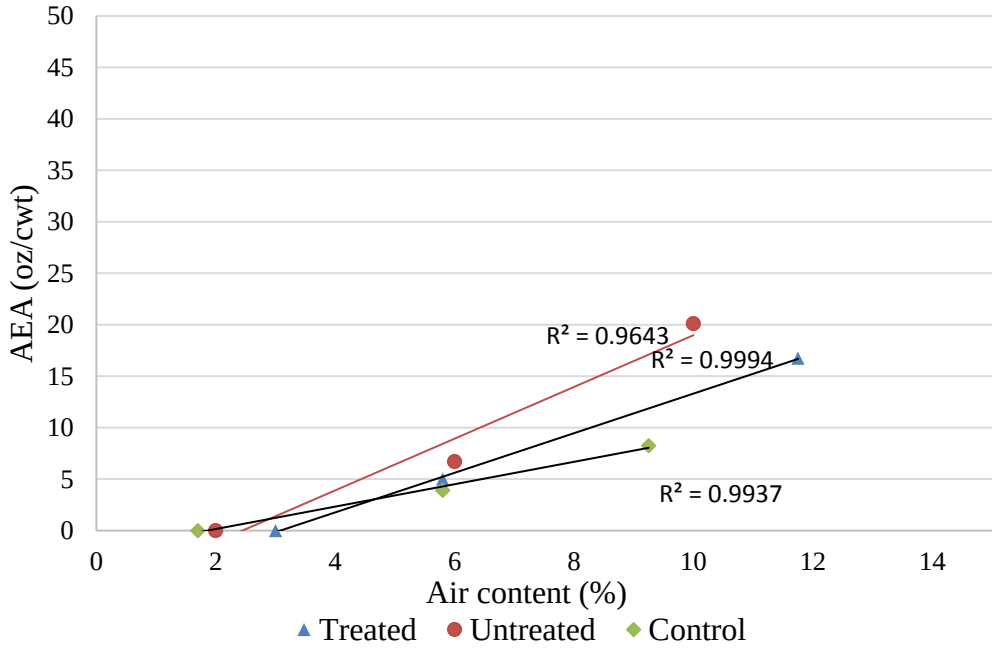

Figure 4.5: Air Content vs Air Dosage for Plant B treated, Untreated and Control Ash

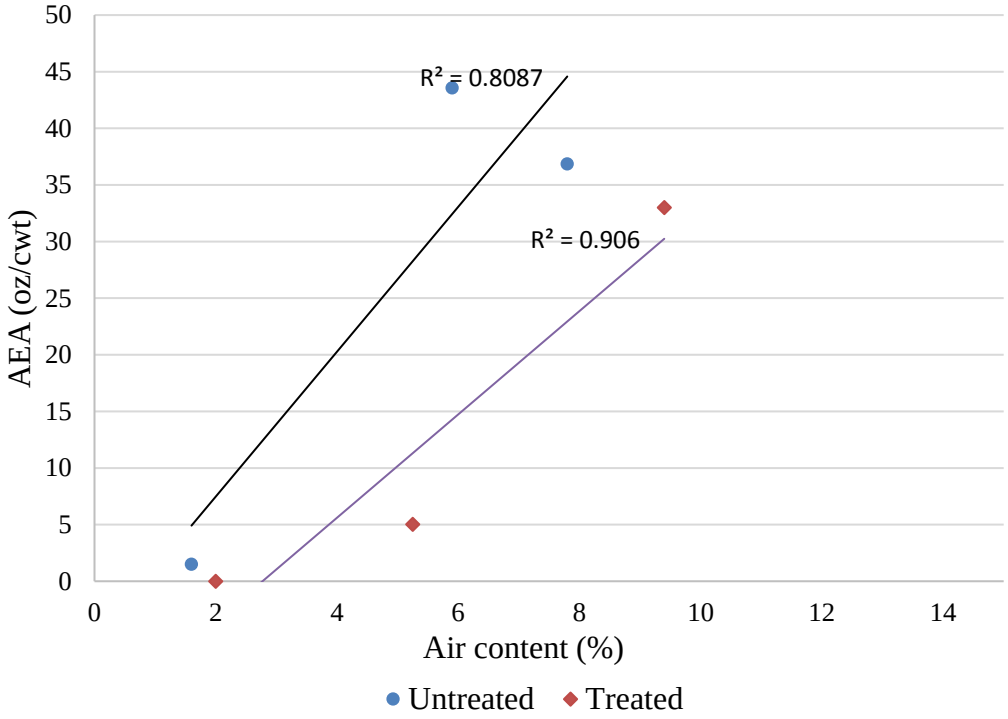

Figure 4.6: Air Content vs Air Dosage for Plant M treated and Untreated Ash

4.3 Mechanical Properties Tests

The results from the mechanical properties tests performed are presented in this section. The mechanical tests results included compressive strength, modulus of elasticity and surface resistivity.

4.3.1 Compressive strength and Modulus of Elasticity Tests

The results from the compressive strength and modulus of elasticity test performed are presented in Table 4.5. Table 4.5 presents compressive strength test results at 7, 28, 56 and 90 days, and modulus of elasticity at 28 days of curing. In Table 4.5, PANN is a control mixture with 5 % air content which does not contain fly ash. These results are shown graphically in Figure 4.8, Figure 4.9, Figure 4.10 and Figure 4.11 while Figure 4.12 shows the average value 28 day strength of three specimens with standard deviation. No trend was obvious in the data other than that

the higher air content mixtures exhibited lower strength compared to low air content mixtures. Also, in comparison to the mixture without fly ash, most of the mixtures showed slow strength gain. However, the 90 day strength for the control mixture without fly ash is similar to most of the mixtures. This slow strength gain could be due to the retarding effect of fly ash on strength. The mixtures that contain treated ash are denoted with "T" preceded by the first letter of the fly ash plant name while the mixtures that contain untreated ash are denoted with "U" preceded by the first letter of the fly ash plant name . The number at the end of the specimen ID represents the low, target and high air content ranges. For instance, MT1 is specimen made with treated ash from Plant M with low air content of between 0 % - 4.5 %

Table 4.5: Compressive Strength and Modulus of Elasticity

Specimen ID	**Compressive Strength (psi)**				**Modulus of Elasticity (psi)**
	7 days	28 days	56 days	90 days	
MT1	4230	5370	5945	6535	3030000
MT2	3255	3795	4800	5245	2450000
MT3	1965	2415	2795	2800	2360000
MU1	4210	5445	5925	6430	2590000
MU2	2385	3065	3580	3785	2820000
MU3	2295	3035	3450	3605	2630000
BC1	4375	5420	5890	6635	2460000
BC2	3015	3625	4300	4880	2340000
AT1	4235	5155	5800	6345	3200000
AT2	3900	4495	5705	6200	2500000
AT3	2895	3170	3800	4260	2620000
AU1	3570	4435	5200	5740	2840000
AU2	2880	3420	4520	4950	2630000
AU3	1650	1870	2345	2860	2550000
BT1	3745	4790	5180	5850	3150000
BT2	3120	3860	4205	4580	2770000
BT3	1500	1935	2275	2490	2460000
BU1	3755	4525	5095	5720	2350000
BU2	3005	3610	4420	4875	2250000
BU3	1600	1885	2230	2855	2150000
PANN	4080	5400	-	6060	3410000

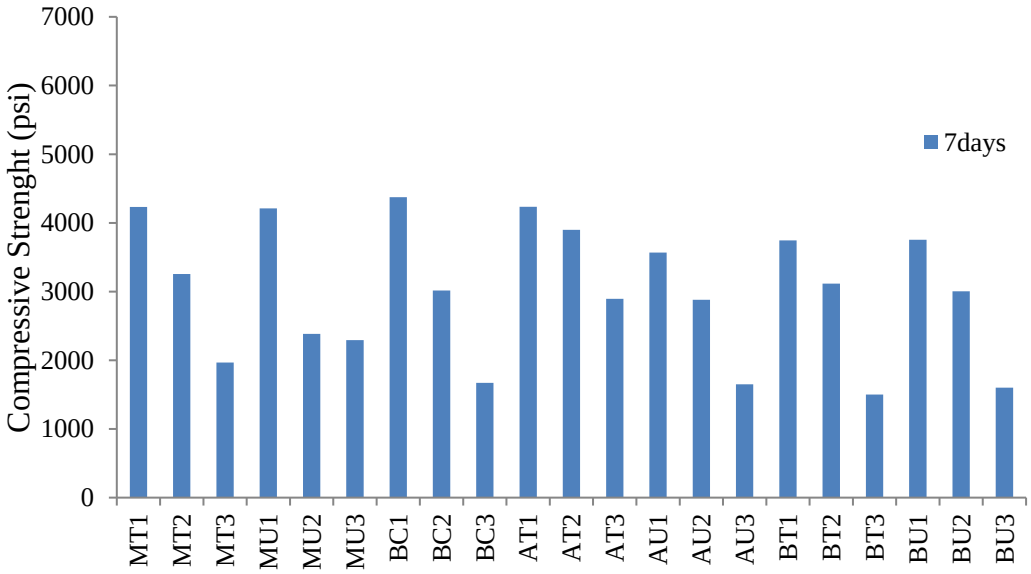

Figure 4.8: Compressive strength at 7 days

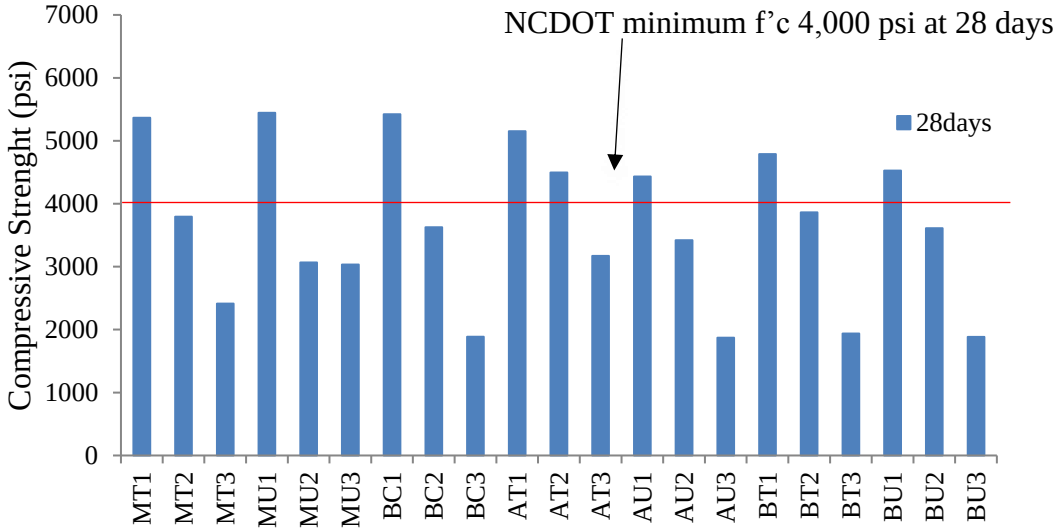

Figure 4.9: Compressive strength at 28 day

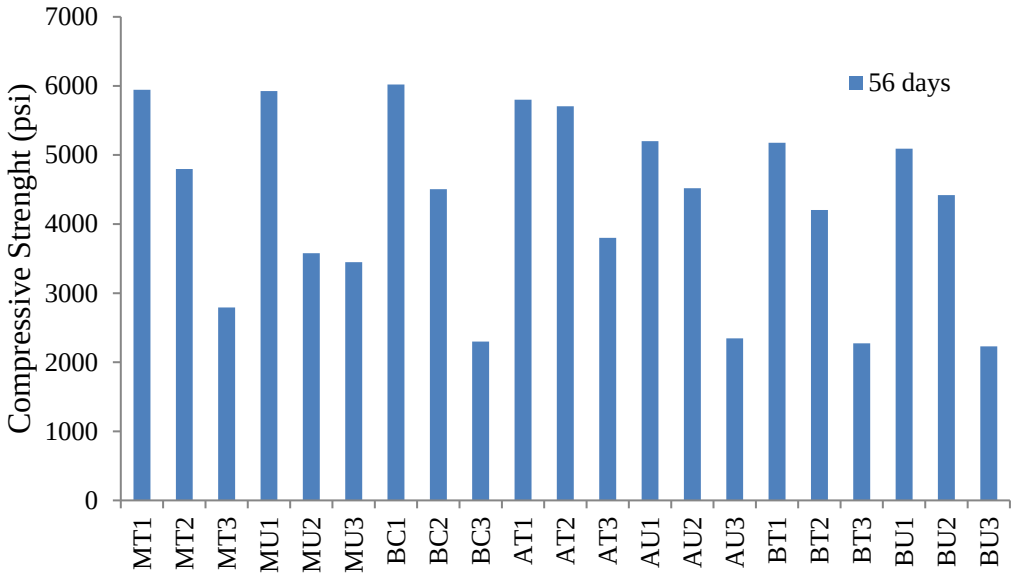

Figure 4.10: Compressive strength at 56 days

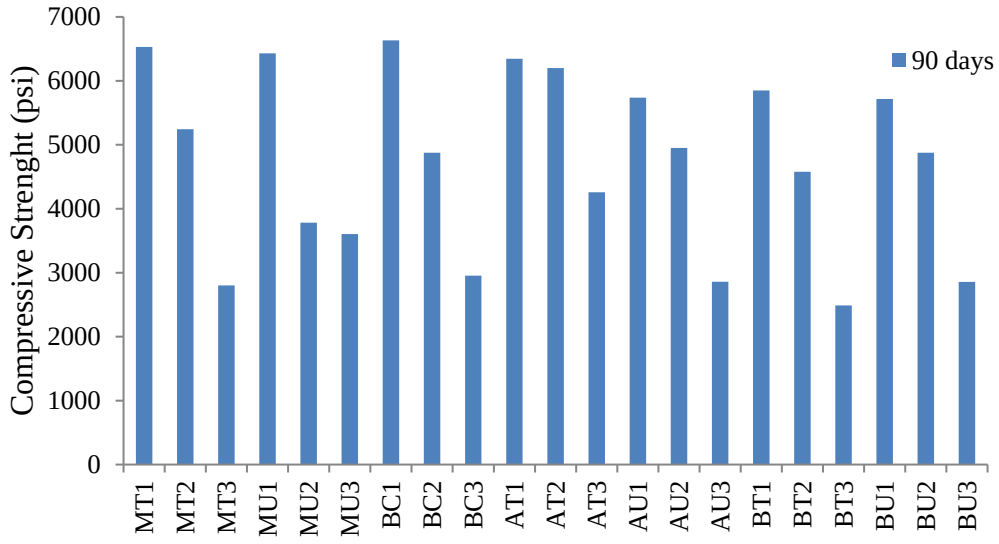

Figure 4.11: Compressive strength at 90 days

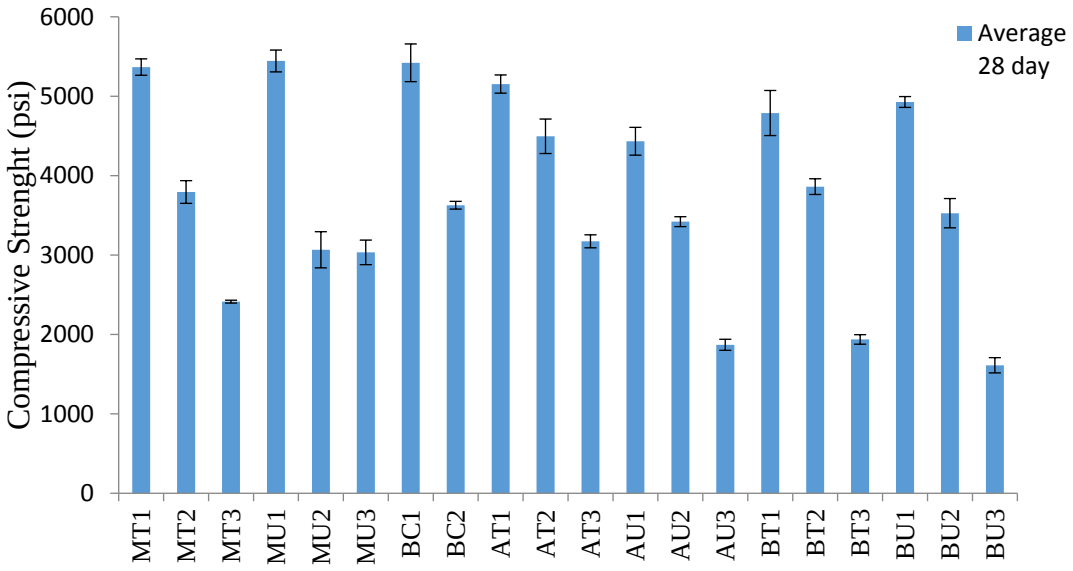

Figure 4.12: Average 28 day compressive strength with standard deviation

4.3.2 Surface Resistivity

The surface resistivity results indicate the susceptibility of the mixtures to chloride ion penetration. Table 4.6 presents the surface resistivity results performed at 7 days, 28 days, 56 days and 90 days. The results are also presented graphically in Figure 4.13, Figure 4.14, Figure 4.15, Figure 4.16 and the average of three specimens for 28 day with standard deviation is presented in Figure 4.17. From Table 4.6, generally the surface resistivity increases as the air content increases. This implies that the high air content mixtures have lower susceptibility to chlorine penetration compared to the low air content mixtures. However, few of the mixtures didn't follow this trend and this could be due to variation in making the specimen as well as tampering of the concrete.

Table 4.6: Surface Resistivity Results

Specimen ID	**Surface Resistivity (KiloOhms/cm)**			
	7 days	28 days	56 days	90 days
MT1	6.8	9.8	18.3	28.5
MT2	7.3	10	18.5	28.0
MT3	7.9	11.5	18.3	32.0
MU1	6.4	10.8	18.3	28.6
MU2	6.9	11.7	19.5	32.7
MU3	6.5	10.8	18.6	29.5
BC1	7.3	11	19.1	31.0
BC2	7.5	11.5	19.5	32.3
BC3	7.8	11.9	19.8	32.8
AT1	6.5	9.8	18.6	30.0
AT2	7.1	11.8	19.5	31.1
AT3	7.6	12.8	20.6	33.0
AU1	5.8	8.9	15.6	22.5
AU2	6.4	9.7	16.6	24.1
AU3	6.7	10.4	18.5	29.5
BT1	4.9	8.1	15.4	22.6
BT2	5.8	9.6	16.4	24.2
BT3	7.2	11.1	19.2	30.3
BU1	4.6	7.2	14.9	21.4
BU2	5.0	8.9	15.8	23.3
BU3	6.8	10.5	19.0	28.9

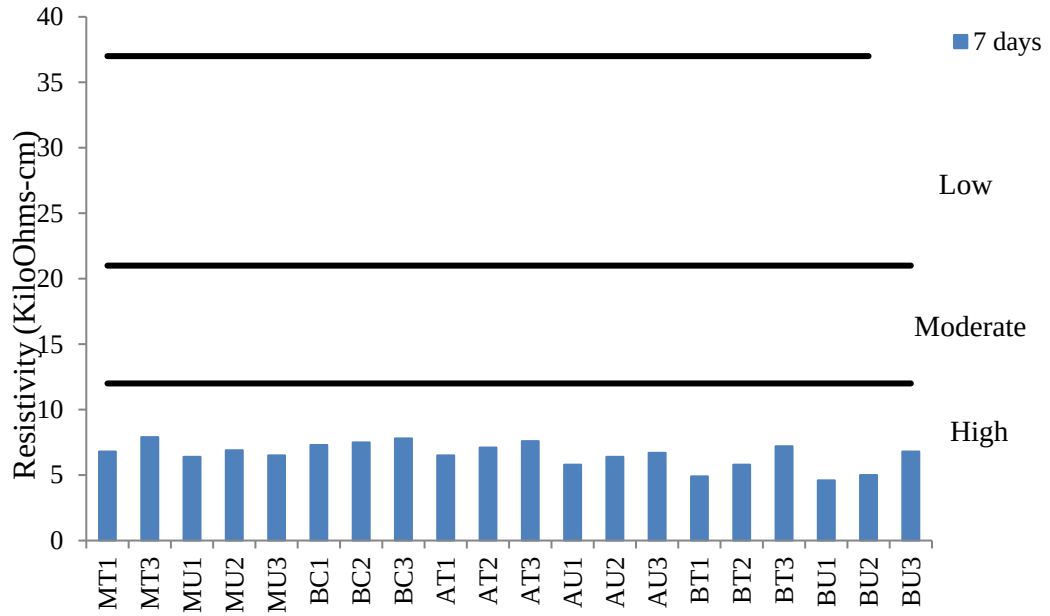

Figure 4.13: Surface resistivity at 7 days

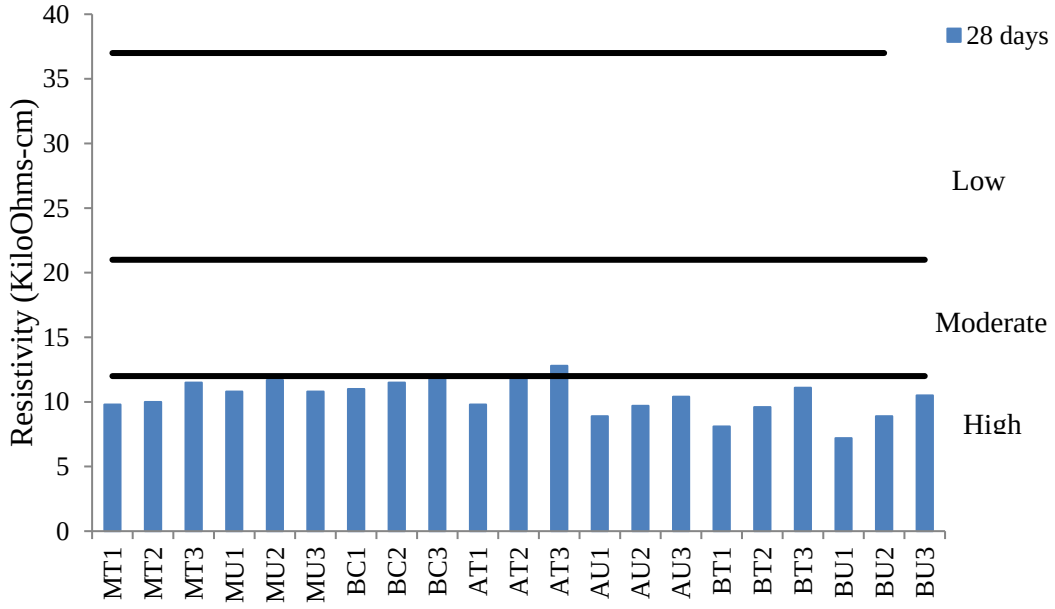

Figure 4.14: Surface resistivity at 28 days

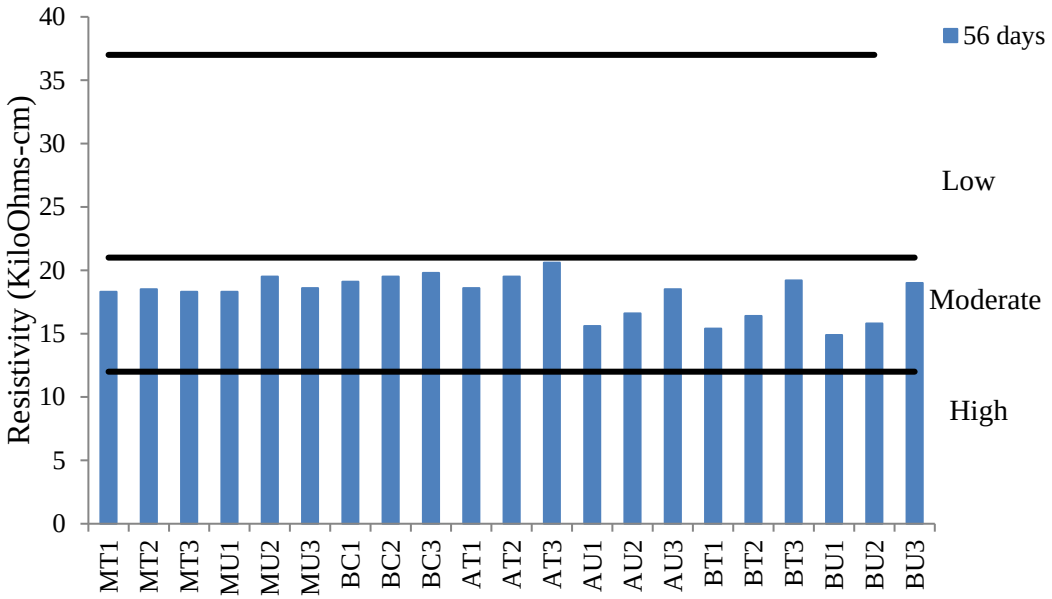

Figure 4.15: Surface Rresistivity at 56 days

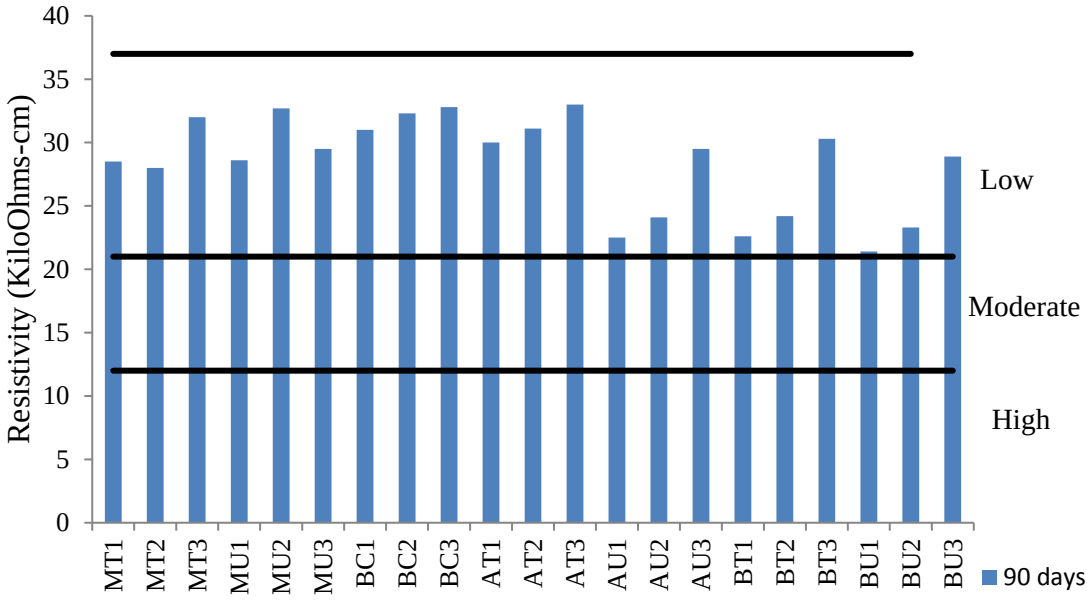

Figure 4.16: Surface resistivity at 90 days

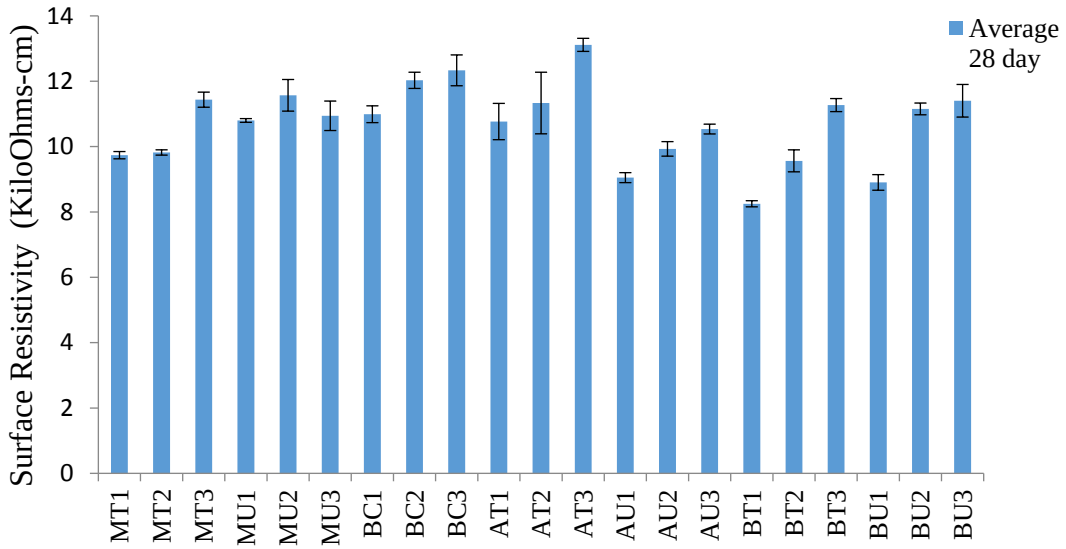

Figure 4.17: Average 28 day surface resistivity with standard deviation

4.3.3 Freeze Thaw Testing

The freeze thaw test results are presented in the following sections below. The results of this laboratory investigation are expressed in terms of the parameters that were measured during testing and calculated. The measured parameters are change in weight and change in fundamental transverse frequency while the calculated parameters are the dynamic modulus and durability factor. The results are subdivided into physical changes and loss of dynamic modulus (durability factor, or DF). The physical change outlines the deterioration and damages associated with the specimens while the durability factor is calculated from the fundamental frequencies.

4.3.3.1 Physical Deterioration

The major physical change that occurred to all the specimens was surface scaling. However, the degree of surface scaling varies from one specimen to the other. Some specimens with low entrained air experienced concrete scaling in addition to expansion of aggregates which subsequently led to disintegration of the specimens as exposure to freeze and thawing cycles increased. Figure 4.18 shows images of

specimens after cycling after failure. The cracks, separation of the coarse aggregates and cement part were caused by the action of freezing and thawing cycles.

Figure: 4.18 Specimen MU1-3 at 30 cycles

Figure: 4.19 Specimen MT1-2 at 90 cycles

4.3.3.2 Dynamic Modulus and Durability Factor

The calculated relative dynamic modulus of elasticity (P_c) and durability factor (*DF*) after different cycles of freeze thaw exposure are presented in Table 4.8. As was previously stated, three specimens were tested for each mixture, hence the DF and dynamic modulus obtained by averaging the results for each of the three replicate specimens representing each mixture are also presented in Table 4.8.

The DF. which is the relative measure of the ability of laboratory concrete specimens to resist frost action by application of a laboratory freeze and thaw test as described in ASTM C666[76] was calculated for the specimens at the end of 300 cycles of freeze thaw. However, as stated by ASTM C666[76] the test was stopped for some of the specimens when the P_c fell below 60 % and *DF* was calculated at that cycle at which it fell below 60 %. P_c was calculated as stated in ASTM C666 [76] and shown in Equation 3. In the same vein, some of the specimens also didn't response to fundamental frequency test after exposure to additional freeze thaw cycles, hence the *DF* was calculated at that number of cycles at which the specimen stopped responding to fundamental frequency test as shown in Table 4.8. The *DF* was calculated as stated in ASTM C666 [76] by dividing the product of relative dynamic modulus of elasticity at 300 cycles and the number of cycles at which P_c fell below 60% with number of cycles at which exposure was terminated.

$$P_c = \frac{n}{b} \times 100 \qquad (Eq\ 3)$$

P_c = Relative dynamic modulus after c cycles

n = Fundamental transverse frequency at 0 cycles

b = Fundamental transverse frequency after c cycles

Table 4.7: Relative Dynamic Modulus of Elasticity per ASTM C666 (2008) and ASTM C215 (2008) including final durability factor

Specimen Label	**P_c (%)**										**Average P_c (%)**	***DF* (%)**
	30 Cycles	60 Cycles	90 Cycles	120 Cycles	150 Cycles	180 Cycles	210 Cycles	240 Cycles	270 Cycles	300 Cycles	300 Cycles	
MT1-1	93.31	75.23	12.04	Fell Apart								2.78
MT1-2	92.16	77.44	8.29									
MT1-3	93.41	79.06	7.32									
MT2-1	100.00	97.92	97.92	97.92	97.92	97.92	97.23	97.23	96.88	95.85	96.19	96.19
MT2-2	100.00	97.23	97.23	97.23	97.23	97.23	96.88	96.88	97.23	95.85		
MT2-3	100.00	98.25	98.25	98.95	98.25	98.25	97.91	97.91	97.91	96.86		
MT3-1	98.90	93.48	93.12	93.12	93.12	92.77	92.41	91.71	91.36	90.65	89.18	89.18
MT3-2	98.90	92.10	91.75	91.75	91.75	91.40	90.35	90.35	89.31	88.27		
MT3-3	99.27	91.74	91.74	91.74	92.09	91.74	90.69	89.64	89.29	88.60		
MU1-1	22.20	Test stopped (Pc below 60%)										2.23
MU1-2	25.97											
MU1-3	18.61											
MU2-1	99.30	92.09	92.09	92.09	91.76	91.09	90.42	89.75	88.76	87.76	87.94	87.94
MU2-2	99.30	92.43	92.43	92.43	91.76	90.75	89.75	89.09	88.43	87.43		
MU2-3	100.00	92.74	92.74	92.74	92.40	91.39	90.38	89.72	89.38	88.61		
MU3-1	100.00	95.74	95.39	95.39	94.69	94.69	94.34	93.99	92.60	91.91	92.59	92.59
MU3-2	100.00	96.08	96.08	96.08	96.08	96.08	95.72	95.02	94.67	93.61		
MU3-3	100.00	95.03	95.38	95.03	95.03	94.68	94.33	94.33	93.28	92.24		
BT1-1	99.00	82.81	64.00	Test stopped (Pc below 60%)								17.37
BT1-2	95.04	80.01	53.83									
BT1-3	92.08	73.72	55.87									
BT2-1	100.00	98.96	98.96	98.96	98.96	98.96	97.93	96.56	95.88	95.53	95.75	95.75
BT2-2	100.00	99.31	97.58	97.58	97.58	97.24	96.55	96.21	95.53	94.85		

Table: 4.7 Cont'd: Relative Dynamic Modulus of Elasticity per ASTM C666 (2008) and ASTM C215 (2008) including final durability factor

Specimen Label	P_c										**Average P_c (%)**	***DF* (%)**
	30 Cycles	60 Cycles	90 Cycles	120 Cycles	150 Cycles	180 Cycles	210 Cycles	240 Cycles	270 Cycles	300 Cycles		
BT2-3	100.00	98.95	98.60	98.25	98.25	97.91	97.91	96.87	96.87	96.86		
BT3-1	100.00	100.00	100.00	100.00	100.00	100.00	97.77	95.56	94.46	91.21	92.89	92.89
BT3-2	100.00	100.00	100.00	98.85	98.85	97.71	95.46	93.22	92.12	92.11		
BT3-3	100.00	100.00	100.00	97.66	97.66	96.50	95.35	95.35	95.35	95.34		
BU1-1	65.61	No Response										5.00
BU1-2	42.25											
BU1-3	42.25											
BU2-1	100.00	100.00	100.00	98.95	98.60	97.91	97.91	97.91	95.83	94.80	95.95	95.95
BU2-2	100.00	100.00	100.00	100.00	100.00	99.29	99.29	97.19	97.19	96.15		
BU2-3	100.00	100.00	100.00	97.91	97.91	97.91	97.91	97.91	97.91	96.86		
BU3-1	100.00	100.00	100.00	100.00	100.00	98.78	95.18	94.00	94.00	93.99	94.39	94.39
BU3-2	100.00	100.00	100.00	100.00	100.00	100.00	97.58	97.58	95.18	95.18		
BU3-3	100.00	100.00	100.00	100.00	100.00	98.78	95.18	94.00	94.00	93.99		
AT1-1	93.19	88.47	88.16	81.18	77.65	74.20	67.53	58.12	49.42	Test stopped (Pc below 60%)		48.81
AT1-2	88.58	86.75	85.83	80.47	79.59	74.43	69.44	59.99	55.52			
AT1-3	92.16	94.09	93.12	86.49	82.81	79.21	72.25	67.24	57.76			
AT2-1	98.67	98.67	98.67	94.72	94.72	82.76	83.36	74.46	88.95	88.95	86.79	86.79
AT2-2	94.72	94.72	94.72	94.72	94.72	91.91	93.75	92.78	88.95	85.20		
AT2-3	97.97	97.97	97.97	97.97	97.97	85.28	93.97	90.06	86.22	86.22		
AT3-1	97.91	97.91	97.21	97.21	96.87	96.87	95.83	94.81	93.78	91.75	88.76	88.76
AT3-2	100.00	93.78	93.78	93.78	92.77	91.76	91.76	89.75	87.77	86.78		
AT3-3	100.00	93.78	89.75	89.75	89.75	89.75	89.75	89.75	87.77	87.76		
AU1-1	41.42											

Table: 4.7 Cont'd: Relative Dynamic Modulus of Elasticity per ASTM C666 (2008) and ASTM C215 (2008) including final durability factor

Specimen Label	P_c										**Average P_c (%)**	***DF* (%)**
	30 Cycles	60 Cycles	90 Cycles	120 Cycles	150 Cycles	180 Cycles	210 Cycles	240 Cycles	270 Cycles	300 Cycles		
AU1-2	35.29	Fell Apart										3.55
AU1-3	29.65											
AU2-1	98.95	98.95	98.95	97.91	97.91	97.91	96.87	95.83	94.81	94.80	96.18	96.18
AU2-2	98.95	98.95	98.95	98.95	98.95	98.95	97.91	97.91	97.91	95.83		
AU2-3	100.00	100.00	100.00	97.91	97.91	97.91	96.87	95.83	97.91	97.91		
AU3-1	100.00	100.00	100.00	98.83	98.83	98.83	97.66	97.66	95.35	95.34	96.50	96.50
AU3-2	100.00	100.00	100.00	98.83	98.83	97.66	97.66	97.66	96.50	96.50		
AU3-3	100.00	100.00	100.00	100.00	100.00	100.00	100.00	97.66	97.66	97.66		
BC1-1	21.23	No Response										1.36
BC1-2	11.41											
BC1-3	8.30											
BC2-1	100.00	100.00	100.00	98.95	97.91	97.91	97.91	97.91	96.87	96.86	96.87	96.87
BC2-2	100.00	100.00	100.00	97.91	97.91	97.91	97.91	97.91	96.87	96.86		
BC2-3	100.00	100.00	99.30	97.91	97.56	97.20	97.18	97.10	97.10	96.90		

4.3.4 Air Void Parameters

The results from the automated air void analysis to evaluate the hardened air void parameters that characterize the quality of air void system are presented in Table 4.9 below. Table 4.9 summarizes the traversed length, specific surface, air void, void frequency and spacing factor. There were some outliers in the results which were removed, hence some mixture do not have up to three specimens result presented.

Table 4.8: Air void Parameters

Specimen	mm Traversed	mm Air	Specific Surface (mm)	Air Void	Void Frequency	Spacing Factor	SAM No
MT1-1	4044.8	90.80	17.3	2.245	0.0253	0.567	
MT1-2	4569.6	89.93	21.6	1.968	0.0279	0.514	0.42
MT1-3	4268.8	62.45	20.2	1.463	0.0301	0.476	
MT2-1	4435.2	207.84	25.4	4.686	0.0813	0.176	
MT2-2	4646.4	221.76	26.6	4.773	0.0905	0.158	0.395
MT2-3	4185.6	221.85	26.5	5.300	0.0793	0.181	
MT3-1	3840	420.21	26.7	10.94	0.148	0.0968	
MT3-2	3680	359.32	27.0	9.764	0.171	0.0840	0.175
MT3-3	4288	498.00	29.6	8.633	0.163	0.0879	
MU1-1	2259.2	25.80	18.3	1.142	0.0203	0.708	
MU1-2	3283.2	34.39	18.8	1.047	0.0201	0.715	0.275
MU1-3	4137.6	90.61	17.8	2.190	0.0196	0.731	
MU2-1	4294.4	241.12	26.9	5.615	0.0756	0.190	
MU2-2	3622.4	266.30	29.2	5.352	0.0765	0.188	0.145
MU2-3	3577.6	207.75	27.8	5.807	0.0805	0.178	
MU3-1	4044.8	290.26	31.2	7.176	0.156	0.0920	
MU3-2	4384	379.48	35.2	8.656	0.174	0.0825	0.39
MU3-3	4480	324.91	32.0	7.252	0.162	0.0884	
BT1-1	4659.2	148.80	20.6	3.194	0.0313	0.458	
BT1-2	3923.2	135.45	24.7	3.453	0.0283	0.507	0.905
BT1-3	4012.8	81.514	22.5	2.031	0.0289	0.496	
BT2-1	4256	210.90	29.8	4.956	0.0848	0.169	0.41
BT2-2	4345.6	257.81	26.3	5.933	0.0731	0.196	
BT3-1	4294.4	502.37	31.4	11.70	0.0942	0.152	0.25
BT3-2	4057.6	278.27	33.3	11.58	0.116	0.123	
BT3-3	4300.8	480.08	33.2	11.16	0.101	0.143	

Table 4.8 Cont'd: Air void Parameters

Specimen	mm Traversed	mm Air	Specific Surface (mm)	Air Void	Void Frequency	Spacing Factor (mm)	SAM No
BU1-1	4115.2	47.321	13.9	1.150	0.0212	0.556	
BU1-2	2771.2	31.715	11.5	1.144	0.0223	0.677	0.47
BU1-3	2790.4	58.504	11.9	2.097	0.102	0.642	
BU2-1	4384	189.98	31.6	4.334	0.0945	0.140	
BU2-2	4358.4	288.62	28.2	6.622	0.0865	0.152	0.16
BU2-3	4236.8	267.94	29.7	6.324	0.144	0.166	
BU3-1	4550.4	538.27	31.1	11.83	0.117	0.0998	
BU3-2	4249.6	534.45	34.2	12.58	0.239	0.122	0.23
BU3-3	3865.6	504.21	35.2	13.04	0.0372	0.0602	
AU1-1	4409.6	96.332	22.5	2.185	0.0370	0.386	0.54
AU1-2	4435.2	117.93	20.3	2.659	0.0782	0.388	
AU2-1	4403.2	278.07	36.0	6.315	0.0824	0.184	0.3
AU2-2	4480	294.08	36.0	6.564	0.193	0.174	
AU3-1	4364.8	552.27	27.7	12.65	0.181	0.0744	
AU3-2	4307.2	504.24	32.7	11.71	0.194	0.0791	0.19
AU3-3	4403.2	508.07	31.8	11.54	0.0310	0.0740	
AT1-1	3078.4	140.89	19.8	2.577	0.0328	0.463	0.32
AT1-2	3251.2	79.518	15.7	2.446	0.106	0.437	
AT2-1	4512	238.93	30.6	5.296	0.109	0.134	
AT2-2	4665.6	278.83	33.1	5.976	0.137	0.131	0.15
AT2-3	4262.4	225.92	35.4	5.300	0.128	0.104	
AT3-1	4388	424.65	34.0	9.723	0.137	0.111	
AT3-2	4288	387.55	30.8	9.038	0.117	0.104	0.26
AT3-3	4780.8	469.10	32.6	9.812	0.0283	0.122	
BC1-1	1561.6	21.949	19.4	1.406	0.117	0.508	0.33
BC2-1	3884.8	244.24	31.8	6.287	0.158	0.122	0.19
BC2-2	4384	220.71	33.6	5.034	0.129	0.0908	
BC2-2	3948.8	203.69	30.5	5.158	0.0212	0.111	

CHAPTER 5: ANALYSIS AND DISCUSSION

This chapter presents the analysis of results from the fly ash adsorption tests, compressive strength test and durability tests as well as discussion of results. It also presents statistical analysis that further supports some of the preliminary conclusions.

5.1 Fly ash Adsorption Tests

The LOI test was not always the best measure of AEA adsorption capacity of ash in Portland cement concrete due to its overestimation of the unburned carbon present in the ash, however it is a useful indicator of unburned carbon. For the LOI test, Plant A fly ash exhibited the highest LOI value of 8.67, which suggests that it contains more unburned carbon than Plant B and Plant M ashes. In contrast to this, the foam index and iodine adsorption tests shows that Plant M fly ash had the highest foam index and iodine number, which also shows that Plant M ash had the highest AEA adsorption capacity. The results from the foam index and iodine adsorption tests suggest that the material combusted during the LOI test cannot be used to reliably predict the AEA demand of ash. These findings are similar to the findings of several other researchers. [13] [53] [79]

To further compare the adsorption capacity of the ashes, the correlations between the characterizations tests are presented in Figure 5.1, Figure 5.2 and Figure 5.3. Figure 5.1 presents the correlation between iodine adsorption and LOI tests, Figure 5.2 presents the correlation between iodine adsorption and foam index test and Figure 5.3 presents the correlation between foam index and LOI test.

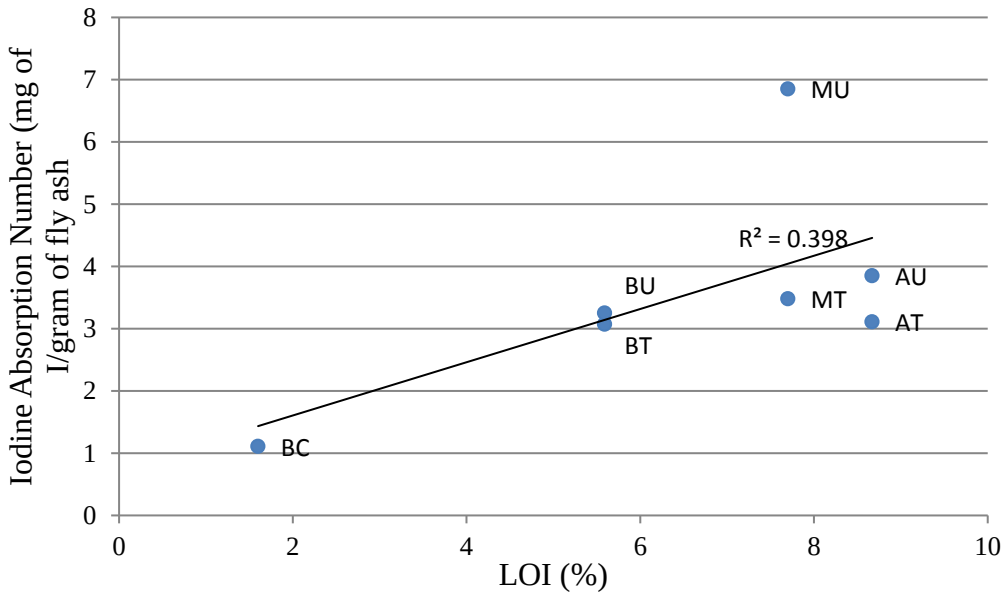

Figure 5.1: Iodine adsorption number vs LOI %

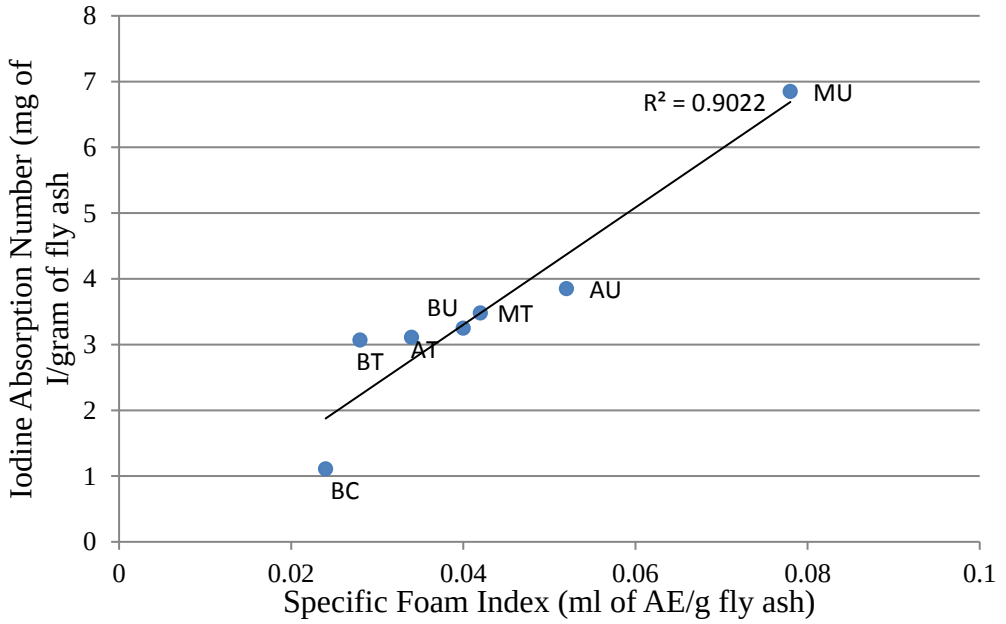

Figure 5.2: Iodine adsorption number vs Specific Foam Index

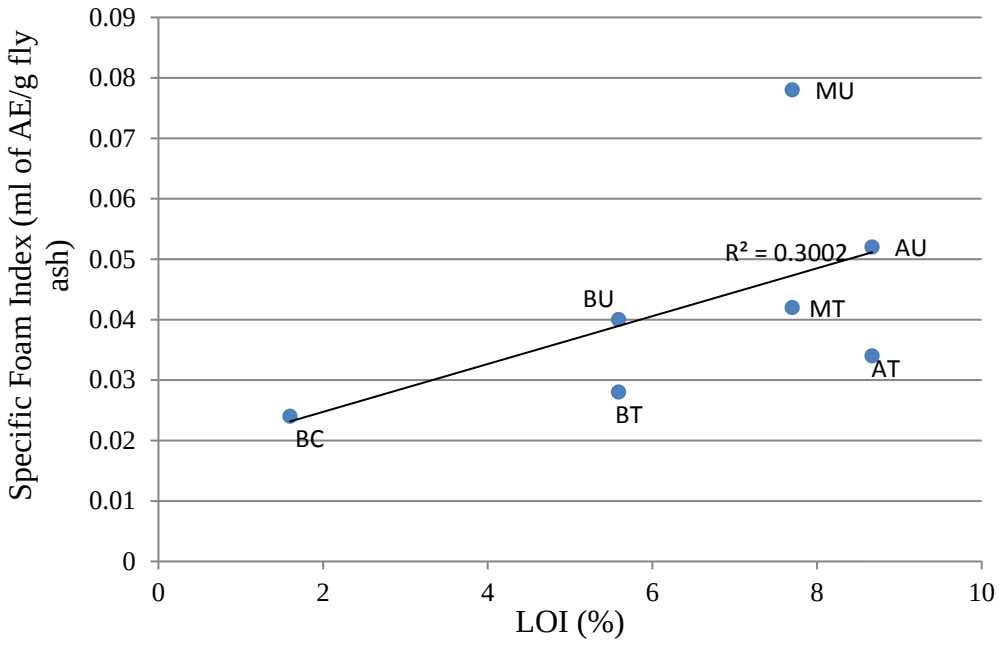

Figure 5.3: Specific Foam Index vs LOI

As shown in Figure 5.1, Figure 5.2 and Figure 5.3 above, LOI test did not show a satisfactory correlation with both foam index and iodine adsorption test. The results of the foam index and iodine adsorption tests were better correlated.

From Figure 5.1 above, it should be noted that treated and untreated ash from the same source have the same LOI values because LOI only estimates the quantity of unburned material in the ash. This material is ignited at 750^{o}C, and since the treatment process does not remove the unburned carbon in ashes, it only reduces the adsorption capacity of the carbon making it ineffective in adsorbing AEA. Unlike LOI, foam index and iodine adsorption relate to the adsorption capacity of the unburned carbon in the ash. This explains why BT, AT and MT ash have different foam index and iodine adsorption number from BU, AU and MU respectively. Each of the treated ashes exhibited a lower foam index and iodine adsorption number than their respective untreated counterparts, demonstrating that the treatment process is effective in rendering the un-burned carbon in ash less absorptive to AEA.

A comparison of LOI and iodine adsorption tests to correctly predict the dosage of AEA needed to stabilize target air content of between 5.5% and 6.5% in fresh concrete is shown in Figure 5.4 and 5.5 respectively.

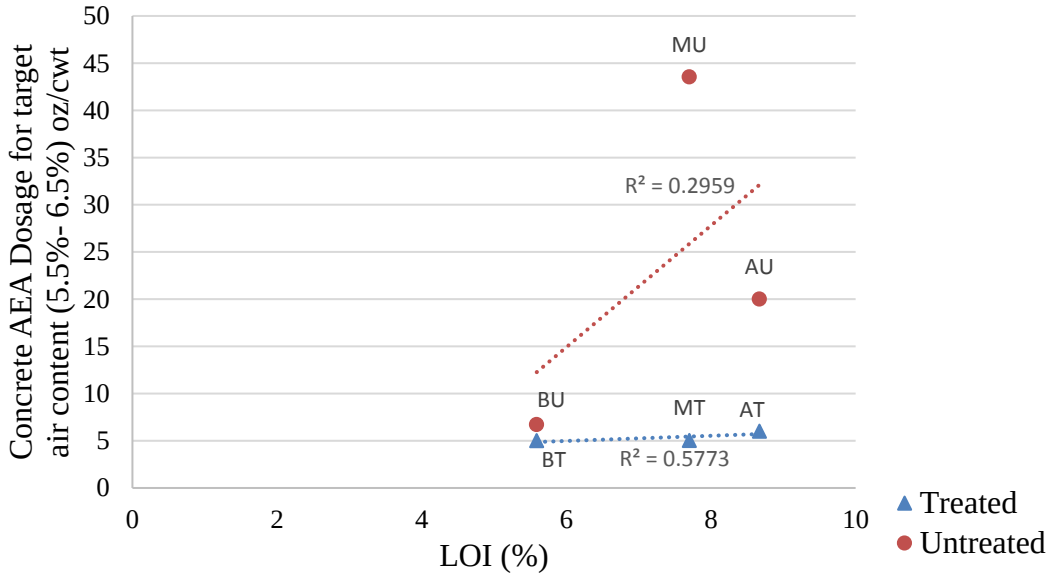

Figure 5.4: Dosage of AEA required to achieve target air (5.5%-6.5%) in concrete versus LOI value of fly ash.

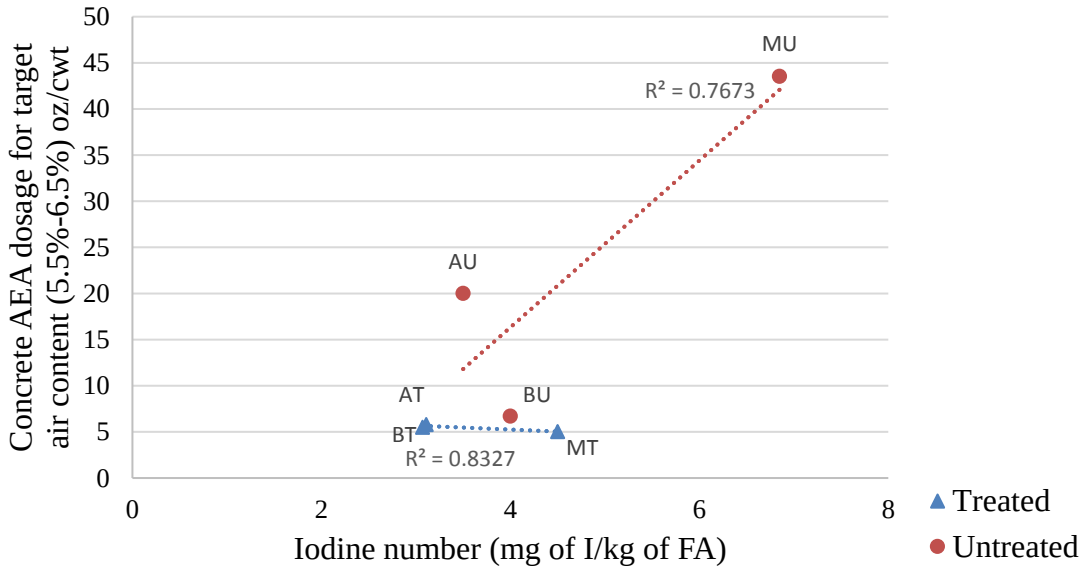

Figure 5.5: Dosage of AEA required to achieve target air (5.5%-6.5%) in concrete versus Iodine number value of fly ash.

It can be seen from the comparison of LOI values and the dose of AEA needed to stabilize target air content in fresh concrete shown in Figure 5.4 above, that the loss on ignition values do not give a good correlation between LOI and dosage required. This further confirms that the LOI test overestimates the unburned carbon present in fly ash. In contrast, the iodine adsorption values are well correlated with the AEA dosage required to stabilize between 5.5 % and 6.5 % air in fresh concrete as shown in Figure 5.5. Since the R^2 value is closer to 1, this suggests that the iodine values are a good indicator of the adsorption capacity of un-burned carbon in the fly ashes and can be used to predict dose of AEA needed in the field.

5.2 Variable Air Dosage

The relationship between AEA dosage and air content have been reported by various researchers to consistently fit a linear trend [13] [60]. However, for off-spec fly ash, this is not the case because it's difficult to predict the air content and dosage relation. As illustrated in Figure 5.6 below, the relationship between air entraining admixture (AEA) dosage and air content generated was linear for the Plant M treated ash while that for the Plant M untreated ash was scattered and inconsistent. An increase in AEA dosage from 1.5 oz/cwt to 43.56 oz/cwt led to an increase of air content from 1.6 % to 5.9 %, whereas reducing the dosage from 43.56 oz/cwt to 36.85 oz/cwt generated higher air content of 7.8 %. Also from Figure 4.4 through Figure 4.6 in Section 4.2, to stabilize 5 % air the range of AEA dosage for treated ashes is 5 oz/cwt - 10 oz/cwt while that for untreated ashes is 7 oz/cwt – 35 oz/cwt which is too wide to predict the quantity needed. Additionally, the recommended dosage rate for Master Air AE 200 is between 0.125 to 1.5 oz/cwt (8-98 mL/100 kg) of cement [80], this means that to stabilize target air content of between 5.5 % -6.5 %, about twenty-

eight times the recommended dosage will be needed. To achieve proper air content in untreated ashes, the required dosage of AEA is too high which is impractical.

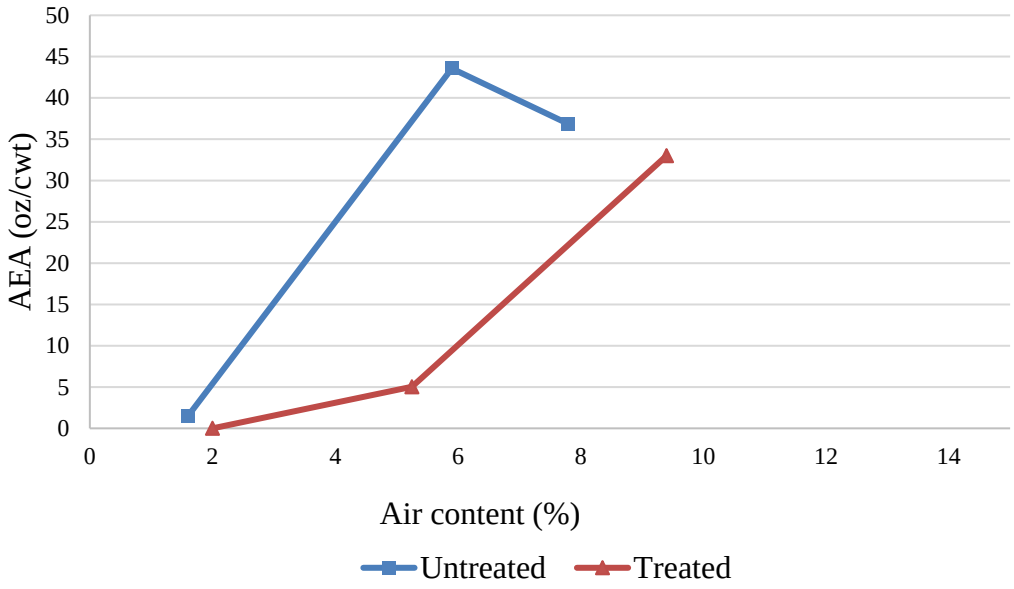

Figure 5.6: Air dosage vs air content generation relationship for Plant M treated and untreated Ash.

Additionally, Table 5.1 shows the linearity of the AEA dosage used and the air content generated. The AEA dosage and air content is shown graphically in section 4.2. For plant A, the AEA dosage vs air content generated for treated ash has an R^2 value of 96.1% while the untreated ash has an R^2 value of 95.4%. This trend was the same for all the ashes investigated. It can be concluded that it is easy to predict the quantity of AEA needed for concrete made with treated ashes to be frost resistant.

Table 5.1: R^2 value of AEA vs Air Content Generated Graph

Ash	**Plant A treated**	**Plant A untreated**	**Plant B treated**	**Plant B untreated**	**Plant B control**	**Plant M treated**	**Plant M untreated**
R^2 value (%)	96.1	95.4	96.4	96.4	99.4	90.6	80.9

5.3 Strength and Surface Resistivity

The relationship between surface resistivity and air content is presented in Figure 5.7 and Figure 5.8. Figure 5.7 shows the relationship between 28 day surface resistivity and air content while Figure 7.8 shows the relationship between 90 day surface resistivity and air content. As shown in Figure 5.7, the typical trend that can be seen is that the surface resistivity for all the ashes increased as air content of the mixture increased. However, this trend is not true for the Plant M untreated mixture. For the Plant M untreated mixture, the surface resistivity increased between the low air content and target air content of Plant M untreated mixture but decreased at the higher air content mixture of Plant M. These could be due to variations in the mixing and making of the cylinders. These results were taken from averaging four different measurement points per cylinder, and then averaging the total resistivity of three cylinders.

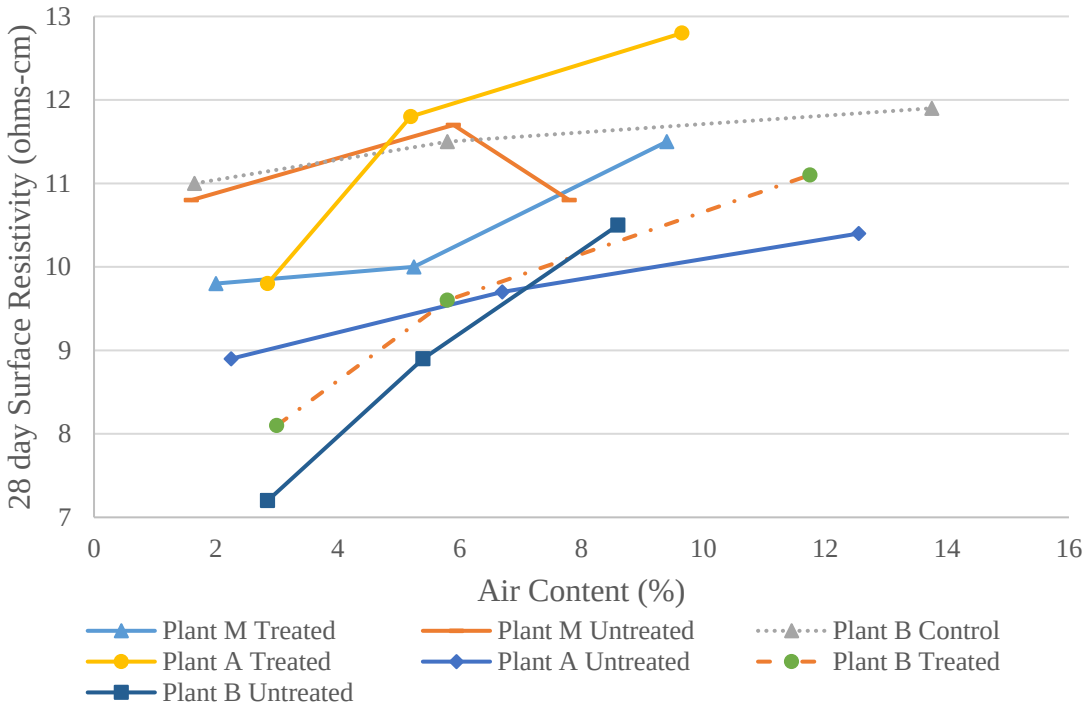

Figure 5.7: Relationship between 28 day surface resistivity and air content

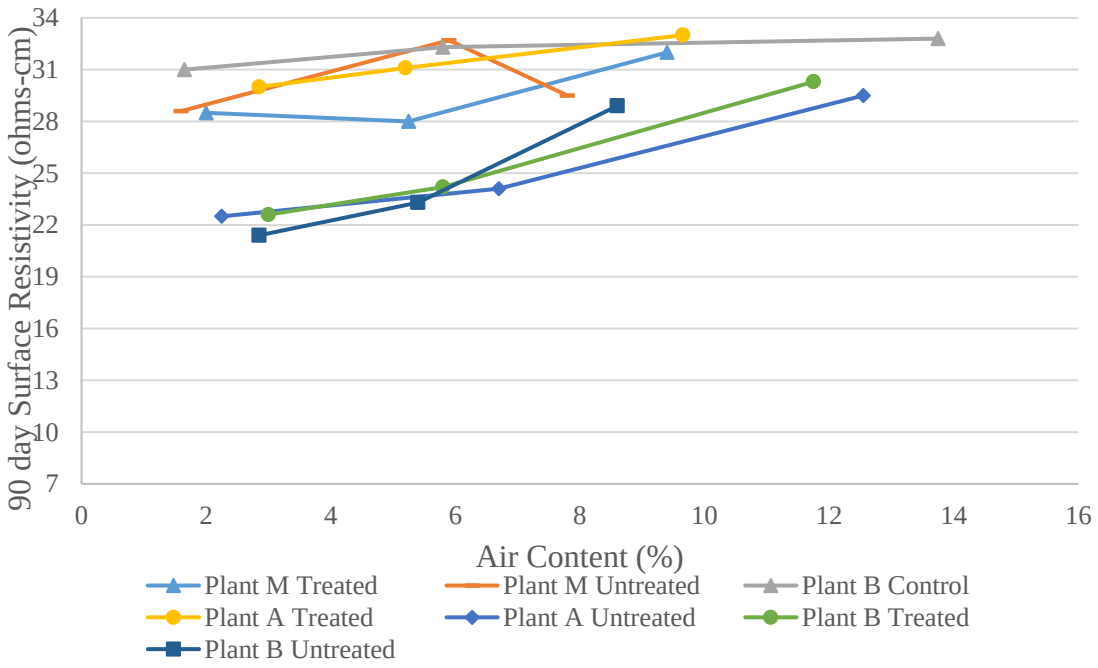

Figure 5.8: Relationship between 90 day surface resistivity and air content

As shown n Figure 5.8, just like the 28 day resistivity, the typical trend that can be seen is that the surface resistivity for all the ashes increased as air content of the mixture increased. However, this trend is not true for Plant M untreated mixture. For Plant M untreated mixture, the surface resistivity increased between the low air content and target air content of Plant M untreated mixture but decreased at the higher air content mixture of Plant M. This could be due to variations in the making of the cylinders because air is a good insulator, it is expected that the resistivity will increase as air content increases. Also, as the age of the concrete increases, the resistivity increases which shows that the concrete has low susceptibility to chlorine ion penetration. These results were obtained by averaging four different measurement points, two times per cylinder for a total of eight measurements and then averaging the total resistivity of three cylinders.

Since the concrete mixtures do not have a constant air content, comparison between the compressive strength gained cannot be easily made between treated and untreated ashes. As shown in Figure 5.9 below, concrete mixtures with higher air contents typically have lower strength compared to low air content mixtures.

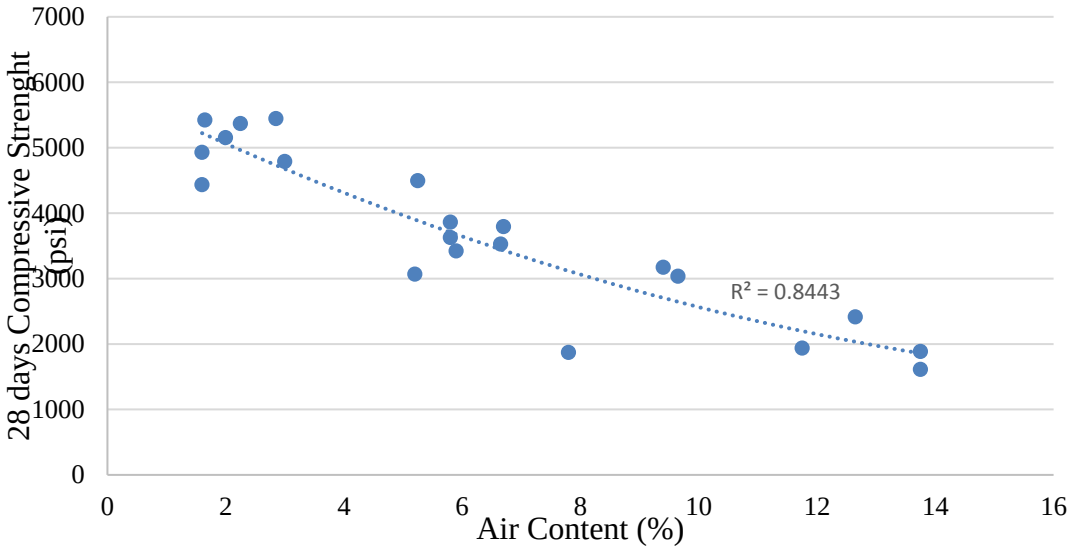

Figure 5.9: Relationship between 28 days compressive strength and air content

However, to analyze the strength of the mixtures an approach based on linear regression of the strength and air content is used. This is illustrated in Figure 5.9 through Figure 5.16. It should be noted that a generally observed for strength reduction in concrete is about 5 % or 250 psi per 1% increase of air content [81] [82]. For concrete without fly ash, 28-day strength is usually used for comparison. However, because of the retarding effects of fly ash on strength, it is more usual to use 56-day strength for comparison, hence the 56-day strength of all the mixtures was used in this analysis.

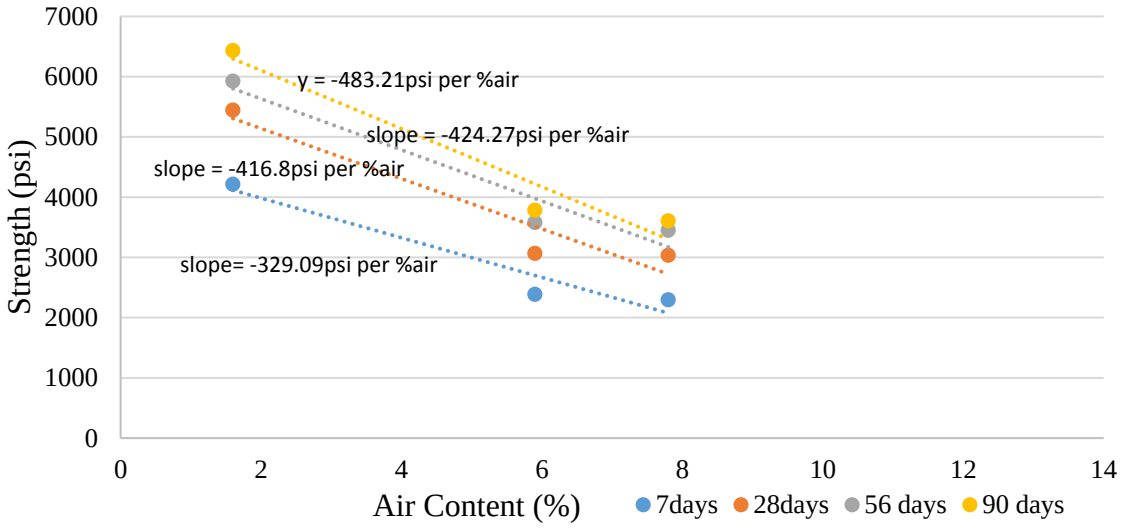

Figure 5.10: Relationship between compressive strength and air content for Plant M Untreated

As illustrated in Figure 5.10, the relationship between strength and air content for Plant M untreated was a reduction of 424 psi for every 1 % increase in air content. If the best fit line is interpolated to 6 % air content (target air content), the average 56-day strength would be about 3900 psi. A similar approach can be used for Plant M treated ash as shown in Figure 5.11 below.

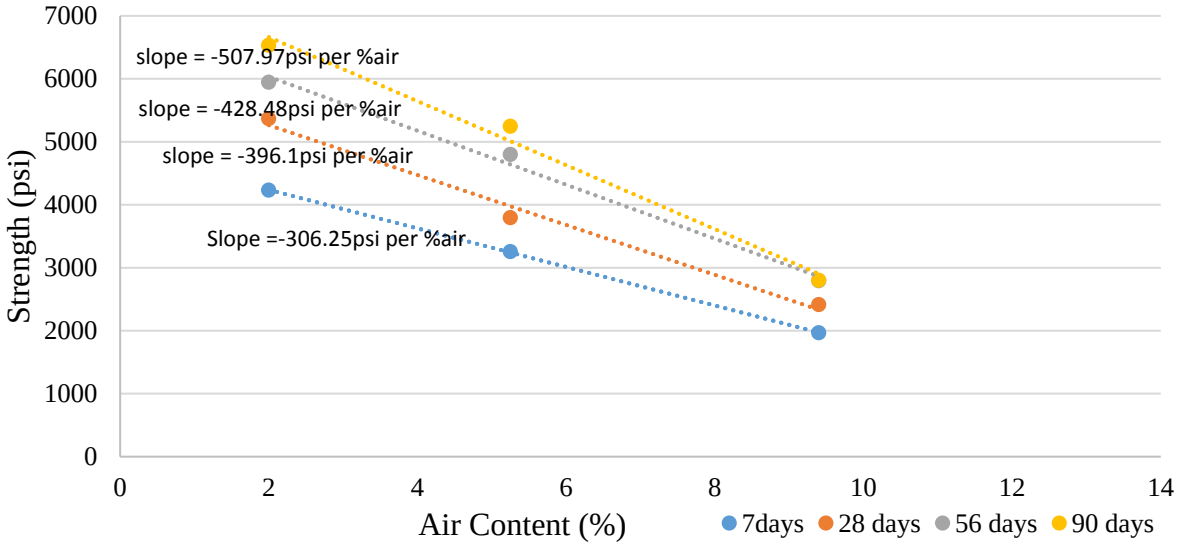

Figure 5.11: Relationship between compressive strength and air content for Plant M treated

Referring to Figure 5.11, the 56-day strength of Plant M treated ash has a high reduction of 428 psi per 1% increase in air content. Interpolation of the trend line to 6% air content means that the average compressive strength would be about 4300 psi. This shows that the treatment process had no effect on the compressive strength of the Plant M treated mixture.

In a similar approach, Figure 5.12 and Figure 5.13 show the relationship between compressive strength and air content for Plant A untreated and treated ash respectively.

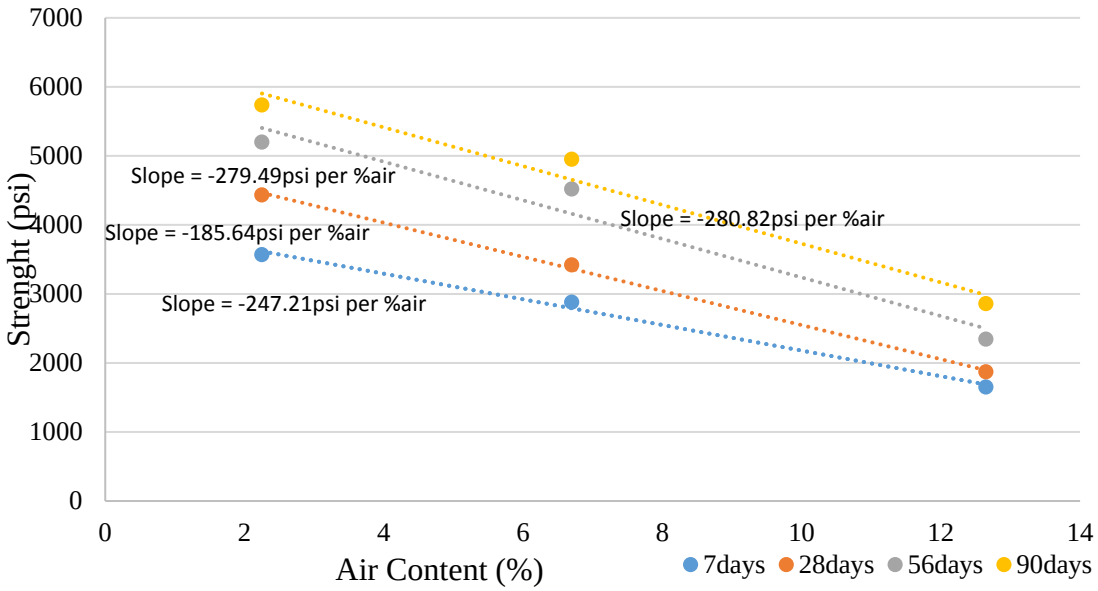

Figure 5.12: Relationship between compressive strength and air content for Plant A untreated ash

As shown in Figure 5.12, the relationship between strength and air content for Plant A untreated ash was 280 psi reduction for every 1% increase in air content. Interpolation of the trend line to 6% air content means the mixture would have an average 56-day strength of about 4400 psi.

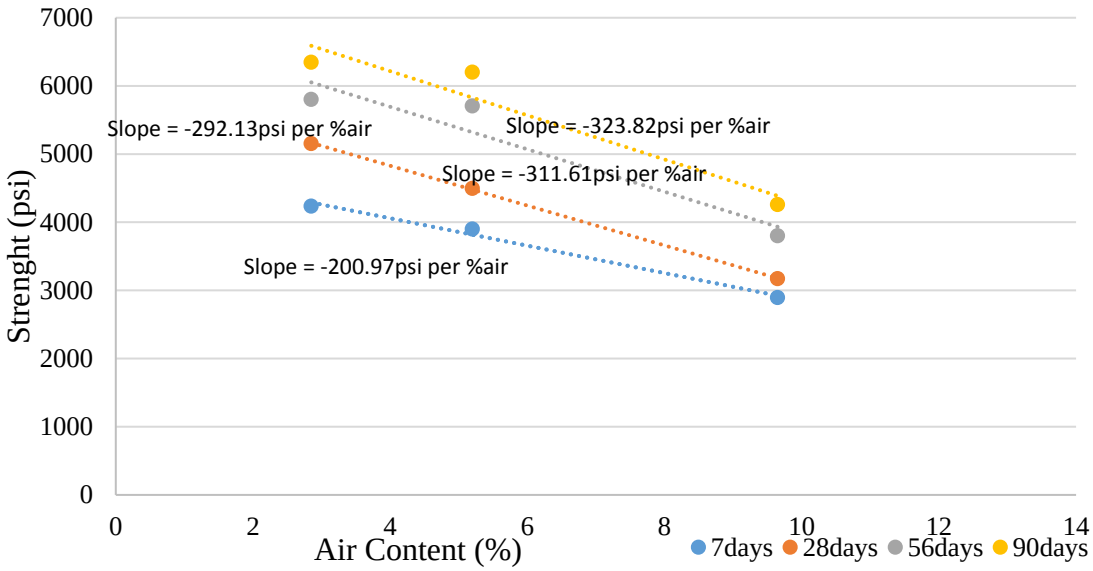

Figure 5.13: Relationship between compressive strength and air content for Plant A treated ash

Referring to Figure 5.13, the air content and strength relationship for Plant A treated ash was 312 psi for every 1% increase in the air content. By interpolating the trend line to 6% air content, the 56-day compressive strength would be about 5000 psi. This shows that the treatment process did not compromise the compressive strength of the concrete. The air content and strength relationship for Plant B control, untreated and treated ashes is illustrated in Figure 5.14, Figure 5.15 and Figure 5.16 respectively.

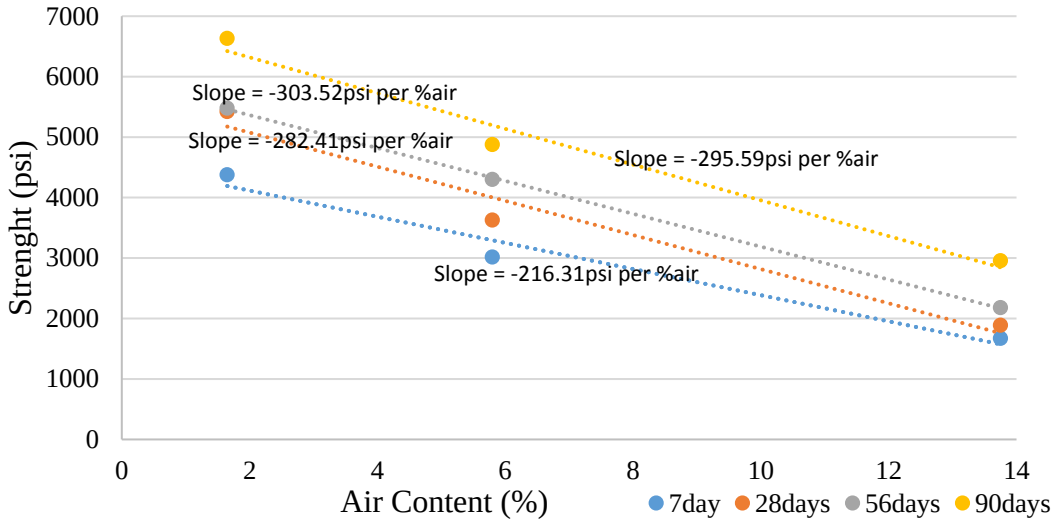

Figure 5.14: Relationship between compressive strength and air content for Plant B control

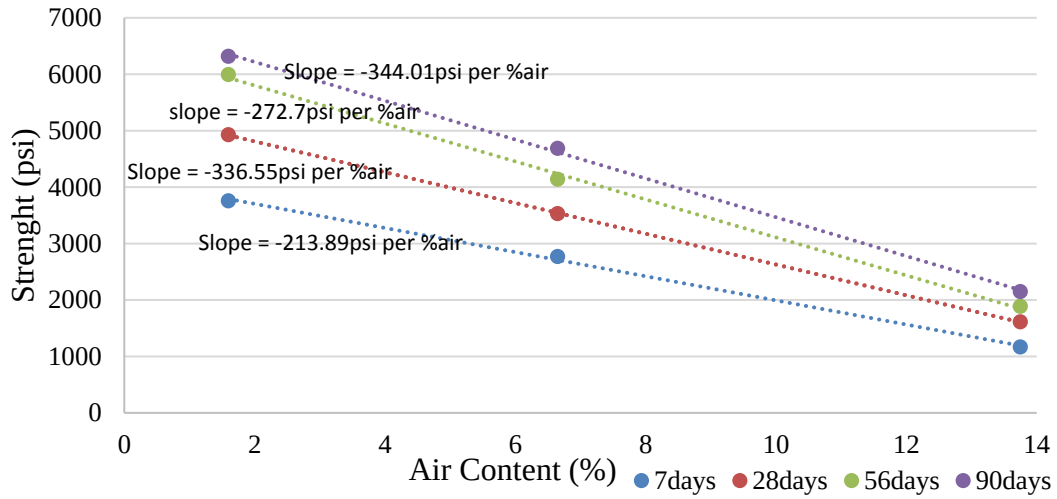

Figure 5.15: Relationship between compressive strength and air content for Plant B untreated

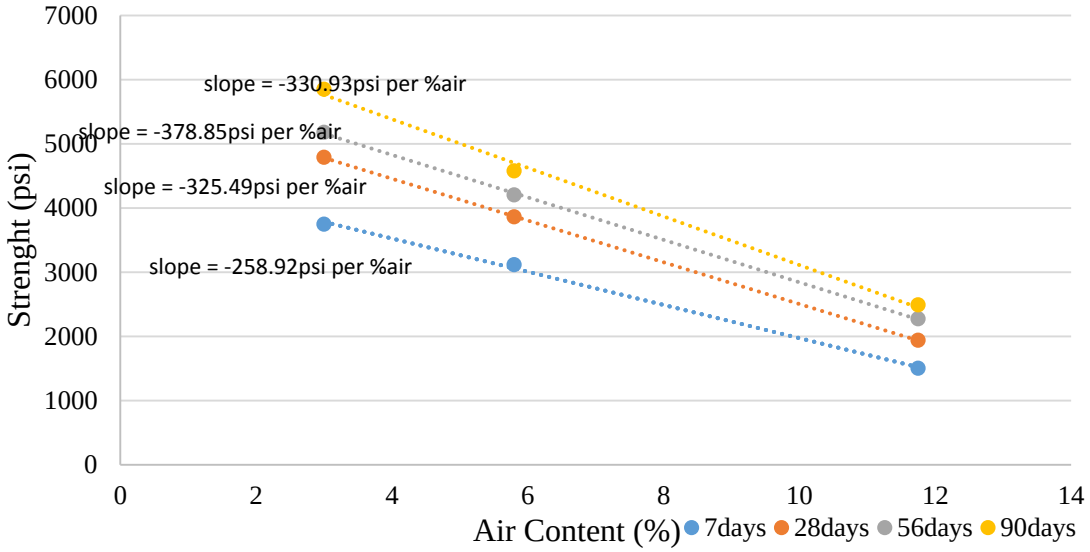

Figure 5.16: Relationship between compressive strength and air content for Plant B treated

From Figure 5.14 above, the relationship between air content and compressive strength for Plant B control mixture was a reduction of 304 psi for every 1 % increase in air content. If the trend line is interpolated to 6 % air content, this implies that the 56-day compressive strength would be 4200 psi. Similarly, from Figure 5.15, the relationship between air content and compressive strength for Plant B untreated ash mixture was a reduction of 273 psi for every 1 % increase in air content. Interpolating the trend line to 6 % air content would imply that the 56-day compressive strength would be 4400 psi. Lastly, from Figure 5.16, the relationship between air content and strength for Plant B treated ash mixture was a reduction of 379 psi for every 1 % increase in air content. If the trend line is interpolated to 6 % air content, the 56-day compressive strength would be 4200 psi. Figure 5.17 shows a bar chart of the interpolated 6 % air content compressive strength of all the ash types at 56-day.

Overall, the average compressive strength exceeds 4000 psi for all the mixtures. There is no indication to suggest that the treatment process influenced the

compressive strength. Treating ash to reduce the adsorption capacity of AEA by unburned carbon does not compromise the strength of the concrete produced.

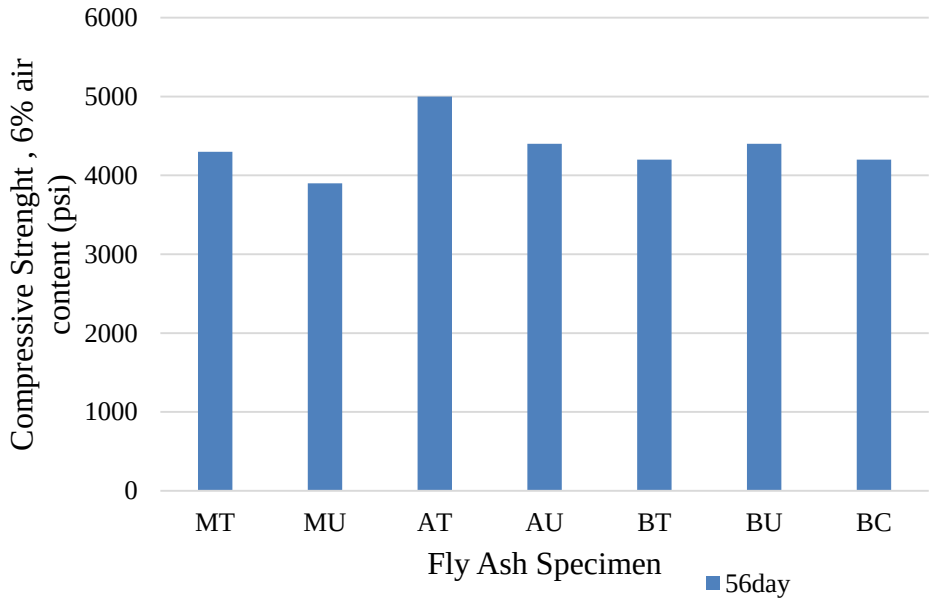

Figure 5.17: 56-day compressive strength of the interpolated 6% air content for all ash specimen

5.3.1 Statistical Analysis for Compressive Strength

To determine the effect of production variables on the resulting output variables and to confirm trends observed from direct pairwise comparison above, a statistical analysis procedure called analysis of covariance (ANCOVA) was conducted. ANCOVA is used to test main effects and interaction of categorical variable with continuous dependent variable, controlling for effects associated with continuous variable. In other words, ANCOVA allows to compare one variable in two or more groups considering the variability of other variables where the control variable is called the covariates. This analysis technique blends analysis of variance (ANOVA) and regression by estimating the regression of covariates on the dependent variable first, after which the dependent variable scores and means are adjusted to remove the linear effects of covariates before analysis of variance is carried out on

these adjusted values. Applying the ANCOVA technique to this study allowed the impact of changes in ash type (whether treated or untreated), AEA dosage and air content to be on the compressive strength to be explored.

For this project, the ANCOVA analysis using general linear model fitting tools in Minitab 17[84] statistical analysis software. As described previously, the use of ANCOVA accommodates for the effects of air content and AEA dosage on observed compressive strength allowing the effect of ash type on strength to be fully explored. The continuous variables of air content and AEA dosage were treated as covariates while ash type was treated as categorical variable. The variance inflation factor (VIF) provides an index that measures how much variance of an estimated regression coefficient is increases because of multicollinearity. Multicollinearity results in unstable parameter estimates which makes difficult to assess the true effect of independent variables on dependent variable. A covariate is an independent continuous variable which also can increase the accuracy of the analysis

The summary of the results of the ANCOVA analyses carried out is presented in Table 5.1. From the analyses, the variance inflation factor (*VIF*) for each of the factors considered were each less than 10, which indicates that multicollinearity did not influence the regression results. In statistical analysis, a factor is significant if the *p-value* is less than 0.05. Consequently, the p-values for the air content, ash type and AEA dosage are 0, 0.339 and 0.179 respectively which indicates that only the air content was the only statistical significant factor in the compressive strength results. The ash type whether treated or untreated was not statistically significant as observed in general trends in previous section. In summary, the ANCOVA model for compressive strength had an R^2 value of 91.98 % which shows that approximately 92

% of the observed variation can be explained by the variables included in the analysis (AEA dosage, ash type, and air content).

Table 5.2: Summary of ANCOVA analyses

Source	df	Adjusted sum of squares	Adjusted mean of Square	F-value	P value	VIF
Air content	1	10088717	10088717	75.96	0.000	1.95
AEA dosage	1	128956	128956	0.97	0.339	2.26
Ash type	1	467069	467069	3.52	0.l79	1.27
Error	16	2125113	132820			
Total	19	26507826				
Model Equation						
Ash type Untreated Strength = 5463 - 306.7 Air - 9.06 AEA Treated Strength = 5809 - 306.7 Air - 9.06 AEA						

5.4 Freeze Thaw

5.4.1 Durability Factor

The primary objective of this portion of the study was to determine the relative resistance to cyclical freezing and thawing of concrete specimens made with treated ashes as a percentage replacement of cement compared to untreated ashes. This discussion is centered on comparison of durability factor (DF) of specimens made with the same type of ash.

Figure 5.18 through Figure 5.20 show the durability factor versus freeze thaw cycles for various ashes. ASTM C666 [76] does not explicitly state DF limit for satisfactory performance in the test. However, many research studies have identified DF values from the ASTM C666 test that correlate to satisfactory performance of concrete in the field. One research study identifying a threshold DF was performed

by Cordon and Merrill, who indicate that DF above 80% meets desired performance standards [83].

As seen in Figure 5.18, the DF for Plant A untreated mixture with target air content (AU2) decreased more slowly than the Plant A treated mixture with target air content (AT2). It is not probable that the treatment had any effect on the freeze thaw durability but the more probable reason for this lies in the difference in air content between AU2 and AT2. This difference in rate of change of DF could be attributed to AU2 slightly having higher air content than AT2, however both mixtures achieve a durability factor greater than 80 %. In the same vain, the DF of Plant A untreated mixture with low air content (AU1) decrease rapidly compared to Plant A treated mix with low air content (AT1). After 30 cycles, the DF of AU1 falls below 60% while AT1 progresses to 240 cycles before falling below 60% which is the cessation point as recommended by ASTM C666 [76]. In general, all the Plant A ash mixtures with fresh air content above 5 % showed good durability while the Plant A mix with fresh air contents below 5 % had poor durability as expected.

Figure 5.19 shows the DF versus freeze and thaw cycle for Plant M ash. The air content and compressive strength of each mixture is included in the legend. The average rate of change of DF of Plant M treated mixture with target air content (MT2) is low compared to the untreated mixture (MU2). Conversely, this is different for the high air content mixtures, the rate of change of DF for MU3 is higher than the MT3 mixture, however all the mixtures above 5 % fresh air content showed good durability performance over the 300 freeze-thaw cycles. On the other hand, the low air content mixtures for both Plant M treated and untreated mixture showed poor durability and low freeze thaw resistance as expected.

Critical to the freeze thaw performance is the quality of the air content of the specimens and the strenght. The amount and quality of the air void can greatly contribute to the freeze thaw resistance of the concrete specimens. Some mixtures definitely had higher strengths than others, and would therefore have the potential to resist freeze-thaw stresses via the concrete matrix, not just air. Overall, all the specimens with fresh air content above 5% had good freeze and thaw durability.

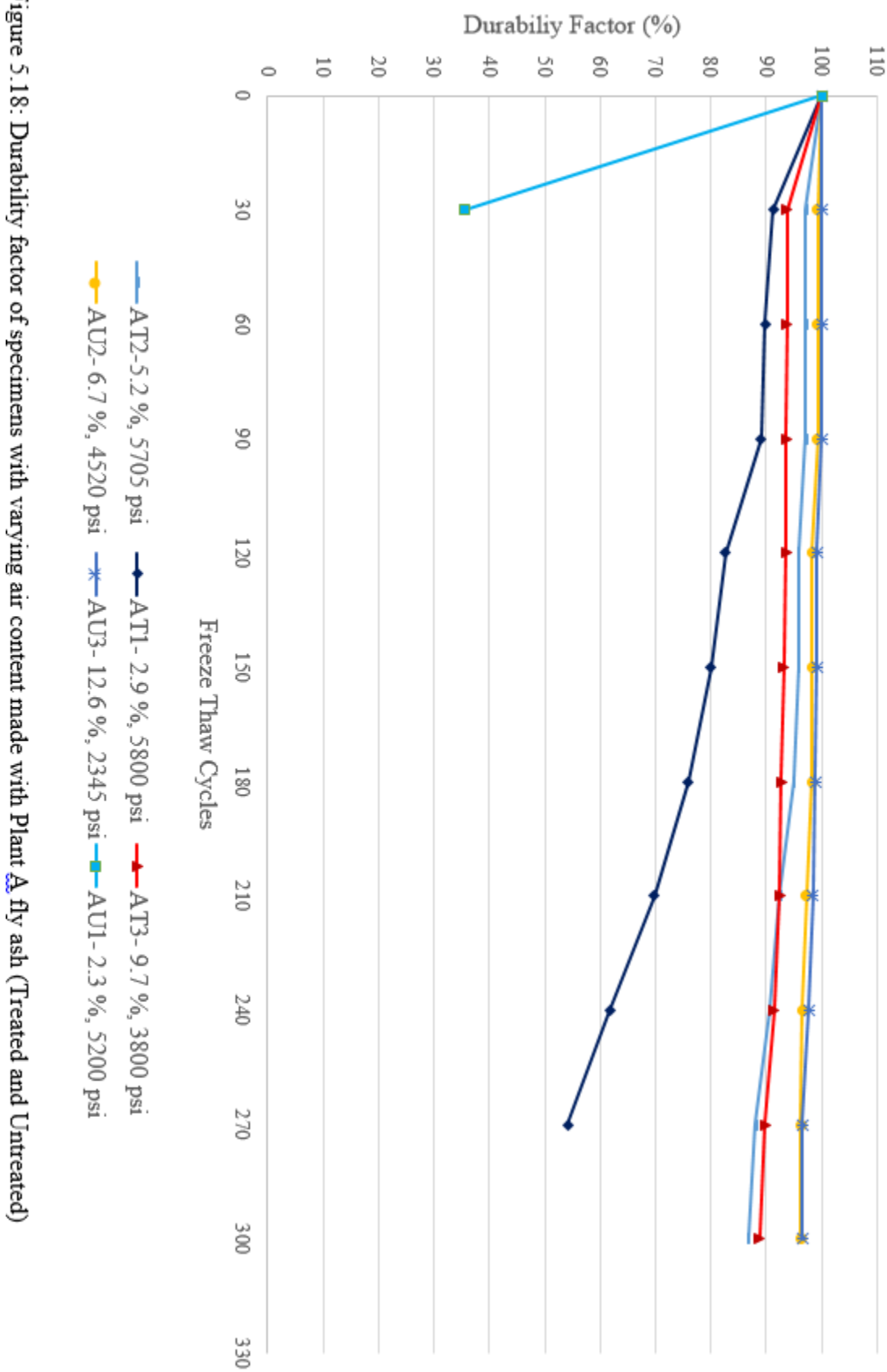

Figure 5.18: Durability factor of specimens with varying air content made with Plant A fly ash (Treated and Untreated)

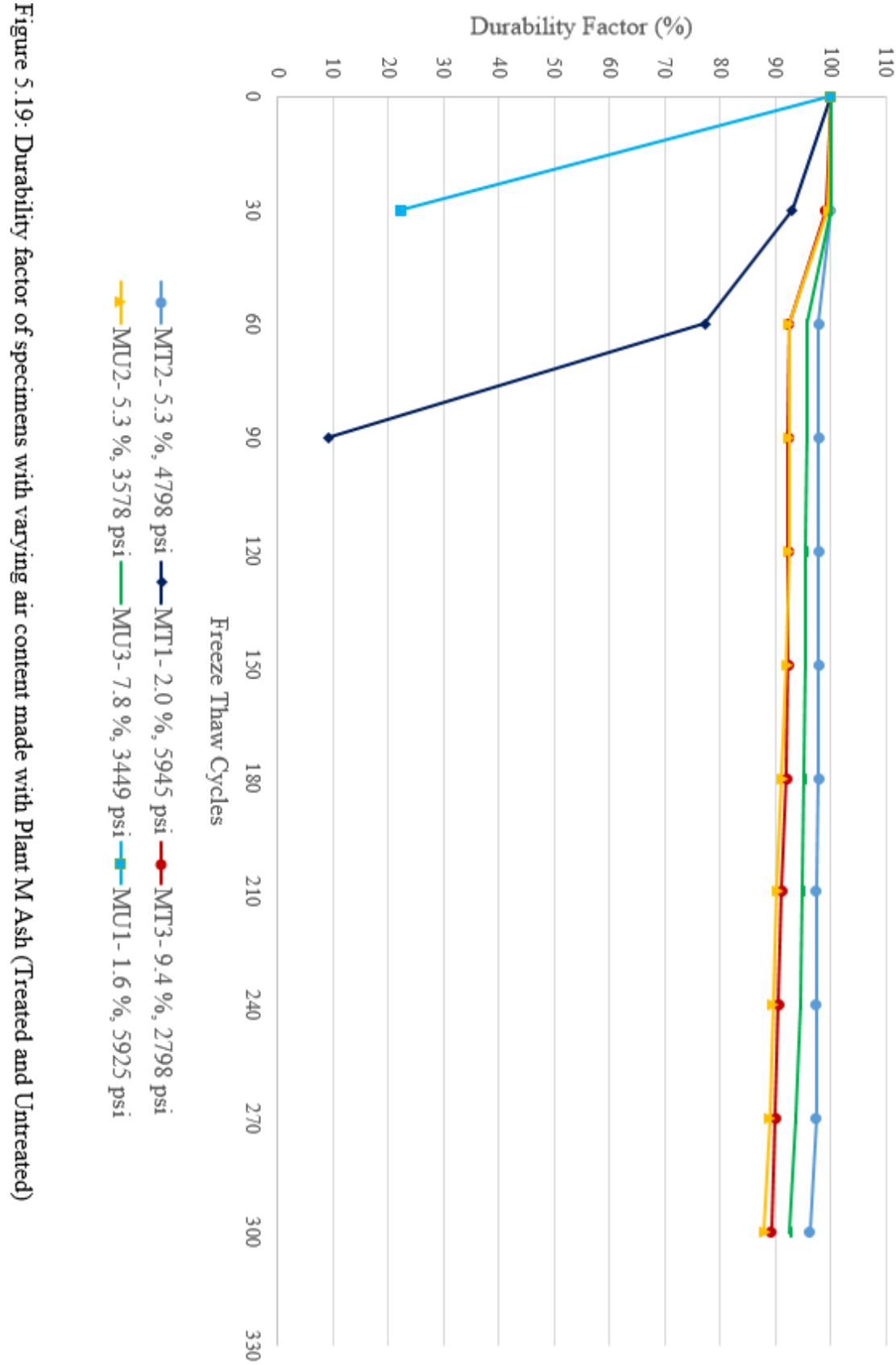

Figure 5.19: Durability factor of specimens with varying air content made with Plant M Ash (Treated and Untreated)

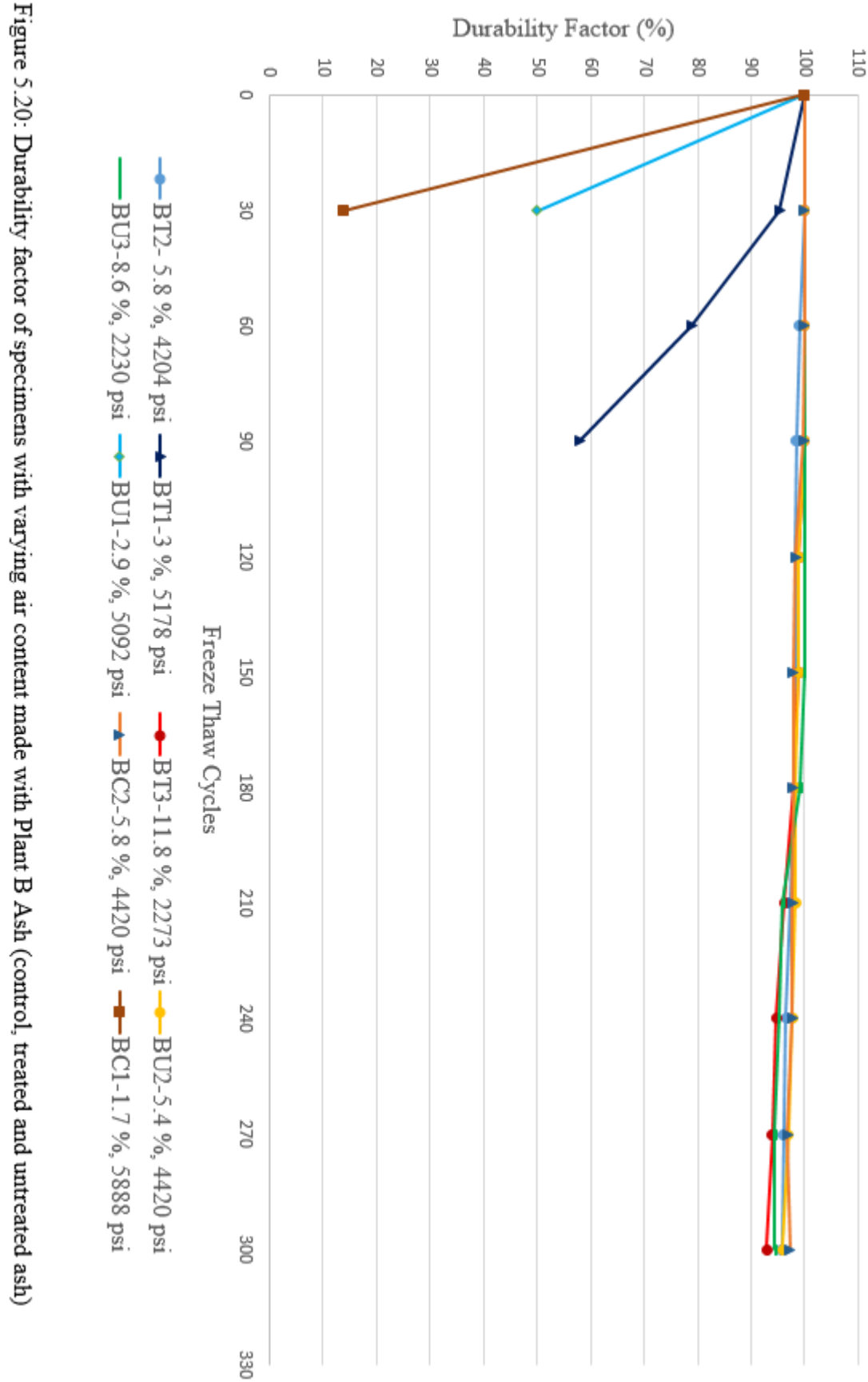

Figure 5.20: Durability factor of specimens with varying air content made with Plant B Ash (control, treated and untreated ash)

5.4.2 Statistical Analysis for Durability Factor

ANCOVA analysis was also performed for response of durability factor (DF) using general linear model fitting tools in Minitab 17[84] statistical analysis software, to assess the effect of air content and AEA dosage (continuous variables) on durability factor allowing for the influence of ash type (treated or untreated) to be explored. Compressive strength was identified as a predictor which highly correlated with other predictors with a VIF value of greater than 10, hence the compressive strength was removed from the model by the software model algorithm due to multicollinearity. The continuous variables of air content and AEA dosage were treated as covariates, while ash type was treated as categorical variable.

The summary of the results of the ANCOVA analyses carried out is presented in Table 5.2. From the analyses, the variance inflation factor (VIF) for each of the factors considered were less than 10, indicating that multicollinearity did not influence the regression results. In statistical analysis, a factor is significant if the *p-value* is less than 0.05. Consequently, the p-values for the air content, ash type and AEA dosage are 0.005, 0.579 and 0.585 respectively, indicating that only the air content was a statistically significant factor influencing the DF. The ash type whether treated or untreated was not statistically significant as observed in general trends in previous section. In summary, the ANCOVA model for DF had an R^2 value of 61.77 % which shows that approximately 62 % of the observed variation can be explained by these variables included in the analysis.

Table 5.3: Summary of ANCOVA analyses

Source	df	Adjusted sum of squares	Adjusted mean of Square	F-value	P-value	VIF
Air content	1	7989.7	7989.7	10.39	0.005	1.95
AEA dosage	1	246.5	246.5	0.97	0.32	2.26
Ash type	1	239.0	239.0	3.52	0.31	1.27
Error	16	12299.5	768.7			
Total	19	32173.8				
Model Equation						
Ash type Untreated D.F = 5.5 + 8.63 Air + 0.396 AEA Treated D.F = 13.3 + 8.63 Air + 0.396 AEA						

5.4.3 Mass Loss

Figure 5.21 through Figure 5.24 give the mass loss after different cycles of freeze thaw cycles for Plant M, Plant A, Plant B (treated and untreated) and Plant B control ash respectively. One trend that can be observed was that all the specimens with low entrained air experienced mass gain in the early stage of the freeze thaw cycles before failure except for AT1. As stated earlier, this mass gain is attributed to concrete cracks formation because of freeze and thaw action on the specimens, this allowed the specimens to absorb more water through the cracks.

As shown in Figure 5.21 through Figure 5.24, the influence of freeze thaw on the mass loss for treated specimens with target air content (mixtures designated with '2', for instance: MT1-2) were lesser compared to the untreated counterpart. This trend was observed for all the ash types except for BT2 and BU2, which both seemed to be experiencing mass loss at the same rate. The mass variation is caused my movement in and out of water which leads to surface scaling of the concrete specimens.

The test results show that the average mass loss of BC2 which is the control mixture was 12.38 percent compared with 4.6 percent for BT2 and 5.37 percent for BU2 after 300 cycles of freeze-thaw. For the other specimens, the maximum of mass loss was 18.78 percent after 300 cycles of freeze-thaw which occurred in AT3. It should be noted that since air and mass are related, the specimens with highest masses failed the test due to the low air content in the mixture. Overall, the mass loss did not present any trend in relation to ash type whether treated or untreated.

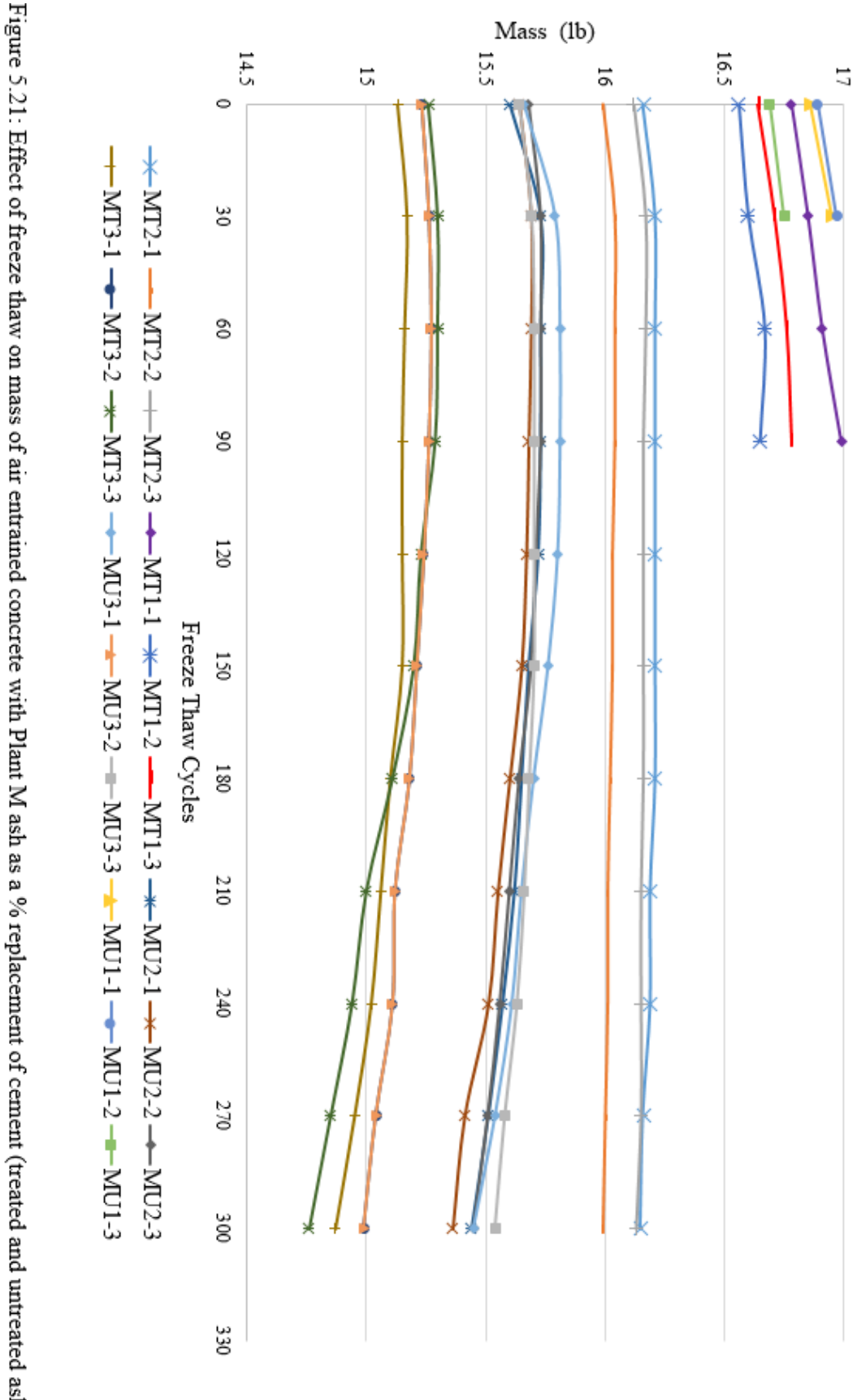

Figure 5.21: Effect of freeze thaw on mass of air entrained concrete with Plant M ash as a % replacement of cement (treated and untreated ash)

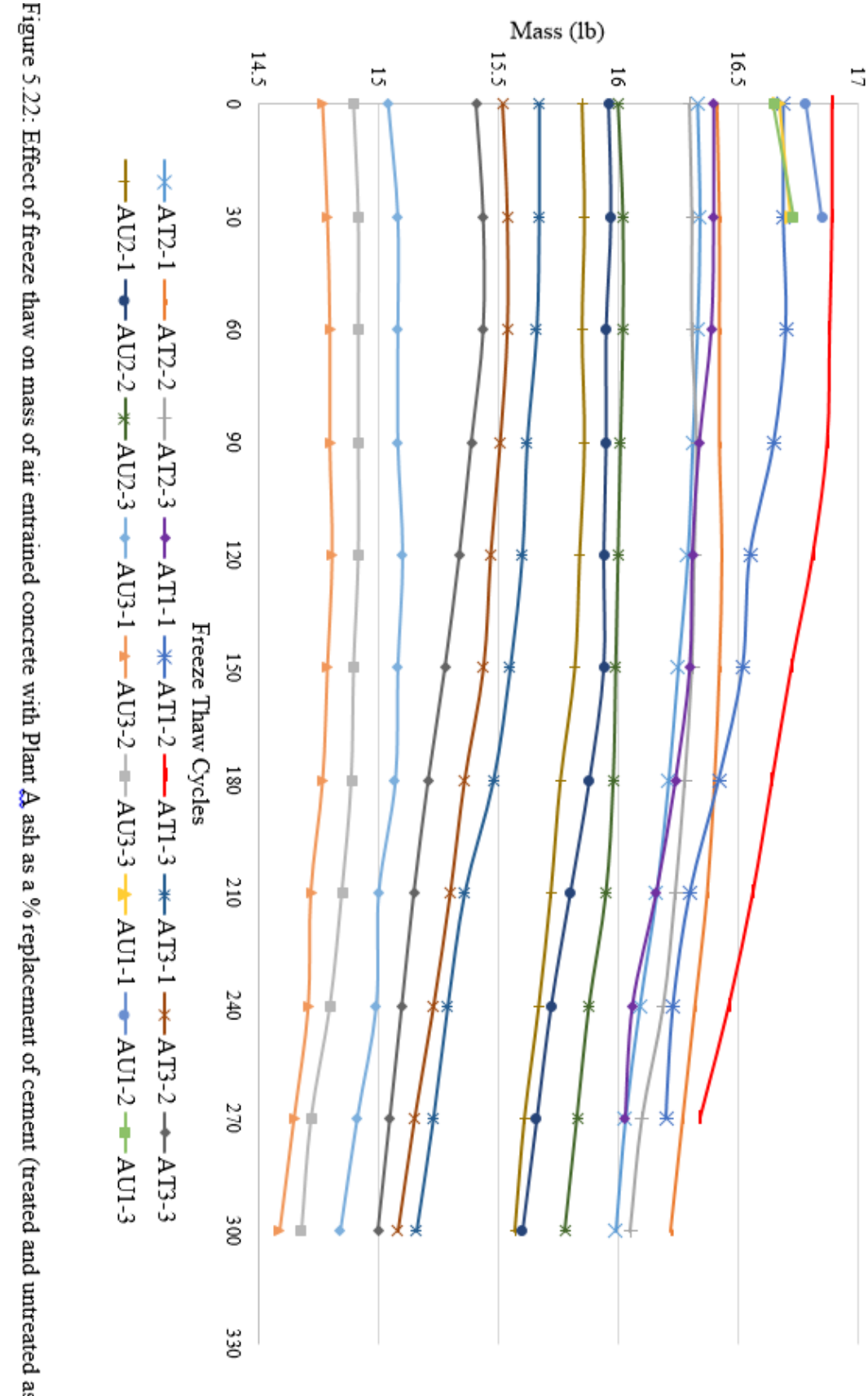

Figure 5.22: Effect of freeze thaw on mass of air entrained concrete with Plant A ash as a % replacement of cement (treated and untreated ash)

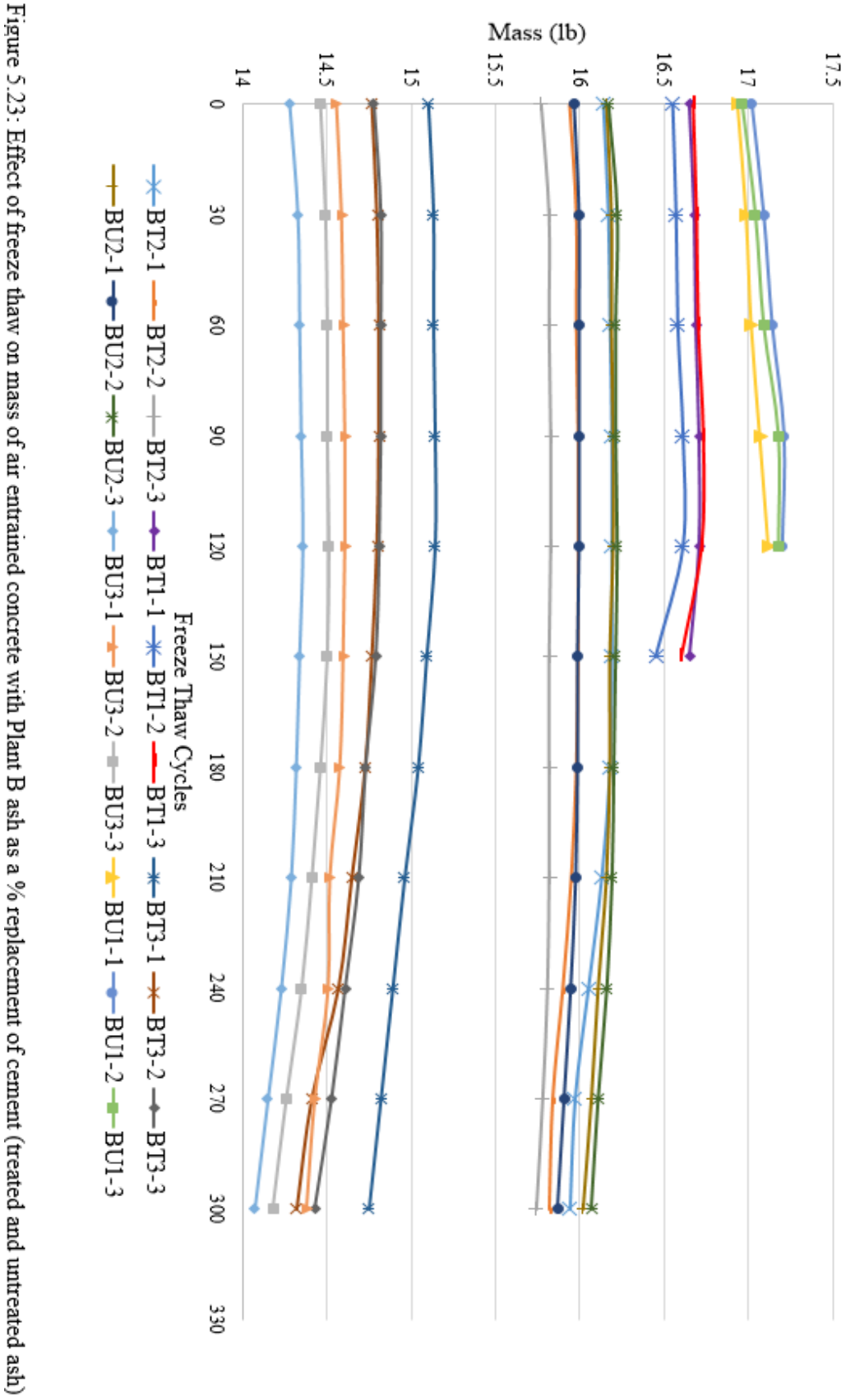

Figure 5.23: Effect of freeze thaw on mass of air entrained concrete with Plant B ash as a % replacement of cement (treated and untreated ash)

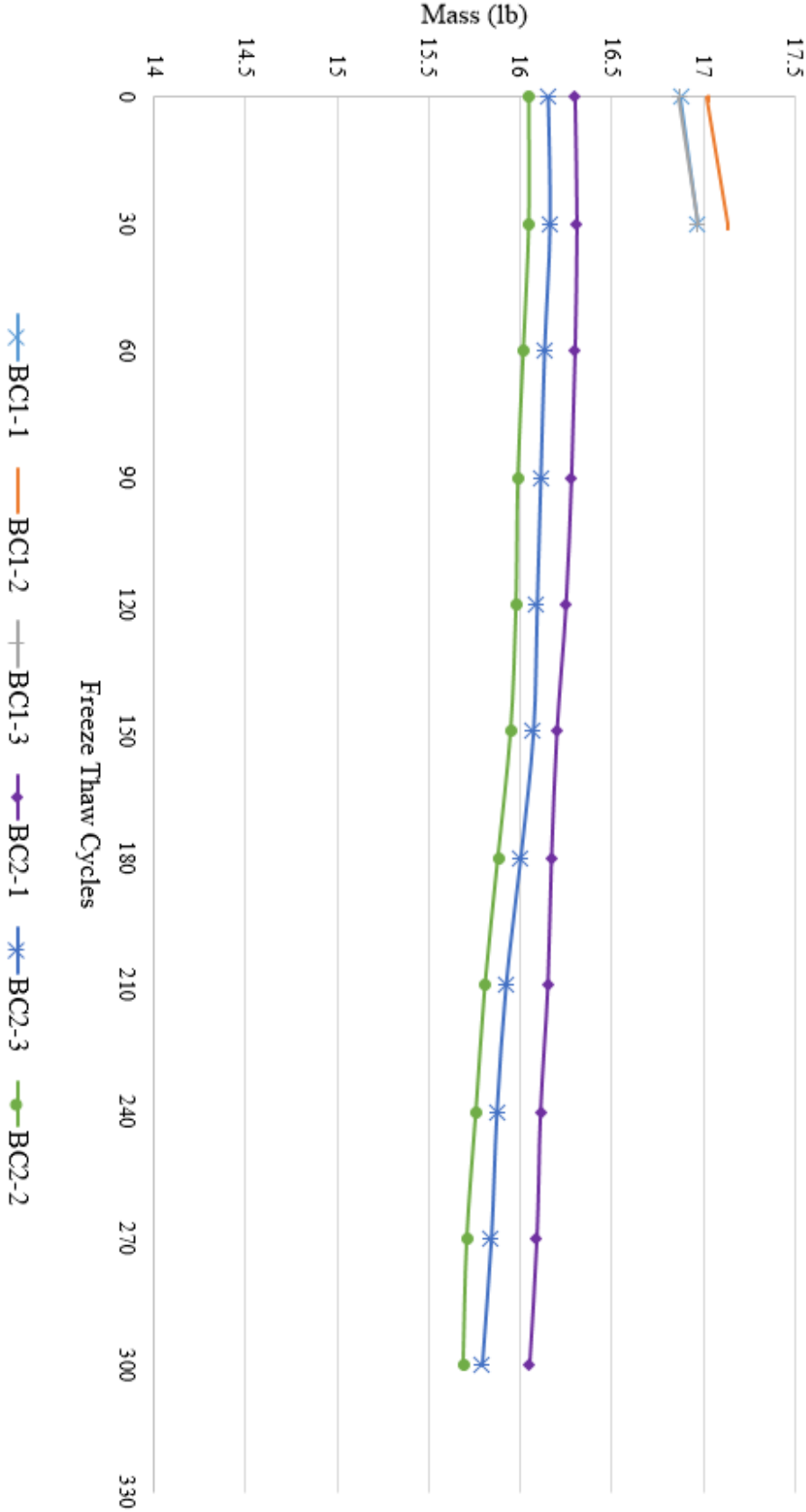

Figure 5.24: Effect of freeze thaw on Mass of air entrained concrete with Plant B control ash as a % replacement of cement

5.5 Air Void System

Section 4.4 shows that good frost protection was achieved when the air content was greater than 5 %. This observation was consistent regardless whether the fly ash was treated or untreated. However, one of the major factors that influences freeze-thaw durability is the quality of the air void system (including parameters such as spacing factor and specific surface). Figure 5.25 presents a bar chart of the spacing factor of all the specimens. As described in Section 2.1.2 and Section 3.6.5.1 of this document, the spacing factor is the relative distance between the voids in concrete and it is the important parameter used to indicate the distribution of air voids in the concrete. The higher the spacing factor the farther a typical air void is from the next closest air void. As described in Section 2.1.2, if the spacing factor is too high, this means that the concrete could be susceptible to freeze and thaw action.

In terms of the air void system, American Concrete Institute, ACI 201[16] suggest that the spacing factor in concrete should be 0.008in (0.2mm) or below for frost durability. This limit is shown in Figure 5.25 with an orange horizontal line. As seen in Figure 5.25, all the specimens with 5 % or more had spacing factors less than 0.008 in (0.2 mm). There is no noticeable difference in the spacing factor between mixtures that contain treated or untreated ash. This suggests that once a target air content within recommendation is achieved and freeze-thaw resistant coarse aggregate is used, the concrete will be resistant to distress from freezing and thawing.

Figure 5.26 shows the correlation between average relative dynamic modulus and average spacing factor for each mixture tested. ASTM C666 [76] failure limit of 60% for DF for specimen undergoing laboratory freeze thaw testing is also shown in Figure 5.26. However this study uses a limit of 80 % as a good durability which is also suggested by Cordon and Merrill [83]. A clear trend with a correlation of 88% that

can be seen is that as the spacing factor increases the DF decreases. Figure 5.27 shows the correlation between SAM number and average spacing factor for each mixture tested .Overall, an adequate air void network appears to have been produced in the specimens, since the spacing factor meets the requirement for frost resistant as outlined by American Concrete Institute, ACI 201[16] and there is no indication that treatment process had any negative effect on the air void system.

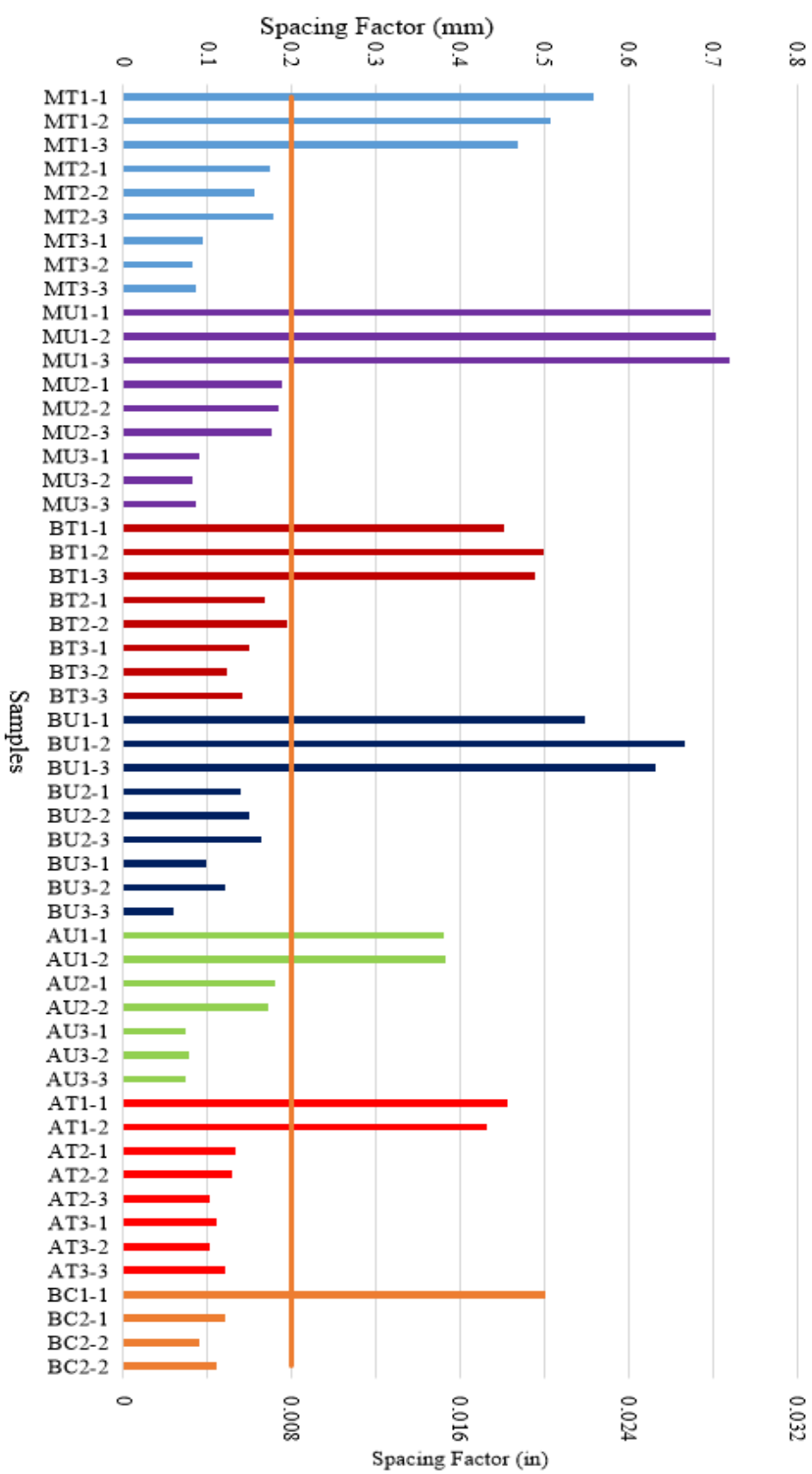

Figure 5.25: Spacing factor bar chart

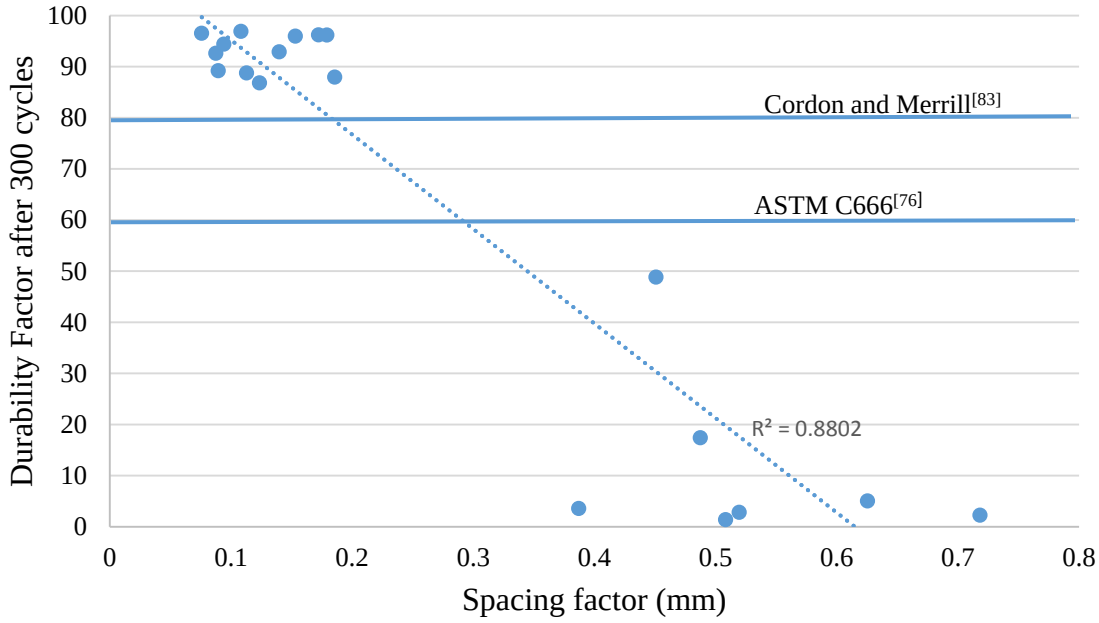

Figure 5.26: Average durability factor versus spacing factor

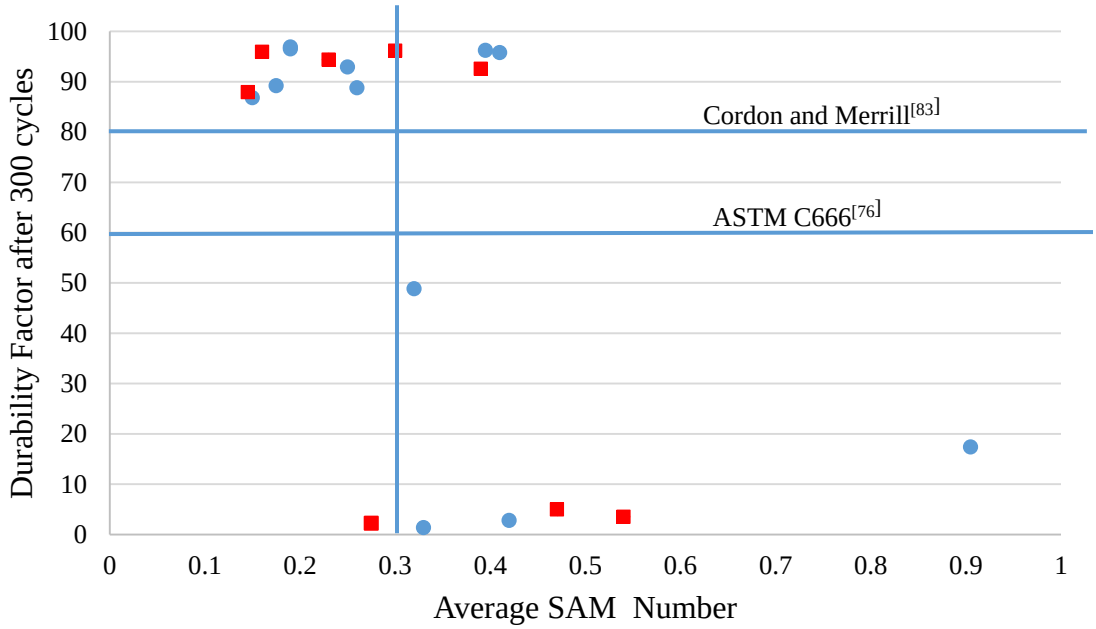

Figure 5.27: Average durability factor versus average SAM Number

5.4.1 Statistical Analysis for Spacing Factor

ANCOVA analysis was also performed for response of spacing factor (SF) using general linear model fitting tools in Minitab 17[84] statistical analysis software, to assess the effect of air content, slump and mixing temperature (continuous variable) on spacing factor allowing for the influence of ash type (treated or untreated) to be explored. The continuous variables of air content, slump and AEA were treated as covariates while ash type was treated as categorical variable.

The summary of the results of the ANCOVA analyses carried out is presented in Table 5.3. From the analyses, the variance inflation factor (VIF) for each of the variables considered was less than 10, indicating that multicollinearity did not influence the regression results. In statistical analysis, a variable is significant if the *p-value* is less than 0.05. Consequently, the p-values for the air content, ash type, slump and temperature are 0.000, 0.532, 0.605 and 0.871 respectively which indicates that only the air content was the only statistical significant variable in the spacing factor. The ash type whether treated or untreated was not statistically significant as observed in general trends in previous section. In summary, the ANCOVA model for spacing factor had an R^2 value of 66.70 % which shows that approximately 67% of the observed variation can be explained by the variables included in the analysis.

Table 5.4: Summary of ANCOVA analyses

Source	df	Adjusted sum of squares	Adjusted mean of Square	F-value	P value	VIF
Air content	1	0.491775	0.491775	27.35	0.000	1.95
Slump	1	0.005032	0.005032	0.41	0.532	2.26
Ash type	1	0.007349	0.007349	0.28	0.605	1.27
Temperature	1	0.000492	0.000492	0.03	0.871	
Error	15	0.269667	0.017978			
Total	19	0.809866				
Model Equation						
Ash type Untreated Spacing Factor = 0.736 - 0.05006 Air - 0.0114 Slump - 0.00146 temp Treated Spacing Factor = 0.696 - 0.05006 Air - 0.0114 Slump - 0.00146 temp						

CHAPTER 6: CONCLUSIONS

6.1 Conclusions

This study evaluates the performance of off-specification fly ashes by treatment with sacrificial absorbents to make them suitable for use in Portland cement concrete with air entrainment. The main objectives of this study were to:

- Analyze the reliability of the treatment process to produce ash that will consistently achieve a targeted level of air entrainment
- Analyze the air bubble size and spacing to see if treatment impacted the air void system
- Evaluate the role of parameters such as air content, fly ash treatment and compressive strength on freeze thaw durability.

The testing methodology consisted of three fly ash types with a portion of each ash treated with chemical absorbent to inhibit the un-burn carbon from adsorbing AEA and the following key findings are presented:

- The treated ashes generally showed low adsorptive capacity compared to the untreated ashes
- It was easier to predict the amount of air entraining admixture (AEA) dosage required to properly entrain air in treated ashes than for untreated ashes
- The treatment did not affect the air void system of the concrete and the compressive strength

- Adding carbon blocker did not affect the durability performance of the concrete produced

The variable air dosage was a set of tests to evaluate the reliability in achieving target air content in concrete mixture as well as the relationship between air content generated and AEA dosage. In this study, it was found that for the treated ash the relationship between air entraining admixture (AEA) dosage and air content generated was linear for treated ashes while that for the untreated ashes it was scattered and inconsistent. This trend was very evident in Plant M ash with LOI of 7.7 %. As the AEA dosage was increased from 1.5 oz/cwt to 43.56oz/cwt the air content increased from 1.6 % to 5.9 %, whereas reducing the dosage from 43.56 oz/cwt to 36.85oz/cwt generated higher air content of 7.8 %. This shows that increasing AEA dosage in untreated ashes does not always generate increased air content and vice versa; dosage prediction proves to be erratic in untreated ashes.

In terms of compressive strength, direct interpolation of the air content versus compressive strength graph showed that the treated mixtures had better strength than the untreated mixtures. This was true for all the fly ashes investigated except for Plant B ash. The Plant B treated mixture had a compressive strength of 4200 psi while the Plant B untreated mixture had a strength of 4400psi, however, there is no enough evidence to conclude that the treatment process influenced the strength gain since the Plant B control mixture also had a strength of 4200 psi. It can be concluded that the treatment process did not have any adverse effect on the strength gain. This conclusion is also buttressed by Statistical analysis using ANCOVA to adjust the regression model for air content and

AEA, ANCOVA analysis did not find the ash type as a statistical significant factor in the compressive strength (*P-value* > 0.05).

The air void system was evaluated using an automated system called bubble counter. The air bubbles spacing, and size are characterized by the terms called spacing factor and specific surface respectively. Based on the data, treated and untreated mixtures with an air content greater than or equal to 5% meets the required specification for spacing factor and specific surface to be frost resistant. This implies that all these mixtures had adequate air void network and the air void system consisted of evenly spaced air bubbles which is essential for frost resistance. All the mixes with adequate spacing factor and specific surface also passed the laboratory freeze thaw testing while mixtures with air content less than 4.5% fail the laboratory freeze thaw test. In other words, when 5% entrained air is properly achieved in a treated mixture, an adequate air void system was also present. Consequently, it can be concluded that the ash treatment process does not adversely affect the air bubble size and spacing. This conclusion is also buttressed by statistical analysis using ANCOVA to adjust the regression model for air content, slump, and mixing temperature, ANCOVA analysis did not find the ash type as a statistical significant factor in the air void system (*P-value* > 0.05).

Based on the data from this study, it was found that concrete mixtures with an air content greater than or equal to 5 % were generally frost resistant using standard laboratory freeze thaw testing as per ASTM C 666. All concrete mixes with air contents below 4.5 % were not resistant to freeze and thaw action. This trend was observed in all the fly ash from all sources and it can be concluded that that when an acceptable AEA is used and an air content that meets specification is achieved in a concrete mixture, the

concrete will be frost resistant. Overall it can be concluded that the treatment process was able to inhibit the effect of the unburned carbon in off-specification fly ash to achieve target air content. Statistical analysis using ANCOVA to adjust the regression model for air content and AEA showed that the ash type is not a statistically significant factor in the durability factor (*P-value* > 0.05). It can be concluded that treatment process did not have any adverse effect on the durability as well as compressive strength of the concrete mixtures produced.

6.2 Recommendations for Future Work

To better characterize the unburned carbon in fly ash and evaluate freeze thaw resistance, the following recommendations are made for future research:

- There is need to establish a criterion based on the adsorption capacity and properties of the differing forms of unburned carbon to identify suitable fly ashes for use in concrete since it is not known whether ash that contains predominantly inertinite will have the same adsorption capacity as one which contains isotropic carbon.
- Based on statistical analysis, this research concluded that the treatment process had no effect on the compressive strength of the concrete produced. However, the treated mixture of two out of the three fly ashes source used had better strength than their untreated counterparts, an in-depth evaluation of air entrained concrete with the same air content needs to be performed to examine the strength performance of chemically beneficiated fly ash mixture.

REFERENCES

[1] US Environmental Protection Agency. "The Clean Air Act Amendments of 1990, A Guide for Small Businesses." (1992).

[2] American Society for Testing and Materials (ASTM), ASTM C 618, 2015, Standard Specification for Coal Fly Ash and Raw or Calcined Natural Pozzolan for Use in Concrete, ASTM International, West Conshohocken, PA, 2015

[3] NCDOT Standard Specification for Roads and Structures Manual, North Carolina Department of Transport Raleigh. January 2012

[4] AASHTO M295 Coal Fly Ash and Raw or Calcined Natural Pozzolan for Use in Concrete. Washington, D.C.: American Association of State Highway and Transportation Officials, 2011.

[5] Powers, T.C, 1949. "The Air Requirement of Frost-Resistant Concrete." Proceedings of the Highway Research Board, PCA Bulletin 33, Portland Cement Association, Skokie Il, 29, 184- 211

[6] Penttala, V. 1998. "Freezing-Induced Strains and Pressures in Wet Porous Materials and Especially in Concrete Mortars." Advanced Cement Based Materials, 7, 8-19.

[7] Kamran N, 2015, Durability of Concrete, lecture notes, Concrete Technology, University of Washington, delivered winter 2015

[8] Pigeon, M., Prevost, J., and Simard, J.M. (1985). "Freeze-Thaw Durability versus Freezing Rate Closure." ACI Journal, September-October 684-692.

[9] Yang, Z., Brown, H., Cheny, A. (2006). "Influence of Moisture Conditions on Freeze and Thaw Durability of Portland Cement Pervious Concrete." Construction and Building Materials, 21, pp 1034.

[10] Powers, T.C., "A Working Hypothesis for Further Studies of Frost resistance of Concrete," ACI Journal, Proceedings, vol. 41, no. 4, February 1945, pp. 245–272

[11] Powers, T.C., and Helmuth, R.A., "Theory of Volume Changes in Hardened Portland Cement Paste During Freezing", Research and Developments Laboratories of the Portland Cement Association, Research Department Bulletin 46, September 1953, Proceedings of the Highway Research Board, vol. 32, pp. 285–297, RX 046.

[12] Pigeon, M. and Pleau R. Durability of concrete in cold climates. CRC Press, 2010.

[13] Folliard, K.J., Hover, K.C., Harris, N., Ley, M.T. and Naranjo, A., 2009. Effects of Texas Fly Ash on Air-Entrainment in Concrete: Comprehensive Report (No. FHWA/TX-08/0-5207-1).

[14] Hover, K., 1993 'Why is there Air in Concrete', http://www.concreteconstruction.net/_view-object?id=00000153-964c-dbf3-a177-967ddaf60000 [Accessed 02/10/2017]

[15] Thomas, J., Jennings, H., 2008 "The Science of Concrete". Centre for Advanced Concrete Based Materials Research, Northwestern University, 2008

[16] Reading, T.J., Adams, R.F., Barnes, B.D., Burmeister, R.A., Clear, K.C., Cook, H.K., Cordon, W.A., Erlin, B., Farkas, E., Famili, H. And Gjorv, O., 1977. "Guide to Durable Concrete". *J. Am. Conc. Inst.*, *74*, Pp.573-581.

[17] Ramachandran, V. S. 1996. Concrete admixtures handbook: properties, science and technology. William Andrew.

[18] American Society for Testing and Materials (ASTM), ASTM C 457, 1998 "Standard Test Method for Microscopical Determination of Parameters of the Air-Void Content and Parameters of the Air-Void System in Hardened Concrete", ASTM International, West Conshohocken, PA, 1998

[19] Felice, R., Freeman, J.M. and Ley, M.T., 2014. "Durable Concrete with Modern Air-Entraining Admixtures". *Concrete international*, *36*(8), pp.37-45.

[20] Ley, M. T., 2007. "The Effects of Fly Ash on the Ability to Entrain and Stabilize Air in Concrete," Dissertation, University of Texas at Austin, August 2007.

[21] Klieger, P., 1952. "Effect of Entrained Air on Strength and Durability of Concrete Made with Various Maximum Sizes of Aggregate," Proceedings, Highway Research Board, Vol. 31, 1952, pp. 177-201; Bulletin No. 40, Research and Development Laboratory, Portland Cement Association, Skokie, IL.

[22] American Society for Testing and Materials (ASTM), ASTM C231, 2014. ''Standard Test Method for Air Content of Freshly Mixed Concrete by the Pressure Method''. American Society of Testing Materials. 2014

[23] American Society for Testing and Materials (ASTM), ASTM C173, 2014. ''Standard Test Method for Air Content of Freshly Mixed Concrete by the Volumetric Method''. American Society of Testing Materials. 2014

[24] Ley, M.T. and Tabb, B., 2014. “A Test Method to Measure the Freeze Thaw Durability of Fresh Concrete using Overpressure”. In *T&DI Congress 2014: Planes, Trains, and Automobiles* (pp. 79-87)

[25] Ley, M.T., Welchel, D., Peery, J., Khatibmasjedi, S. and LeFlore, J., 2017. Determining the air-void distribution in fresh concrete with the Sequential Air Method. Construction and Building Materials, 150, pp.723-737.

[26] Energy Information Administration (EIA), U.S. DOE, "International Energy Outlook 2011," www.eia.gov. [Cited: June 6, 2017.] http://www.eia.gov/forecasts/ieo/pdf/0484%282011%29.pdf.

[27] Energy Information Administration (EIA), U.S. DOE, "Electricity Generation by Energy Source," www.eia.doe.gov. [Cited: June 6, 2017.] https://www.eia.gov/energyexplained/images/charts/outlet-graph-large.jpg

[28] American Coal Ash Association, 2015. “Coal Combustion Product (CCP) Production & Use Survey Report” [Cited: June 6, 2017.] https://www.acaa-usa.org/Portals/9/Files/PDFs/News-Release-Coal-Ash-Production-and-Use-2015.pdf

[29] American Coal Ash, 2015. ‘’ARTBA final forcast’’ [Cited: June 6, 2017.] https://www.acaa-usa.org/Portals/9/Files/PDFs/ReferenceLibrary/ARTBA-final-forecast.compressed.pdf

[30] Costa, J.M. and Mercer, A.D., 1993. “Progress in the Understanding and Prevention of Corrosion”. V. 2. The Institute of Materials, UK; 1993. P. 619

[31] Thomas, M., 2007. “Optimizing the use of fly ash in concrete”, IS548, Portland Cement Association, Skokie, Illinois

[32] Hower, J.C., Rathbone, R.F. and Graham, U.M., 1995. “Approaches to the petrographic characterization of fly ash” (No. CONF-9505231--). Vanguard Solutions, Inc., Ashland, KY (United States).

[33] Maroto-Valer, M.M., Taulbee, D.N. and Hower, J.C., 2001. "Characterization of differing forms of unburned carbon present in fly ash separated by density gradient centrifugation," Fuel, V. 80, 2001, 795-800.

[34] Veranth, J. M., Pershing, D.W., Sarofim, A.F., and Shield J.E., 1998. "Sources of unburned carbon in the fly ash produced from low-NOx pulverized coal combustion" Proceedings of the Combustion Institute, V. 27, 1998, pp.1737–1744

[35] Gebler, S. and Klieger, P., 1983., "Effect of Fly Ash on the Air-Void Stability of Concrete," Fly Ash Silica Fume, Slag and Other Mineral By-Products in Concrete, SP- 79, American Concrete Institute, Detroit, pp. 103-142.

[36] Whiting, D.A., Nagi, M.A., 1998, "Manual of control of air content in concrete", Portland Cement Association, Skokie, IL

[37] Freeman, E., Gao, Y-M., Hurt, R., and Suuberg, E., 1997. "Interaction of Carbon-Containing Fly Ash with Commercial Air-Entraining Admixtures for Concrete". Fuel, 76(8):761-765, 1997

[38] American Society for Testing and Materials (ASTM), ASTM C 260, 2016, Standard Specification for Air Entraining Admixtures for Concrete ASTM International, West Conshohocken, PA, 2016

[39] Nagi, M.A., Okamoto, P.A., Kozikowski, R.L. and Hover, K.C., 2006. "Procedures for Evaluating Air Entraining Admixtures for Highway Concrete" (No. NCHRP Project 18-10).

[40] "Air Entraining Agents" http://www.navodayaengg.in/wp-content/uploads/2015/12/4_L3_Unit2-word.pdf (Accessed 2/26/2017)

[41] Torrans P.H., and. Ivey, D., (1968) 'Air Entrainment in Concrete' Research Report Texas Transportation Institute, Texas A&M University College Station, Texas

[42] Dodson, V., Chapter 6, "Air-Entraining Admixtures," Concrete Admixtures, Van Nostrand Reinhold, New York, New York, 1990, pp. 129-158.

[43] American Society for Testing and Materials (ASTM), ASTM C226-12,2012, Standard Specification for Air-Entraining Additions for Use in the Manufacture of Air-Entraining Hydraulic Cement, ASTM International, West Conshohocken, PA, 2012, www.astm.org

[44] Ansari, F., Zhang, Z., Luke, A., & Maher, A. 1999. "Effects of Synthetic Air Entraining Agents on Compressive Strength of Portland Cement Concrete-Mechanism of Interaction and Remediation Strategy" (No. FHWA NJ 2001-021,)

[45] Tanesi, J. and Meininger, R., 2007. "Freeze-thaw resistance of concrete with marginal air content." Transportation Research Record: Journal of the Transportation Research Board 2020 (2007): 61-66.

[46] American Society for Testing and Materials (ASTM), ASTM C 311, 2016. Standard Test Methods for Sampling and Testing Fly Ash for Use in Portland Cement Concrete ASTM International, West Conshohocken, PA, 2016, www.astm.org

[47] American Society for Testing and Materials (ASTM), ASTM C 114, 2015. Standard Test Methods for Chemical Analysis of Hydraulic Cement ASTM International, West Conshohocken, PA, 2015, www.astm.org

[48] Fan, M. and Brown, R.C., 2001. "Comparison of the Loss-on-Ignition and Thermogravimetric Analysis Techniques in Measuring Unburned Carbon in Coal Fly Ash". Energy & fuels, 15(6), pp.1414-1417.

[49] Mohebbi, M., Rajabipour, F. and Scheetz, B.E., 2015, "Reliability of Loss on Ignition Test for Determining the Unburned Carbon Content in Fly Ash," in Proceedings of 2015 World of coal ash conference-Products in Concrete, 2015

[50] Harris, N.J., Hover, K.C., Folliard, K.J., Ley, T., 2006. "Variable Affecting the ASTM Standard C 311 Loss on Ignition Test for Fly Ash", Journal of ASTM International, Vol.3, Issue 8, 2006

[51] Harris, N.J., Hover, K.C., Folliard, K.J. and Ley, M.T., 2008. The use of the foam index test to predict AEA dosage in concrete containing fly ash: Part I—Evaluation of the state of practice. Journal of ASTM International, 5(7), pp.1-15.

[52] Ahmed, Z. T. 2012. "The Quantification of the Fly Ash Adsorption Capacity for Charecterization and Use in Concrete". PhD Thesis, Michigan Technological University: Houghton, MI, 2012.

[53] Sutter, L. L.; Hooton, R.D.; and Schlorholtz, S., 'Research Description and Findings Specifications and Protocols for Acceptance Tests of Fly Ash Used in Highway Concrete, ''NCHRP Report 749, National Cooperative Highway Research Board of National Academics Washington, DC, 2013A,329 pp

[54] American Society for Testing and Materials (ASTM), ASTM D1510-16a, 2016. Standard Test Method for Carbon Black—Iodine Adsorption Number, ASTM International, West Conshohocken, PA, 2016, www.astm.org

[55] American Society for Testing and Materials (ASTM), ASTM WK47573. New Test Method for Determination of Iodine Number of Coal Fly Ash, ASTM International, West Conshohocken, PA, 2014, www.astm.org

[56] Fox, J. 2005. "Changes in fly ash with thermal treatment." 2005 International Ash Utilization Symosia and the World of Coal Ash Conference, Cement and Concrete 5

[57] Giampa, V.M. and Plaza, O.P., 1999. "Ammonia Removal from Coal Fly Ash by Carbon Burn-Out". In Proceedings: 14th International Symposium on Management and Use of Coal Combustion Products (CCPs) (Vol. 1). Electric Power Research Institute.

[58] John J. P, Peter H. ‘’Carbon Burn-out system, Wateree Station’’ – Presentation to the ASME Research Committee on Power & Environmental Chemistry Lexington, Kentucky, October 12-14, 1988.

[59] Keppeler, J. G., 2001. “Carbon Burn-out: An Update on Commercial Applications”. 2001 International Ash Utilization Symposium, Centre for Applied Energy Research, University of Kentucky, Paper 61

[60] Miller, R. and Taylor, T. 2007 “Verification of the Use of a Carbon Blocking Agent for Fly Ash in Concrete”. ODOT Final Report SJN 134317, 2008, Ohio Department of Transportation. Columbus, OH 43223

[61] James. T.E., James P., Guy. W. 2015. “Chemical treatment of coal ash for beneficial use application/by product treatment via calcium polysulfide”. In Proceedings: World of Coal Ash Conference, Nashville, Tennessee. May 5-7, 2015.

[62] Bittner, J.D., Hrach, F.J., Gasiorowski, S.A., Canellopoulus, L.A. and Guicherd, H., 2014. Triboelectric belt separator for beneficiation of fine minerals. Procedia Engineering, 83, pp.122-129

[63] Stencel, J.M., Li, T.X., Gurupira, T., Jones, C., Neathery, J.K., Ban, H. and Altman, R. 1999. “Technological Development for Carbon-Ash Beneficiation by Pneumatic Transport, Triboelectric Processing”. 1999 International Ash Utilization Symosium, Center for Applied Energy Research, University of Kentucky, Paper #85

[64] Bittner, J.D. and Gasiorowski, S.A., 2005. ‘’Triboelectrostatic Fly Ash Beneficiation: An update on Separation Technologies International Operations. Separation Technologies, LLC. Hampton Avenue, Needham MA

[65] Thompson, A, Hamley P., Lester, E..,Cloke, M. and Poliaoff, M., 2001. “The Removal of carbon from fly ash using supercritical water oxidation.” 2001 International Ash Utilisation Symposium, Center for Applied Energy Research University of Kentucky, Paper 85

[66] Abeln, J., Kluth, M., Petrich, G., & Schmieder, H. (2001). Supercritical Water Oxidation (SCWO): A process for the treatment of industrial waste effluents. International Journal of High Pressure Research, 20(1-6), 537-547.

[67] Hurt R, Suuberg E, Gao YM, Burnett A, inventors; Brown University Research Foundation, assignee. Apparatus and method for deactivating carbon in fly ash. United States patent US 6,136,089. 2000 Oct 24.

[68] Hurt, R. H. Gao, Y. M., Shim, H S. and Suuberg, E.M 1997. “Effects of Carbon on Air Entrainment in Fly Ash Concrete: The Role of Soot and Carbon Black”. Energy &Fuels, 11, 457-462

[69] American Society for Testing and Materials (ASTM), 2016. ASTM C33, Standard Specification for Concrete Aggregates, ASTM International, West Conshohocken, PA, 2016, www.astm.org

[70] American Society for Testing and Materials (ASTM), ASTM C192 / C192M-16a, Standard Practice for Making and Curing Concrete Test Specimens in the Laboratory, ASTM International, West Conshohocken, PA, 2016, www.astm.org

[71] American Society for Testing and Materials (ASTM), ASTM C143 / C143M-15a, Standard Test Method for Slump of Hydraulic-Cement Concrete, ASTM International, West Conshohocken, PA, 2015, www.astm.org

[72] AASHTO, TP95, 2011 “Standard Method of Test for Surface Resistivity Indication of Concrete’s Ability to Resist Chloride Ion Penetration.”." AASHTO Provisional Standards, 2011 Edition (2011).

[73] American Society for Testing and Materials (ASTM), 2017. ASTM C39, Standard Test Method for Compressive Strength of Cylindrical Concrete Specimens, ASTM International, West Conshohocken, PA, 2017, www.astm.org

[74] American Society for Testing and Materials (ASTM), 2015, ASTM C1231, Standard Practice for Use of Unbonded Caps in Determination of Compressive Strength of Hardened Cylindrical Concrete Specimens, ASTM International, West Conshohocken, PA, 2015, www.astm.org

[75] American Society for Testing and Materials (ASTM), ASTM C469, Standard Test Method for Static Modulus of Elasticity and Poisson’s Ratio of Concrete in Compression, ASTM International, West Conshohocken, PA, 2014, www.astm.org

[76] American Society for Testing and Materials (ASTM), ASTM C666 / C666M-15, Standard Test Method for Resistance of Concrete to Rapid Freezing and Thawing, ASTM International, West Conshohocken, PA, 2015, www.astm.org

[77] American Society for Testing and Materials (ASTM), ASTM C215, Standard Test Method for Fundamental Transverse, Longitudinal, and Torsional Resonant Frequencies of Concrete Specimens, ASTM International, West Conshohocken, PA, 2014, www.astm.org

[78] Peterson, Karl, Raymond Swartz, Lawrence Sutter, and Thomas Van Dam. "Hardened concrete air void analysis with a flatbed scanner." Transportation Research Record: Journal of the Transportation Research Board 1775 (2001): 36-43.

[79] Ley, M.T., Harris, N.J., Folliard, K.J. and Hover, K.C., 2008. “Investigation of Air-Entraining Admixture Dosage in Fly Ash Concrete”. Materials Journal, 105(5), pp.494-498.

[80] AE200 data sheet https://assets.master-builders-solutions.basf.com/Shared%20Documents/EB%20Construction%20Chemcials%20-%20US/Admixture%20Systems/Data%20Sheets/MasterAir/basf-masterair-ae-200-tds.pdf [Accessed 12th November, 2017]

[81] Urban, D. (2004). “Air supply: a producer in Wisconsin studied strength loss variable in air entrained concrete”. The Concrete Producer, http://findarticles.com/p/articles/mi_m0NSY/is_4_22/ai_n6134039 [Accessed 15th December 2017]

[82] What is Concrete? http://www.carnationconstruction.com/Materials/02-Materials-Concrete.html [Accessed 15th December 2017]

[83] Cordon, W. A., and Merrill, D. (1963). "Requirements for Freezing and Thawing Durability for Concrete." ASTM, 63, 1026-1036

[84] Minitab, Inc. "MINITAB release 17: statistical software for windows." Minitab Inc, USA (2014).

APPENDIX A: SUPPLEMENTAL INFORMATION FOR CHAPTER 3

BASF
We create chemistry

3

03 30 00	Cast-in-Place Concrete
03 40 00	Precast Concrete
03 70 00	Mass Concrete

MasterAir® AE 200

Air-Entraining Admixture

Formerly Micro Air*

Description

MasterAir AE 200 air-entraining admixture provides concrete with extra protection by creating air bubbles that are ultrastable, small and closely spaced – a characteristic especially useful in the types of concrete known for their difficulty to entrain and maintain the air content desired.

Even when used at a lower dosage than standard air-entraining admixtures, MasterAir AE 200 admixture meets the requirements of ASTM C 260, AASHTO M 154, and CRD-C 13.

Applications

Recommended for use in:

- Concrete exposed to cyclic freezing and thawing
- Production of high-quality normal or lightweight concrete (heavyweight concrete normally does not contain entrained air)

Features

- Ready-to-use in the proper concentration for rapid, accurate dispensing
- Greatly improved stability of air-entrainment
- Ultra stable air bubbles

Benefits

- Increased resistance to damage from cyclic freezing and thawing
- Increased resistance to scaling from deicing salts
- Improved plasticity and workability
- Improved air-void system in hardened concrete
- Improved ability to entrain and retain air in low-slump concrete, concrete containing high-carbon content fly ash, concrete using large amounts of fine materials, concrete using high-alkali cements, high-temperature concrete, and concrete with extended mixing times
- Reduced permeability – increased watertightness
- Reduced segregation and bleeding

Performance Characteristics

Concrete durability research has established that the best protection for concrete from the adverse effects of freezing and thawing cycles and deicing salts results from: proper air content in the hardened concrete, a suitable air-void system in terms of bubble size and spacing and adequate concrete strength, assuming the use of sound aggregates and proper mixing, transporting, placing, consolidation, finishing and curing techniques. MasterAir AE 200 admixture can be used to obtain adequate freezing and thawing durability in a properly proportioned concrete mixture, if standard industry practices are followed.

MASTER® BUILDERS SOLUTIONS

Figure A1: Technical data sheet for Master Air AE200

Air Content Determination: The total air content of normal weight concrete should be measured in strict accordance with ASTM C 231, "Standard Test Method for Air Content of Freshly Mixed Concrete by the Pressure Method" or ASTM C 173/C 173M, "Standard Test Method for Air Content of Freshly Mixed Concrete by the Volumetric Method."

The air content of lightweight concrete should only be determined using the Volumetric Method. The air content should be verified by calculating the gravimetric air content in accordance with ASTM C 138/C 138M, "Standard Test Method for Density (Unit Weight), Yield, and Air Content (Gravimetric) of Concrete." If the total air content, as measured by the Pressure Method or Volumetric Method and as verified by the Gravimetric Method, deviates by more than 1.5%, the cause should be determined and corrected through equipment calibration or by whatever process is deemed necessary.

Guidelines for Use

Dosage: There is no standard dosage for MasterAir AE 200 admixture. The exact quantity of air-entraining admixture needed for a given air content of concrete varies because of differences in concrete making materials and ambient conditions. Typical factors that might influence the amount of air entrained include: temperature, cementitious materials, sand gradation, sand-aggregate ratio, mixture proportions, slump, means of conveying and placement, consolidation and finishing technique.

The amount of MasterAir AE 200 admixture used will depend upon the amount of entrained air required under actual job conditions. In a trial mixture, use 0.125 to 1.5 fl oz/cwt (8-98 mL/100 kg) of cement. In mixtures containing water-reducing or set-control admixtures, the amount of MasterAir AE 200 admixture needed is somewhat less than the amount required in plain concrete. Due to possible changes in the factors that can affect the dosage of MasterAir AE 200 admixture, frequent air content checks should be made during the course of the work. Adjustments to the dosage should be based on the amount of entrained air required in the mixture at the point of placement. If an unusually high or low dosage of MasterAir AE 200 admixture is required to obtain the desired air content, consult your Local sales representative. In such cases, it may be necessary to determine that, in addition to a proper air content in the fresh concrete, a suitable air-void system is achieved in the hardened concrete.

Dispensing and Mixing: Add MasterAir AE 200 admixture to the concrete mixture using a dispenser designed for air-entraining admixtures; or add manually using a suitable measuring device that ensures accuracy within plus or minus 3% of the required amount. For optimum, consistent performance, the air-entraining admixture should be dispensed on damp, fine aggregate or with the initial batch water. If the concrete mixture contains lightweight aggregate, field evaluations should be conducted to determine the best method to dispense the air-entraining admixture.

Precaution

In a 2005 publication from the Portland Cement Association (PCA R&D Serial No. 2789), it was reported that problematic air-void clustering that can potentially lead to above normal decreases in strength was found to coincide with late additions of water to air-entrained concretes. Late additions of water include the conventional practice of holding back water during batching for addition at the jobsite. Therefore, caution should be exercised with delayed additions to air-entrained concrete. Furthermore, an air content check should be performed after post-batching addition of any other materials to an air-entrained concrete mixture.

Product Notes

Corrosivity – Non-Chloride, Non-Corrosive: MasterAir AE 200 admixture will neither initiate nor promote corrosion of reinforcing and prestressing steel embedded in concrete, or of galvanized steel floor and roof systems. No calcium chloride or other chloride-based ingredients are used in the manufacture of this admixture.

Compatibility: MasterAir AE 200 admixture may be used in combination with any BASF admixture, unless stated otherwise on the data sheet for the other product. When used in conjunction with other admixtures, each admixture must be dispensed separately into the mixture.

Figure A1 Cont'd: Technical data sheet for Master Air AE200

Storage and Handling

Storage Temperature: MasterAir AE 200 admixture should be stored and dispensed at 35 °F (2 °C) or higher. Although freezing does not harm this product, precautions should be taken to protect it from freezing. If it freezes, thaw and reconstitute by mild mechanical agitation. Do not use pressurized air for agitation.

Shelf Life: MasterAir AE 200 admixture has a minimum shelf life of 18 months. Depending on storage conditions, the shelf life may be greater than stated. Please contact your Local sales representative regarding suitability for use and dosage recommendations if the shelf life of MasterAir AE 200 admixture has been exceeded.

Safety: MasterAir AE 200 admixture is a caustic solution. Chemical goggles and gloves are recommended when transferring or handling this material. (See SDS and/or product label for complete information.)

Packaging

MasterAir AE 200 admixture is supplied in 55 gal (208 L) drums, 275 gal (1040 L) totes and by bulk delivery.

Related Documents

Safety Data Sheets: MasterAir AE 200 admixture

Additional Information

For suggested specification information or for additional product data on MasterAir AE 200 admixture, contact your local sales representative.

The Admixture Systems business of BASF's Construction Chemicals division is the leading provider of solutions that improve placement, pumping, finishing, appearance and performance characteristics of specialty concrete used in the ready-mixed, precast, manufactured concrete products, underground construction and paving markets. For over 100 years we have offered reliable products and innovative technologies, and through the Master Builders Solutions brand, we are connected globally with experts from many fields to provide sustainable solutions for the construction industry.

Limited Warranty Notice

BASF warrants this product to be free from manufacturing defects and to meet the technical properties on the current Technical Data Guide, if used as directed within shelf life. Satisfactory results depend not only on quality products but also upon many factors beyond our control. BASF MAKES NO OTHER WARRANTY OR GUARANTEE, EXPRESS OR IMPLIED, INCLUDING WARRANTIES OF MERCHANTABILITY OR FITNESS FOR A PARTICULAR PURPOSE WITH RESPECT TO ITS PRODUCTS. The sole and exclusive remedy of Purchaser for any claim concerning this product, including but not limited to, claims alleging breach of warranty, negligence, strict liability or otherwise, is shipment to purchaser of product equal to the amount of product that fails to meet this warranty or refund of the original purchase price of product that fails to meet this warranty, at the sole option of BASF. Any claims concerning this product must be received in writing within one (1) year from the date of shipment and any claims not presented within that period are waived by Purchaser. BASF WILL NOT BE RESPONSIBLE FOR ANY SPECIAL, INCIDENTAL, CONSEQUENTIAL (INCLUDING LOST PROFITS) OR PUNITIVE DAMAGES OF ANY KIND.

Purchaser must determine the suitability of the products for the intended use and assumes all risks and liabilities in connection therewith. This information and all further technical advice are based on BASF's present knowledge and experience. However, BASF assumes no liability for providing such information and advice including the extent to which such information and advice may relate to existing third party intellectual property rights, especially patent rights, nor shall any legal relationship be created by or arise from the provision of such information and advice. BASF reserves the right to make any changes according to technological progress or further developments. The Purchaser of the Product(s) must test the product(s) for suitability for the intended application and purpose before proceeding with a full application of the product(s). Performance of the product described herein should be verified by testing and carried out by qualified experts.

* Micro Air became MasterAir AE 200 under the Master Builders Solutions brand, effective January 1, 2014.

BASF Corporation
Admixture Systems
www.master-builders-solutions.basf.us

United States
23700 Chagrin Boulevard
Cleveland, Ohio 44122-5544
Tel: 800 628-9990 ■ Fax: 216 839-8821

Canada
1800 Clark Boulevard
Brampton, Ontario L6T 4M7
Tel: 800 387-5862 ■ Fax: 905 792-0651

Figure A1 Cont'd: Technical data sheet for Master Air AE200

Table A.1: Coarse aggregate sieve analysis

Sieve Size	Percent Passing	ASTM C 33 Specification, % Passing
1"	100	100
3/4"	96	90-100
1/2"	55	---
3/8"	33	20-55
No.4	5	0-10
No.8	2	0-5
No.200 Decant, %	0.3	1.0/1.5

Table A.2: Fine aggregate sieve analysis

Sieve Size	Percent Passing	ASTM C 33 Specification, % Passing
3/8	100%	100.0%
No. 4	99.9%	95-100%
No. 8	98.8%	80-100%
No. 16	79.5%	50-85%
No. 30	34.9%	25-60%
No. 50	5.6%	5-30%
No. 100	0.9%	0-10%
No. 200	0.3%	0-3%

APPENDIX B: FLY ASH CHARACTERIZATION TEST DATA

Table: B.1 Iodine adsorption test data.

Fly Ash	Volume of AEA (ml)	Volume of AEA (ml)	Average Volume (ml)
Plant B Treated	19.90	19.52	19.71
Plant B Control	16.12	17.72	16.92
Plant B Untreated	20.67	19.35	20.01
Plant A Treated	18.96	20.58	19.77
Plant A Untreated	20.98	21.22	21.10
Plant M Treated	21.04	19.8	20.42
Plant M Untreated	28.76	29.02	28.89

Table: A.2 Loss on Ignition test data

Fly Ash	Weight of Crucible (g)	Weight of Dry Fly Ash + Crucible (g)	Wight of Fly Ash after Cooling (g)
Plant B Treated	75.268	76.270	76.214
Plant B Control	72.749	73.749	73.733
Plant B Untreated	75.378	76.379	76.437
Plant A Treated	77.634	76.638	76.730
Plant A Untreated	77.378	78.378	78.291
Plant M Treated	77.383	78.386	78.309
Plant M Untreated	78.383	79.384	79.305

APPENDIX C: COMPRESSIVE STRENGHT DATA

Table: C.1 7 days Compressive strength data of specimen.

Specimen Code	Load (lbs)		
	Specimen 1	Specimen 2	Specimen 3
MT1	52395	53440	53585
MT2	42120	39335	41210
MT3	22775	26240	25070
MU1	53440	52800	52456
MU2	28455	31810	29620
MU3	29170	29830	27420
BC1	54350	54900	55630
BC2	36965	38750	37900
AT1	53100	52900	53573
AT2	54350	54900	55630
AT3	36965	36278	35790
AU1	44678	43345	46419
AU2	36165	36278	36073
AU3	20640	19760	21760
BT1	50615	44405	46140
BT2	40070	41955	35410
BT3	19465	18260	18840
BU1	49510	45705	46310
BU2	35345	34320	34590
BU3	15110	14455	14405

Table: C.2 28 days Compressive strength data of specimens.

Specimen Code	Load (lbs)		
	Specimen 1	Specimen 2	Specimen 3
MT2	45120	48725	49110
MT1	69240	66470	66525
MT3	30035	30330	30585
MU2	42525	36055	36955
MU3	40765	37375	36170
BT2	49590	46765	49150
BT1	57925	65175	57335
BT3	23270	24895	24830
BU3	18635	21540	20555
BU1	62225	60715	62730
BU2	42721	42600	47575
AU3	24515	22375	23569
AU2	41985	43905	42988
AU1	53370	58635	55035
MU1	68280	70550	66310
AT2	59735	53050	56620
AT1	66740	63935	63503
BC1	71555	68420	64280
BC2	46365	45435	44890
AT3	41100	38585	39865

Table: C.3 56 days Compressive strength data of specimens

Specimen Code	Load (lbs)		
	Specimen 1	Specimen 2	Specimen 3
MT2	62175	60265	58355
MT1	74710	74030	75250
MT3	40040	34700	30500
MU2	44675	45190	44960
MU3	44080	43060	42830
BT2	55180	54365	48865
BT1	64485	65840	64810
BT3	29650	24980	31010
BU3	22705	23250	25135
BU1	74145	74140	77500
BU2	48990	54505	52450
AU3	29875	29345	29130
AU2	59700	56750	53870
AU1	64560	64640	66750
MU1	74708	73968	74600
AT2	72108	71569	71300
AT1	72800	72358	73400
BC1	73565	74720	73575
BC2	53900	53980	54180
AT3	47250	48060	47900

Table: C.3 90 days Compressive strength data of specimens

Specimen Code	Load (lbs)		
	Specimen 1	Specimen 2	Specimen 3
MT2	66527	66755	64305
MT1	87685	78695	79695
MT3	37390	36495	31620
MU2	50135	42500	49875
MU3	46890	44340	44580
BT2	58355	57800	56315
BT1	74740	70120	75525
BT3	31685	30095	31995
BU3	26580	26945	27415
BU1	79005	77525	81475
BU2	58240	59270	59035
AU3	35450	34980	37250
AU2	62170	61590	62775
AU1	71780	72500	71890
MU1	80072	81900	80356
AT2	77250	78130	78225
AT1	79960	78960	80150
BC1	82890	81389	85620
BC2	61100	60734	61900
AT3	53215	54160	53078

APPENDIX D: MODULUS OF ELASTICITY DATA

Table D1: Data for Modulus of Elasticity

Code	Load (lb)				Strain Stress (psi)	40% Ultimate Load Stress (psi)	Modulus of Elasticity (psi)			
	Specimen 1	Specimen 2	Specimen 3	Ultimate			E1	E2	E3	
MT2	6700	7000	7030	50000	244.4287	1768.659	0.0092	0.0122	0.01	0.010466667
MT1	8330	8250	7685	70000	286.1101	2476.123	0.0119	0.0115	0.0128	0.012066667
MT3	4225	5650	5000	30000	175.3921	1061.196	0.0069	0.0063	0.0063	0.0065
MU2	6945	5830	5501	40000	215.4935	1414.927	0.007	0.007	0.0079	0.0073
MU3	4450	5765	6210	40000	193.6682	1414.927	0.0088	0.0075	0.0075	0.007933333
BT2	6715	6145	5845	50000	220.5518	1768.659	0.0098	0.0086	0.0099	0.009433333
BT1	7710	6730	7140	60000	254.4511	2122.391	0.0086	0.0105	0.0108	0.009966667
BT3	5290	5000	5225	25000	182.9383	884.3297	0.005	0.0049	0.0053	0.005066667
BU3	6045	5335	4095	20000	182.4667	707.4637	0.004	0.0045	0.005	0.0045
BU1	7900	8445	8430	60000	292.1236	2122.391	0.0097	0.0083	0.008	0.008666667
BU2	7910	6565	7360	45000	257.4578	1591.793	0.0066	0.0081	0.0071	0.007266667
AU3	3800	5000	5000	30000	162.7167	1061.196	0.0057	0.007	0.0057	0.006133333
AU2	6300	5000	7000	50000	215.7764	1768.659	0.0105	0.0098	0.0095	0.009933333
AU1	7400	5300	6300	60000	224.0302	2122.391	0.0103	0.0122	0.0111	0.0112
MU1	5000	6200	6000	70000	202.8063	2476.123	0.0159	0.0129	0.0149	0.014566667
AT2	5000	6200	7200	45000	216.9555	1591.793	0.0103	0.0098	0.0078	0.0093
AT1	6200	7000	7600	70000	245.2541	2476.123	0.0122	0.012	0.0108	0.011666667
BC1	5500	5000	5500	70000	188.657	2476.123	0.0145	0.01566	0.016	0.015386667
BC2	5000	5500	5800	50000	192.1943	1768.659	0.0115	0.0119	0.0104	0.011266667
AT3	5800	6200	6200	45000	214.5973	1591.793	0.009	0.0089	0.0088	0.0089

152

APPENDIX E: FREEZE THAW DATA

Table E1: Fundamental Frequency Data (0 Cycles)

Specimen Code	Freq 1 (kHz)	Freq 2 (kHz)	Freq 3 (kHz)	Avg Freq (kHz)
MT2-1	1.910	1.910	1.910	1.910
MT2-2	1.910	1.910	1.910	1.910
MT2-3	1.900	1.900	1.900	1.900
MT1-1	1.020	1.020	1.020	1.020
MT1-2	1.010	1.020	1.020	1.017
MT1-3	1.200	1.200	1.200	1.200
MT3-1	1.810	1.810	1.810	1.810
MT3-2	1.820	1.820	1.820	1.820
MT3-3	1.820	1.820	1.810	1.817
MU2-1	1.900	1.900	1.900	1.900
MU2-2	1.900	1.900	1.900	1.900
MU2-3	1.900	1.890	1.890	1.893
MU3-1	1.860	1.860	1.850	1.857
MU3-2	1.860	1.850	1.840	1.850
MU3-3	1.860	1.860	1.840	1.853
BT2-1	1.930	1.920	1.910	1.920
BT2-2	1.920	1.920	1.910	1.917
BT2-3	1.900	1.900	1.900	1.900
BT1-1	2.000	2.000	2.000	2.000
BT1-2	1.990	1.990	1.990	1.990
BT1-3	1.980	1.980	1.980	1.980
BT3-1	1.780	1.780	1.780	1.780
BT3-2	1.740	1.740	1.740	1.740
BT3-3	1.700	1.700	1.700	1.700
BU3-1	1.640	1.640	1.640	1.640
BU3-2	1.640	1.640	1.640	1.640
BU3-3	1.640	1.640	1.640	1.640
BU1-1	2.000	2.000	2.000	2.000
BU1-2	2.000	2.000	2.000	2.000
BU1-3	2.000	2.000	2.000	2.000
BU2-1	1.900	1.900	1.900	1.900
BU2-2	1.900	1.880	1.880	1.887
BU2-3	1.900	1.900	1.900	1.900
AU3-1	1.700	1.700	1.700	1.700
AU3-2	1.700	1.700	1.700	1.700
AU3-3	1.700	1.700	1.700	1.700
AU2-1	1.900	1.900	1.900	1.900
AU2-2	1.900	1.900	1.900	1.900

Table E1 Cont'd: Fundamental Frequency Data (0 Cycles)

Specimen Code	Freq 1 (kHz)	Freq 2 (kHz)	Freq 3 (kHz)	Avg Freq (kHz)
AU2-3	1.900	1.900	1.900	1.900
AU1-1	2.020	2.020	2.020	2.020
AU1-2	2.020	2.020	2.020	2.020
AU1-3	2.020	2.020	2.020	2.020
MU1-1	2.080	2.080	2.080	2.080
MU1-2	2.080	2.080	2.080	2.080
MU1-3	2.040	2.040	2.040	2.040
AT2-1	2.000	2.000	1.980	1.993
AT2-2	2.000	2.000	1.980	1.993
AT2-3	1.960	1.960	1.960	1.960
AT1-1	2.020	2.020	2.020	2.020
AT1-2	2.040	2.040	2.040	2.040
AT1-3	2.000	2.000	2.000	2.000
BC1-1	2.040	2.040	2.040	2.040
BC1-2	2.040	2.000	2.000	2.013
BC1-3	2.040	2.000	2.000	2.013
BC2-1	1.900	1.900	1.900	1.900
BC2-2	1.900	1.900	1.900	1.900
BC2-3	1.900	1.900	1.900	1.900
AT3-1	1.900	1.900	1.900	1.900
AT3-2	1.900	1.900	1.900	1.900
AT3-3	1.900	1.900	1.900	1.900

Table E2: Fundamental Frequency Data (30 Cycles)

Specimen Code	Freq 1 (kHz)	Freq 2 (kHz)	Freq 3 (kHz)	Avg Freq (kHz)
MT2-1	1.910	1.910	1.910	1.91
MT2-2	1.910	1.910	1.910	1.91
MT2-3	1.900	1.900	1.900	1.90
MT1-1	0.980	0.980	0.980	0.98
MT1-2	1.000	1.000	1.000	1.00
MT1-3	1.150	1.150	1.150	1.15
MT3-1	1.800	1.800	1.800	1.80
MT3-2	1.810	1.810	1.810	1.81
MT3-3	1.810	1.810	1.810	1.81
MU2-1	1.890	1.890	1.900	1.89
MU2-2	1.900	1.890	1.890	1.89
MU2-3	1.900	1.890	1.890	1.89
MU3-1	1.860	1.860	1.850	1.86
MU3-2	1.860	1.850	1.840	1.85
MU3-3	1.860	1.860	1.840	1.85
BT2-1	1.930	1.920	1.910	1.92
BT2-2	1.920	1.920	1.910	1.92
BT2-3	1.900	1.900	1.900	1.90
BT1-1	1.990	1.990	1.990	1.99
BT1-2	1.940	1.940	1.940	1.94
BT1-3	1.900	1.900	1.900	1.90
BT3-1	1.780	1.780	1.780	1.78
BT3-2	1.740	1.740	1.740	1.74
BT3-3	1.700	1.700	1.700	1.70
BU3-1	1.640	1.640	1.640	1.64
BU3-2	1.640	1.640	1.640	1.64
BU3-3	1.640	1.640	1.640	1.64
BU1-1	1.620	1.620	1.620	1.62
BU1-2	1.300	1.300	1.300	1.30
BU1-3	1.300	1.300	1.300	1.30
BU2-1	1.900	1.900	1.900	1.90
BU2-2	1.900	1.880	1.880	1.89
BU2-3	1.900	1.900	1.900	1.90
AU3-1	1.700	1.700	1.700	1.70
AU3-2	1.700	1.700	1.700	1.70
AU3-3	1.700	1.700	1.700	1.70
AU2-1	1.890	1.890	1.890	1.89
AU2-2	1.890	1.890	1.890	1.89
AU2-3	1.900	1.900	1.900	1.90
AU1-1	1.300	1.300	1.300	1.30

AU1-2	1.200	1.200	1.200	1.20
AU1-3	1.100	1.100	1.100	1.10

Table E2 Cont'd: Fundamental Frequency Data (30 Cycles)

Specimen Code	**Freq 1 (kHz)**	**Freq 2 (kHz)**	**Freq 3 (kHz)**	**Avg Freq (kHz)**
MU1-1	0.980	0.980	0.980	0.98
MU1-2	1.060	1.060	1.060	1.06
MU1-3	0.880	0.880	0.880	0.88
AT2-1	1.980	1.980	1.980	1.98
AT2-2	1.940	1.940	1.940	1.94
AT2-3	1.940	1.940	1.940	1.94
AT1-1	1.950	1.950	1.950	1.95
AT1-2	1.960	1.960	1.840	1.92
AT1-3	1.960	1.960	1.840	1.92
BC1-1	0.940	0.940	0.940	0.94
BC1-2	0.680	0.680	0.680	0.68
BC1-3	0.580	0.580	0.580	0.58
BC2-1	1.900	1.900	1.900	1.90
BC2-2	1.900	1.900	1.900	1.90
BC2-3	1.900	1.900	1.900	1.90
AT3-1	1.850	1.850	1.850	1.85
AT3-2	1.840	1.840	1.840	1.84
AT3-3	1.800	1.800	1.800	1.80

Table E3: Fundamental Frequency Data (60 Cycles)

Specimen Code	Freq 1 (kHz)	Freq 2 (kHz)	Freq 3 (kHz)	Avg Freq (kHz)
MT2-1	1.890	1.890	1.890	1.89
MT2-2	1.890	1.880	1.880	1.88
MT2-3	1.890	1.880	1.880	1.88
MT1-1	0.665	0.665	0.665	0.67
MT1-2	1.000	0.980	0.980	0.99
MT1-3	1.020	1.020	1.020	1.02
MT3-1	1.750	1.750	1.750	1.75
MT3-2	1.760	1.740	1.740	1.75
MT3-3	1.740	1.740	1.740	1.74
MU2-1	1.830	1.820	1.820	1.82
MU2-2	1.830	1.830	1.820	1.83
MU2-3	1.830	1.820	1.820	1.82
MU3-1	1.830	1.820	1.800	1.82
MU3-2	1.820	1.810	1.810	1.81
MU3-3	1.810	1.810	1.800	1.81
BT2-1	1.920	1.910	1.900	1.91
BT2-2	1.910	1.910	1.910	1.91
BT2-3	1.890	1.890	1.890	1.89
BT1-1	1.820	1.820	1.820	1.82
BT1-2	1.780	1.780	1.780	1.78
BT1-3	1.700	1.700	1.700	1.70
BT3-1	1.780	1.780	1.780	1.78
BT3-2	1.740	1.740	1.740	1.74
BT3-3	1.700	1.700	1.700	1.70
BU3-1	1.640	1.640	1.640	1.64
BU3-2	1.640	1.640	1.640	1.64
BU3-3	1.640	1.640	1.640	1.64
BU1-1	1.240	1.240	1.240	1.24
BU1-2	0.880	0.880	0.880	0.88
BU1-3	0.860	0.860	0.860	0.86
BU2-1	1.900	1.900	1.900	1.90
BU2-2	1.900	1.900	1.880	1.89
BU2-3	1.900	1.900	1.900	1.90
AU3-1	1.700	1.700	1.700	1.70
AU3-2	1.700	1.700	1.700	1.70
AU3-3	1.700	1.700	1.700	1.70
AU2-1	1.890	1.890	1.890	1.89
AU2-2	1.890	1.890	1.890	1.89
AU2-3	1.900	1.900	1.900	1.90

AU1-1	-	-	-	-

Table E3 Cont'd: Fundamental Frequency Data (60 Cycles)

Specimen Code	**Freq 1 (kHz)**	**Freq 2 (kHz)**	**Freq 3 (kHz)**	**Avg Freq (kHz)**
AU1-2	-	-	-	
AU1-3	-	-	-	-
MU1-1	-	-	-	-
MU1-2	-	-	-	-
MU1-3	-	-	-	-
AT2-1	1.980	1.980	1.980	1.98
AT2-2	1.940	1.940	1.940	1.94
AT2-3	1.940	1.940	1.940	1.94
AT1-1	1.900	1.900	1.900	1.90
AT1-2	1.900	1.900	1.900	1.90
AT1-3	1.940	1.940	1.940	1.94
BC1-1	-	-	-	-
BC1-2	-	-	-	-
BC1-3	-	-	-	-
BC2-1	1.900	1.900	1.900	1.90
BC2-2	1.900	1.900	1.900	1.90
BC2-3	1.900	1.900	1.900	1.90
AT3-1	1.850	1.850	1.850	1.85
AT3-2	1.840	1.840	1.840	1.84
AT3-3	1.840	1.840	1.840	1.84

Table E4: Fundamental Frequency Data (90 Cycles)

Specimen Code	Freq 1 (kHz)	Freq 2 (kHz)	Freq 3 (kHz)	Avg Freq (kHz)
MT2-1	1.890	1.890	1.890	1.89
MT2-2	1.890	1.880	1.880	1.88
MT2-3	1.890	1.880	1.880	1.88
MT1-1	0.340	0.340	0.340	0.34
MT1-2	0.360	0.360	0.360	0.36
MT1-3	0.350	0.350	0.350	0.35
MT3-1	1.750	1.750	1.740	1.75
MT3-2	1.750	1.740	1.740	1.74
MT3-3	1.740	1.740	1.740	1.74
MU2-1	1.830	1.820	1.820	1.82
MU2-2	1.830	1.830	1.820	1.83
MU2-3	1.830	1.820	1.820	1.82
MU3-1	1.830	1.810	1.800	1.81
MU3-2	1.820	1.810	1.810	1.81
MU3-3	1.810	1.810	1.810	1.81
BT2-1	1.920	1.910	1.900	1.91
BT2-2	1.900	1.890	1.890	1.89
BT2-3	1.890	1.890	1.880	1.89
BT1-1	1.600	1.600	1.600	1.60
BT1-2	1.460	1.460	1.460	1.46
BT1-3	1.480	1.480	1.480	1.48
BT3-1	1.780	1.780	1.780	1.78
BT3-2	1.740	1.740	1.740	1.74
BT3-3	1.700	1.700	1.700	1.70
BU3-1	1.640	1.640	1.640	1.64
BU3-2	1.640	1.640	1.640	1.64
BU3-3	1.640	1.640	1.640	1.64
BU2-1	1.900	1.900	1.900	1.90
BU2-2	1.900	1.880	1.880	1.89
BU2-3	1.900	1.900	1.900	1.90
AU3-1	1.700	1.700	1.700	1.70
AU3-2	1.700	1.700	1.700	1.70
AU3-3	1.700	1.700	1.700	1.70
AU2-1	1.890	1.890	1.890	1.89
AU2-2	1.890	1.890	1.890	1.89
AU2-3	1.900	1.900	1.900	1.90
AU1-1	-	-	-	-

AU1-2	-	-	-	-
AU1-3	-	-	-	-

Table E4 Cont'd: Fundamental Frequency Data (90 Cycles)

Specimen Code	**Freq 1 (kHz)**	**Freq 2 (kHz)**	**Freq 3 (kHz)**	**Avg Freq (kHz)**
MU1-1	-	-	-	-
MU1-2	-	-	-	-
MU1-3	-	-	-	-
AT2-1	1.980	1.980	1.980	1.98
AT2-2	1.940	1.940	1.940	1.94
AT2-3	1.940	1.940	1.940	1.94
AT1-1	1.990	1.990	1.890	1.96
AT1-2	1.890	1.890	1.890	1.89
AT1-3	1.930	1.930	1.930	1.93
BC1-1	-	-	-	-
BC1-2	-	-		-
BC1-3	-	-	-	-
BC2-1	1.900	1.900	1.900	1.90
BC2-2	1.900	1.900	1.900	1.90
BC2-3	1.900	1.900	1.880	1.89
AT3-1	1.850	1.850	1.850	1.85
AT3-2	1.840	1.840	1.840	1.84
AT3-3	1.800	1.800	1.800	1.80

Table E5: Fundamental Frequency Data (120 Cycles)

Specimen Code	Freq 1 (kHz)	Freq 2 (kHz)	Freq 3 (kHz)	Avg Freq (kHz)
MT2-1	1.890	1.890	1.890	1.89
MT2-2	1.890	1.880	1.880	1.88
MT2-3	1.890	1.890	1.890	1.89
MT1-1	0.000	0.000	0.000	0.000
MT1-2	0.000	0.000	0.000	0.000
MT1-3	0.000	0.000	0.000	0.000
MT3-1	1.750	1.750	1.740	1.75
MT3-2	1.750	1.740	1.740	1.74
MT3-3	1.740	1.740	1.740	1.74
MU2-1	1.830	1.820	1.820	1.82
MU2-2	1.830	1.830	1.820	1.83
MU2-3	1.830	1.820	1.820	1.82
MU3-1	1.830	1.810	1.800	1.81
MU3-2	1.820	1.810	1.810	1.81
MU3-3	1.810	1.810	1.800	1.81
BT2-1	1.920	1.910	1.900	1.91
BT2-2	1.900	1.890	1.890	1.89
BT2-3	1.910	1.910	1.910	1.91
BT1-1	1.300	1.300	1.300	1.30
BT1-2	1.120	1.120	1.120	1.12
BT1-3	1.280	1.280	1.280	1.28
BT3-1	1.780	1.780	1.780	1.78
BT3-2	1.730	1.730	1.730	1.73
BT3-3	1.680	1.680	1.680	1.68
BU3-1	1.640	1.640	1.640	1.64
BU3-2	1.640	1.640	1.640	1.64
BU3-3	1.640	1.640	1.640	1.64
BU1-1	0.620	0.620	0.620	0.62
BU1-2	0.540	0.540	0.540	0.54
BU2-1	1.890	1.890	1.890	1.89
BU2-2	1.900	1.880	1.880	1.89
BU2-3	1.880	1.880	1.880	1.88
AU3-1	1.690	1.690	1.690	1.69
AU3-2	1.690	1.690	1.690	1.69
AU3-3	1.700	1.700	1.700	1.70
AU2-1	1.880	1.880	1.880	1.88
AU2-2	1.890	1.890	1.890	1.89
AU2-3	1.880	1.880	1.880	1.88
AU1-1	-	-	-	-

AU1-2	-	-	-	-
AU1-3	-	-	-	-

Table E5 Cont'd: Fundamental Frequency Data (120 Cycles)

Specimen Code	**Freq 1 (kHz)**	**Freq 2 (kHz)**	**Freq 3 (kHz)**	**Avg Freq (kHz)**
MU1-1	-	-	-	-
MU1-2	-	-	-	-
MU1-3	-	-	-	-
AT2-1	1.940	1.940	1.940	1.94
AT2-2	1.940	1.940	1.940	1.94
AT2-3	1.940	1.940	1.940	1.94
AT1-1	1.820	1.820	1.820	1.82
AT1-2	1.830	1.830	1.830	1.83
AT1-3	1.860	1.860	1.860	1.86
BC1-1	-	-	-	-
BC1-2	-	-	-	-
BC1-3	-	-	-	-
BC2-1	1.890	1.890	1.890	1.89
BC2-2	1.880	1.880	1.880	1.88
BC2-3	1.880	1.880	1.880	1.88
AT3-1	1.880	1.880	1.880	1.88
AT3-2	1.840	1.840	1.840	1.84
AT3-3	1.800	1.800	1.800	1.80

Table E6: Fundamental Frequency Data (150 Cycles)

Specimen Code	Freq 1 (kHz)	Freq 2 (kHz)	Freq 3 (kHz)	Avg Freq (kHz)
MT2-1	1.890	1.890	1.890	1.89
MT2-2	1.890	1.880	1.880	1.88
MT2-3	1.890	1.880	1.880	1.88
MT1-1	-	-	-	-
MT1-2	-	-	-	-
MT1-3	-	-	-	-
MT3-1	1.750	1.750	1.740	1.75
MT3-2	1.750	1.740	1.740	1.74
MT3-3	1.750	1.740	1.740	1.74
MU2-1	1.820	1.820	1.820	1.82
MU2-2	1.820	1.820	1.820	1.82
MU2-3	1.820	1.820	1.820	1.82
MU3-1	1.820	1.800	1.800	1.81
MU3-2	1.820	1.810	1.810	1.81
MU3-3	1.810	1.810	1.800	1.81
BT2-1	1.920	1.910	1.900	1.91
BT2-2	1.900	1.890	1.890	1.89
BT2-3	1.910	1.910	1.910	1.91
BT1-1	1.060	1.060	1.060	1.06
BT1-2	0.880	0.880	0.880	0.88
BT1-3	-	-	-	-
BT3-1	1.780	1.780	1.780	1.78
BT3-2	1.730	1.730	1.730	1.73
BT3-3	1.680	1.680	1.680	1.68
BU3-1	1.640	1.640	1.640	1.64
BU3-2	1.640	1.640	1.640	1.64
BU3-3	1.640	1.640	1.640	1.64
BU1-1	-	-	-	-
BU1-2	-	-	-	-
BU1-3	-	-	-	-
BU2-1	1.890	1.890	1.880	1.89
BU2-2	1.900	1.880	1.880	1.89
BU2-3	1.880	1.880	1.880	1.88
AU3-1	1.690	1.690	1.690	1.69
AU3-2	1.690	1.690	1.690	1.69
AU3-3	1.700	1.700	1.700	1.70
AU2-1	1.880	1.880	1.880	1.88
AU2-2	1.890	1.890	1.890	1.89
AU2-3	1.880	1.880	1.880	1.88

AU1-1	-	-	-	-
AU1-3	-	-	-	-

Table E6 Cont'd: Fundamental Frequency Data (150 Cycles)

Specimen Code	**Freq 1 (kHz)**	**Freq 2 (kHz)**	**Freq 3 (kHz)**	**Avg Freq (kHz)**
MU1-1	-	-	-	-
MU1-2	-	-	-	-
MU1-3	-	-	-	-
AT2-1	1.940	1.940	1.940	1.94
AT2-2	1.940	1.940	1.940	1.94
AT2-3	1.940	1.940	1.940	1.94
AT1-1	1.780	1.780	1.780	1.78
AT1-2	1.820	1.820	1.820	1.82
AT1-3	1.820	1.820	1.820	1.82
BC1-1	-	-	-	-
BC1-2	-	-	-	-
BC1-3	-	-	-	-
BC2-1	1.880	1.880	1.880	1.88
BC2-2	1.880	1.880	1.880	1.88
BC2-3	1.880	1.880	1.870	1.88
AT3-1	1.870	1.870	1.870	1.87
AT3-2	1.830	1.830	1.830	1.83
AT3-3	1.800	1.800	1.800	1.80

Table E7: Fundamental Frequency Data (180 Cycles)

Specimen Code	Freq 1 (kHz)	Freq 2 (kHz)	Freq 3 (kHz)	Avg Freq (kHz)
MT2-1	1.890	1.890	1.890	1.89
MT2-2	1.890	1.880	1.880	1.88
MT2-3	1.890	1.880	1.880	1.88
MT1-1	-	-	-	-
MT1-2	-	-	-	-
MT1-3	-	-	-	-
MT3-1	1.750	1.740	1.740	1.74
MT3-2	1.740	1.740	1.740	1.74
MT3-3	1.740	1.740	1.740	1.74
MU2-1	1.820	1.810	1.810	1.81
MU2-2	1.923	2.000	1.810	1.91
MU2-3	1.810	1.810	1.810	1.81
MU3-1	1.820	1.800	1.800	1.81
MU3-2	1.820	1.810	1.810	1.81
MU3-3	1.810	1.800	1.800	1.80
BT2-1	1.920	1.910	1.900	1.91
BT2-2	1.890	1.890	1.890	1.89
BT2-3	1.910	1.910	1.910	1.91
BT1-1	-	-	-	-
BT1-2	-	-	-	-
BT1-3	-	-	-	-
BT3-1	1.780	1.780	1.780	0.000
BT3-2	1.720	1.720	1.720	0.000
BT3-3	1.670	1.670	1.670	0.000
BU3-1	1.630	1.630	1.630	1.63
BU3-2	1.640	1.640	1.640	1.64
BU3-3	1.630	1.630	1.630	1.63
BU1-1	-	-	-	-
BU1-2	-	-	-	-
BU1-3	-	-	-	-
BU2-1	1.880	1.880	1.880	1.88
BU2-2	1.880	1.880	1.880	1.88
BU2-3	1.880	1.880	1.880	1.88
AU3-1	1.690	1.690	1.690	1.69
AU3-2	1.680	1.680	1.680	1.68
AU3-3	1.700	1.700	1.700	1.70
AU2-1	1.880	1.880	1.880	1.88
AU2-2	1.890	1.890	1.890	1.89
AU2-3	1.880	1.880	1.880	1.88

AU1-1	-	-	-	-
AU1-3	-	-	-	-

Table E7 Cont'd: Fundamental Frequency Data (180 Cycles)

Specimen Code	**Freq 1 (kHz)**	**Freq 2 (kHz)**	**Freq 3 (kHz)**	**Avg Freq (kHz)**
MU1-1	-	-	-	-
MU1-2	-	-	-	-
MU1-3	-	-	-	-
AT2-1	1.820	1.810	1.810	1.81
AT2-2	1.923	2.000	1.810	1.91
AT2-3	1.810	1.810	1.810	1.81
AT1-1	1.740	1.740	1.740	1.74
AT1-2	1.760	1.760	1.760	1.76
AT1-3	1.780	1.780	1.780	1.78
BC1-1	-	-	-	-
BC1-2	-	-	-	-
BC1-3	-	-	-	-
BC2-1	1.880	1.880	1.880	1.88
BC2-2	1.880	1.880	1.880	1.88
BC2-3	1.880	1.880	1.880	1.88
AT3-1	1.870	1.870	1.870	1.87
AT3-2	1.820	1.820	1.820	1.82
AT3-3	1.800	1.800	1.800	1.80

Table E8: Fundamental Frequency Data (210 Cycles)

Specimen Code	Freq 1 (kHz)	Freq 2 (kHz)	Freq 3 (kHz)	Avg Freq (kHz)
MT2-1	1.890	1.880	1.880	1.88
MT2-2	1.890	1.880	1.870	1.88
MT2-3	1.880	1.880	1.880	1.88
MT1-1	0.000	0.000	0.000	0.000
MT1-2	0.000	0.000	0.000	0.000
MT1-3	0.000	0.000	0.000	0.000
MT3-1	1.740	1.740	1.740	1.74
MT3-2	1.730	1.730	1.730	1.73
MT3-3	1.730	1.730	1.730	1.73
MU2-1	1.810	1.810	1.800	1.81
MU2-2	1.800	1.800	1.800	1.80
MU2-3	1.800	1.800	1.800	1.80
MU3-1	1.810	1.800	1.800	1.80
MU3-2	1.810	1.810	1.810	1.81
MU3-3	1.800	1.800	1.800	1.80
BT2-1	1.920	1.900	1.900	1.91
BT2-2	1.890	1.880	1.880	1.88
BT2-3	1.910	1.910	1.910	1.91
BT1-1	-	-	-	-
BT1-2	-	-	-	-
BT1-3	-	-	-	-
BT3-1	1.760	1.760	1.760	1.760
BT3-2	1.700	1.700	1.700	1.700
BT3-3	1.660	1.660	1.660	1.660
BU3-1	1.600	1.600	1.600	1.600
BU3-2	1.620	1.620	1.620	1.620
BU3-3	1.600	1.600	1.600	1.600
BU1-1	-	-	-	-
BU1-2	-	-	-	-
BU1-3	-	-	-	-
BU2-1	1.880	1.880	1.880	1.88
BU2-2	1.880	1.880	1.880	1.88
BU2-3	1.880	1.880	1.880	1.88
AU3-1	1.680	1.680	1.680	1.68
AU3-2	1.680	1.680	1.680	1.68
AU3-3	1.700	1.700	1.700	1.70
AU2-1	1.870	1.870	1.870	1.87
AU2-2	1.880	1.880	1.880	1.88
AU2-3	1.870	1.870	1.870	1.87

AU1-1	-	-	-	-
AU1-3	-	-	-	-

Table E8 Cont'd: Fundamental Frequency Data (210 Cycles)

Specimen Code	**Freq 1 (kHz)**	**Freq 2 (kHz)**	**Freq 3 (kHz)**	**Avg Freq (kHz)**
MU1-1	-	-	-	-
MU1-2	-	-	-	-
MU1-3	-	-	-	-
AT2-1	1.820	1.820	1.820	1.82
AT2-2	1.930	1.930	1.930	1.93
AT2-3	1.900	1.900	1.900	1.90
AT1-1	1.660	1.660	1.660	1.66
AT1-2	1.700	1.700	1.700	1.70
AT1-3	1.700	1.700	1.700	1.70
BC1-1	-	-	-	-
BC1-2	-	-	-	-
BC1-3	-	-	-	-
BC2-1	1.880	1.880	1.880	1.88
BC2-2	1.880	1.880	1.880	1.88
BC2-3	1.900	1.900	1.900	1.90
AT3-1	1.860	1.860	1.860	1.86
AT3-2	1.820	1.820	1.820	1.82
AT3-3	1.800	1.800	1.800	1.80

Table E9: Fundamental Frequency Data (240 Cycles)

Specimen Code	Freq 1 (kHz)	Freq 2 (kHz)	Freq 3 (kHz)	Avg Freq (kHz)
MT2-1	1.890	1.880	1.880	1.883
MT2-2	1.890	1.880	1.870	1.880
MT2-3	1.880	1.880	1.880	1.880
MT1-1	-	-	-	-
MT1-2	-	-	-	-
MT1-3	-	-	-	-
MT3-1	1.740	1.730	1.730	1.733
MT3-2	1.730	1.730	1.730	1.730
MT3-3	1.720	1.720	1.720	1.720
MU2-1	1.800	1.800	1.800	1.800
MU2-2	1.800	1.790	1.790	1.793
MU2-3	1.800	1.790	1.790	1.793
MU3-1	1.800	1.800	1.800	1.800
MU3-2	1.810	1.800	1.800	1.803
MU3-3	1.800	1.800	1.800	1.800
BT2-1	1.900	1.880	1.880	1.887
BT2-2	1.880	1.880	1.880	1.880
BT2-3	1.900	1.900	1.900	1.900
BT1-1	-	-	-	-
BT1-2	-	-	-	-
BT1-3	-	-	-	-
BT3-1	1.740	1.740	1.740	1.740
BT3-2	1.680	1.680	1.680	1.680
BT3-3	1.660	1.660	1.660	1.660
BU3-1	1.590	1.590	1.590	1.590
BU3-2	1.620	1.620	1.620	1.620
BU3-3	1.590	1.590	1.590	1.590
BU1-1	-	-	-	-
BU1-2	-	-	-	-
BU1-3	-	-	-	-
BU2-1	1.880	1.880	1.880	1.880
BU2-2	1.860	1.860	1.860	1.860
BU2-3	1.880	1.880	1.880	1.880
AU3-1	1.680	1.680	1.680	1.680
AU3-2	1.680	1.680	1.680	1.680
AU3-3	1.680	1.680	1.680	1.680
AU2-1	1.860	1.860	1.860	1.860
AU2-2	1.880	1.880	1.880	1.880
AU2-3	1.860	1.860	1.860	1.860

AU1-1	-	-	-	-
AU1-3	-	-	-	-

Table E9 Cont'd: Fundamental Frequency Data (240 Cycles)

Specimen Code	**Freq 1 (kHz)**	**Freq 2 (kHz)**	**Freq 3 (kHz)**	**Avg Freq (kHz)**
MU1-1	-	-	-	-
MU1-2	-	-	-	-
MU1-3	-	-	-	-
AT2-1	1.720	1.720	1.720	1.720
AT2-2	1.920	1.920	1.920	1.920
AT2-3	1.860	1.860	1.860	1.860
AT1-1	1.540	1.540	1.540	1.540
AT1-2	1.580	1.580	1.580	1.580
AT1-3	1.640	1.640	1.640	1.640
BC1-1	-	-	-	-
BC1-2	-	-	-	-
BC1-3	-	-	-	-
BC2-1	1.880	1.880	1.880	1.880
BC2-2	1.880	1.880	1.880	1.880
BC2-3	1.900	1.900	1.900	1.900
AT3-1	1.850	1.850	1.850	1.850
AT3-2	1.800	1.800	1.800	1.800
AT3-3	1.800	1.800	1.800	1.800

Table E10: Fundamental Frequency Data (270 Cycles)

Specimen Code	Freq 1 (kHz)	Freq 2 (kHz)	Freq 3 (kHz)	Avg Freq (kHz)
MT2-1	1.880	1.880	1.880	1.88
MT2-2	1.890	1.880	1.880	1.88
MT2-3	1.880	1.880	1.880	1.88
MT1-1	0.000	0.000	0.000	0.000
MT1-2	0.000	0.000	0.000	0.000
MT1-3	0.000	0.000	0.000	0.000
MT3-1	1.730	1.730	1.730	1.73
MT3-2	1.720	1.720	1.720	1.72
MT3-3	1.720	1.720	1.710	1.72
MU2-1	1.800	1.790	1.780	1.79
MU2-2	1.790	1.790	1.780	1.79
MU2-3	1.790	1.790	1.790	1.79
MU3-1	1.800	1.780	1.780	1.79
MU3-2	1.800	1.800	1.800	1.80
MU3-3	1.800	1.790	1.780	1.79
BT2-1	1.880	1.880	1.880	1.88
BT2-2	1.880	1.870	1.870	1.87
BT2-3	1.900	1.900	1.880	1.89
BT1-1	-	-	-	-
BT1-2	-	-	-	-
BT1-3	-	-	-	
BT3-1	1.730	1.730	1.730	1.730
BT3-2	1.670	1.670	1.670	1.670
BT3-3	1.660	1.660	1.660	1.660
BU3-1	1.590	1.590	1.590	1.590
BU3-2	1.600	1.600	1.600	1.600
BU3-3	1.590	1.590	1.590	1.590
BU1-1	-	-	-	-
BU1-2	-	-	-	-
BU1-3	-	-	-	-
BU2-1	1.860	1.860	1.860	1.86
BU2-2	1.860	1.860	1.860	1.86
BU2-3	1.880	1.880	1.880	1.88
AU3-1	1.660	1.660	1.660	1.66
AU3-2	1.670	1.670	1.670	1.67
AU3-3	1.680	1.680	1.680	1.68
AU2-1	1.850	1.850	1.850	1.85
AU2-2	1.880	1.880	1.880	1.88
AU2-3	1.880	1.880	1.880	1.88

AU1-1	-	-	-	-
AU1-3	-	-	-	-

Table E10 Cont'd: Fundamental Frequency Data (270 Cycles)

Specimen Code	**Freq 1 (kHz)**	**Freq 2 (kHz)**	**Freq 3 (kHz)**	**Avg Freq (kHz)**
MU1-1	-	-	-	-
MU1-2	-	-	-	-
MU1-3	-	-	-	-
AT2-1	1.880	1.880	1.880	1.88
AT2-2	1.880	1.880	1.880	1.88
AT2-3	1.820	1.820	1.820	1.82
AT1-1	1.420	1.420	1.420	1.42
AT1-2	1.520	1.520	1.520	1.52
AT1-3	1.520	1.520	1.520	1.52
BC1-1	-	-	-	-
BC1-2	-	-	-	-
BC1-3	-	-	-	-
BC2-1	1.870	1.870	1.870	1.87
BC2-2	1.870	1.870	1.870	1.87
BC2-3	1.880	1.880	1.880	1.88
AT3-1	1.840	1.840	1.840	1.84
AT3-2	1.780	1.780	1.780	1.78
AT3-3	1.780	1.780	1.780	1.78

Table E11: Fundamental Frequency Data (300 Cycles)

Specimen Code	Freq 1 (kHz)	Freq 2 (kHz)	Freq 3 (kHz)	Avg Freq (kHz)
MT2-1	1.870	1.870	1.870	1.87
MT2-2	1.870	1.870	1.870	1.87
MT2-3	1.870	1.870	1.870	1.87
MT1-1	-	-	-	-
MT1-2	-	-	-	-
MT1-3	-	-	-	-
MT3-1	1.730	1.720	1.720	1.72
MT3-2	1.710	1.710	1.710	1.71
MT3-3	1.710	1.710	1.710	1.71
MU2-1	1.780	1.780	1.780	1.78
MU2-2	1.780	1.780	1.770	1.78
MU2-3	1.787	1.780	1.780	1.78
MU3-1	1.780	1.780	1.780	1.78
MU3-2	1.790	1.790	1.790	1.79
MU3-3	1.780	1.780	1.780	1.78
BT2-1	1.880	1.880	1.870	1.88
BT2-2	1.870	1.870	1.860	1.87
BT2-3	1.880	1.880	1.880	1.88
BT1-1	-	-	-	-
BT1-2	-	-	-	-
BT1-3	-	-	-	-
BT3-1	1.700	1.700	1.700	1.700
BT3-2	1.670	1.670	1.670	1.670
BT3-3	1.660	1.660	1.660	1.660
BU3-1	1.590	1.590	1.590	1.590
BU3-2	1.600	1.600	1.600	1.600
BU3-3	1.590	1.590	1.590	1.590
BU1-1	-	-	-	-
BU1-2	-	-	-	-
BU1-3	-	-	-	-
BU2-1	1.850	1.850	1.850	1.85
BU2-2	1.850	1.850	1.850	1.85
BU2-3	1.870	1.870	1.870	1.87
AU3-1	1.660	1.660	1.660	1.66
AU3-2	1.670	1.670	1.670	1.67
AU3-3	1.680	1.680	1.680	1.68
AU2-1	1.850	1.850	1.850	1.85
AU2-2	1.860	1.860	1.860	1.86
AU2-3	1.880	1.880	1.880	1.88

AU1-1	-	-	-	-
AU1-3	-	-	-	-

Table E11 Cont'd: Fundamental Frequency Data (300 Cycles)

Specimen Code	**Freq 1 (kHz)**	**Freq 2 (kHz)**	**Freq 3 (kHz)**	**Avg Freq (kHz)**
MU1-1	-	-	-	-
MU1-2	-	-	-	-
MU1-3	-	-	-	-
AT2-1	1.880	1.880	1.880	1.88
AT2-2	1.840	1.840	1.840	1.84
AT2-3	1.820	1.820	1.820	1.82
AT1-1	1.360	1.360	1.360	1.36
AT1-2	1.360	1.360	1.360	1.36
AT1-3	1.400	1.400	1.400	1.40
BC1-1	-	-	-	-
BC1-2	-	-	-	-
BC1-3	-	-	-	-
BC2-1	1.870	1.870	1.870	1.87
BC2-2	1.870	1.870	1.870	1.87
BC2-3	1.880	1.880	1.880	1.88
AT3-1	1.820	1.820	1.820	1.82
AT3-2	1.770	1.770	1.770	1.77
AT3-3	1.780	1.780	1.780	1.78